Time Series Analysis in Astronomy

(Aikasarja-analyysi tähtitieteessä)

Code: PAP 312
Credits: 5

Lauri Jetsu
Department of Physics
University of Helsinki

Introduction

- **Lecturer:** Lauri Jetsu (lauri.jetsu@helsinki.fi)
- **Assistant:** Ari Leppälä (ari.leppala@helsinki.fi)
- **Magenta** colour www-links: symbols ☠ highlight
- **Lecturer's homepage** ☠

- Homepage **"Time Series Analysis in Astronomy"** ☠

Paper I **"Discrete Chi-square Method for Detecting Many Signals" ([15] Jetsu 2020, OJAp)** ☠

- **ONLY** 1 **Paper I**: Print, read and take to lectures
- **Introduces** Discrete Chi-square Method (DCM)
- **Applies** DCM to **simulated data**
- **Compares** DCM to other period analysis methods

Introduction ...

- Homepage **"Variable Stars"** ☠

Paper II **"Say hello to Algol's new companion candidates" ([16]Jetsu 2021)** ☠

- **2 PAPERS Paper I** and **Paper II**: Print, read and take to lectures
- **Introduces** DCM
- **Applies** DCM and other methods to **simulated** and **real** variable star data (e.g. **Paper II**)

- **Different exercises** in courses **"Time Series Analysis in Astronomy"** and **"Variable Stars"** $\longrightarrow$ **Study order** of **"Time Series Analysis in Astronomy"** and **"Variable Stars"** courses **flexible**

Introduction

Figure: @www.nobleworkscards.com

- **Question:** Do last term students have an advantage, because they already know DCM?
- **Answer 1:** Hopefully, they remember something about DCM, because all exercises are new.
- **Answer 2:** Next year: You will have the same advantage $\rightarrow$ Order of courses irrelevant
- **Answer 3:** Your future in Science? Good to learn DCM thoroughly: Artificial and real data analysis & DCM performance versus other methods, like DFT

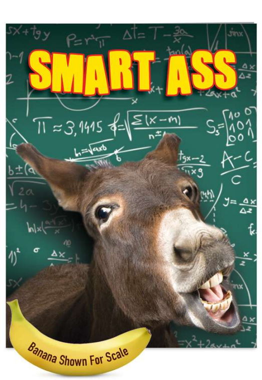

Introduction ...

Status of papers

- **Paper I**: **accepted & published**
- **Paper II**: **accepted & published**

In all lectures

- Both **“Time Series Analysis in Astronomy”** and **“Variable Stars”** courses:
- Symbols of variables
- Equation, Figure, Table and Section numbers
- References
- Abbreviations ...

same as in Paper I and **Paper II**:

$\rightarrow$ **We save a lot of time**

Introduction

- **Exercises** in **python**
- **We try** to use **same** symbols in all **python** program exercises, like
  T= t_i = time, **Y**= y_i = observation
- Important variables are written in **VIOLET capital or small letters** → Use same notations → Assistant can find them in your **python** programs
- DCM is an abstract method. It can be used to analyse arbitrary periodic, not only astronomical, phenomena
- **Observable** variability time scale
  → Can be observed in human time scale
  → DCM analysis possible

Introduction

- For example, stars are variable, not constant, because they evolve
- **Observable periodic changes in variable stars:**
  - Eclipses
  - Starspots
  - Activity cycles
- DCM is general $\rightarrow$ Can be applied to **many periodic** phenomena

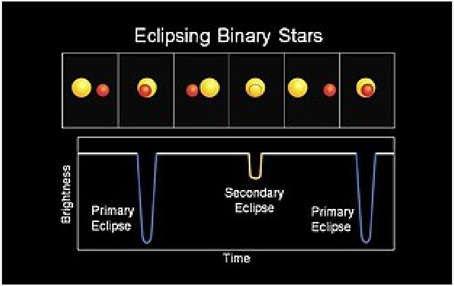

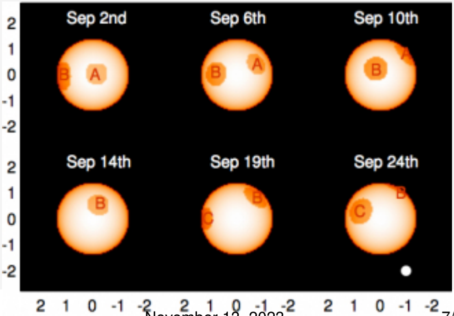

Background

- **First studies** [17](e.g. Jetsu et al. 1990)
- **Power spectrum analysis** [34] (Scargle 1982)
- Aug, 2021: 4741 citations
- Sinusoidal light curve
  $g(t) = A \sin 2\pi f(t - t_{min})$
  $A =$ Amplitude = spot size
  $P = 1/f =$ Rotation period
  $t_{min} =$ Minimum epoch
- **One constant** period for **one starspot**

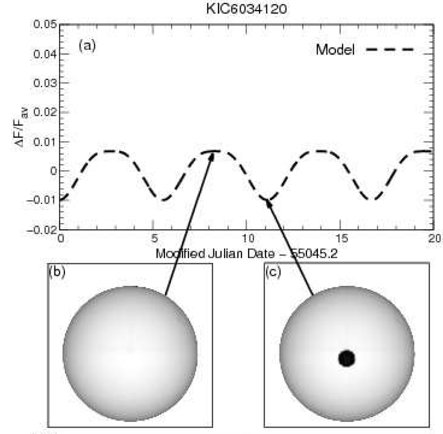

Figure from [35](Shibayama et al. 2013: their Fig. 3)

Background

- **Next studies** [19](e.g. Jetsu et al. 1999)
- **T**hree **S**tage **P**eriod **A**nalysis ([18]Jetsu & Pelt 1999: **TSPA**)
- Data divided into segments (seasons)
- Second order $g(t)$ light curve (double wave)
- P, A, $t_{min,1}$ and $t_{min,2}$ for **two** starspots
- **One constant** period for **two starspots**

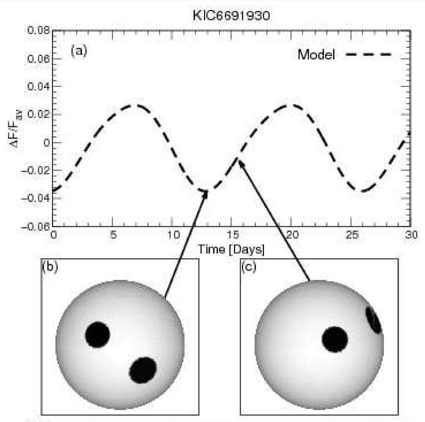

Figure from [35](Shibayama et al. 2013: their Fig. 4)

Background

- **Next studies** [25](e.g. Lehtinen et al. 2016)
- **C**ontinuous **P**eriod **S**earch ([24] Lehtinen et al. 2011: **CPS**)
- Sliding model window
- Best model identified
  - Constant
  - Sine wave
  - Double wave
- **One constant** period for **two starspots**

Figure [24](Lehtinen et al. 2011: their Fig. 7)

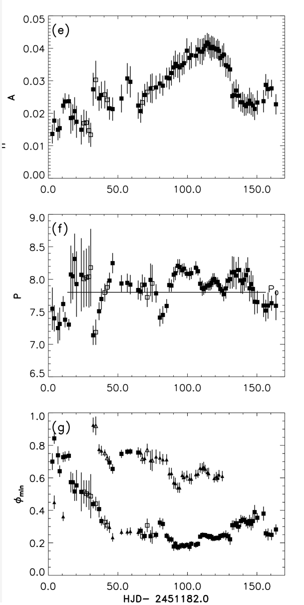

Background

- **Next studies** [13] (e.g. Jetsu 2019a)
- **Preliminary**
  Discrete
  Chi-square
  Method version
  ([15] Jetsu 2020 **DCM**)
- **Two constant** period light curves superimposed on a polynomial trend
- **Incompatibility** of one- and two-dimensional period finding methods, e.g. there are no **“flip-flops”**

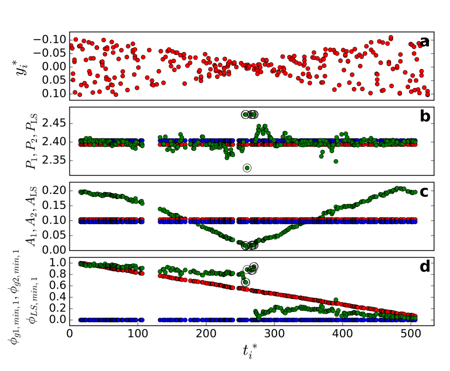

Figure [13](Jetsu 2019, his Fig. 11)

Background (Jetsu 2019a)

Imagine a face with a left eye () and a right eye (). Both eyes can disappear and reappear. At any given moment, the number of eyes may be zero, one or two. The original stationary right eye can disappear and reappear only at fixed locations. The original non-stationary left eye rotates slowly around the head. We see this head spinning. Soon it is impossible to tell which eye is the original left or right eye. The only compatible pictures of this face are snapshots, but none of these snapshots can be used to recognize this constantly changing face. These snapshots can capture only one side of the head, or equivalently only half of the full visible surface of FK Com.

Abstract (Paper I)

Discrete Chi-Square Method for Detecting Many Signals

Unambiguous detection of signals superimposed on unknown trends is difficult for unevenly spaced data. Here, we formulate the Discrete Chi-square Method (DCM) that can determine the best model for many signals superimposed on arbitrary polynomial trends. DCM minimizes the Chi-square for the data in the multi-dimensional tested frequency space. The required number of tested frequency combinations remains manageable, because the method test statistic is symmetric in this tested frequency space. With our known tested constant frequency grid values, the non-linear DCM model becomes linear, and all results become unambiguous. We test DCM with simulated data containing different mixtures of signals and trends. DCM gives unambiguous results, if the signal frequencies are not too close to each other, and none of the signals is too weak. It relies on brute computational force, because all possible free parameter combinations for all reasonable linear models are tested. DCM works like winning a lottery by buying all lottery tickets. Anyone can reproduce all our results with the DCM computer code.

Files (Paper I)

- All **program**, **file** and **other related** items are printed in **violet** colour
- All necessary files are available in **Zenodo** ☠

  dcm.pdf = **Paper I** manuscript

  dcm.py = DCM analysis **python** program

  dcm.dat = DCM control file

  TestData.dat = Simulated data file

  fisher.py = Fisher test **python** program
- **Copy four last files** from Zenodo to the same directory in your own computer
- **Do not use** Zenodo **Paper I** manuscript version (**dcm.pdf**), because it is the **submitted** version

Model (Paper I)

- **Observing times** = $t_i \rightarrow$ **Model zero** point $t = 0$ at t_1
- **Observations and errors** = $y_i = y(t_i) \pm \sigma_i$, $1 \leq i \leq n$
- **Mean** of y_i = m_y, **Standard deviation** of y_i = s_y
- **Model**

$$g(t) = g(t, K_1, K_2, K_3) = h(t) + p(t) \quad (1)$$

- **Periodic part** $h(t)$ is a sum of K_1 signals

$$h(t) = h(t, K_1, K_2) = \sum_{i=1}^{K_1} h_i(t) \quad (2)$$

- **i:th signal** is

$$h_i(t) = \sum_{j=1}^{K_2} B_{i,j} \cos(2\pi j f_i t) + C_{i,j} \sin(2\pi j f_i t) \quad (3)$$

- **Signal order** $= K_2$ (**dcm.py** can test only alternatives $1 \equiv$ sine wave and $2 \equiv$ double sine wave)

Model (Paper I)

- **Aperiodic part** is K_3 order polynomial

$$p(t) = p(t, K_3) = \sum_{k=0}^{K_3} p_k(t) \quad (4)$$

- **k:th** term is

$$p_k(t) = M_k \left[\frac{2t}{\Delta T}\right]^k \quad (5)$$

- It is difficult **to see** what this model means in reality
- **Figure on next page**
  - Three $h_i(t)$ signals ($K_1 = 3$)
  - All signals are sinusoids ($K_2 = 1$)
  - Signals superimposed on second order $p(t)$ polynomial ($K_3 = 2$)

Model (Paper I)

- **Time** = x-axis
- **Data** = y-axis

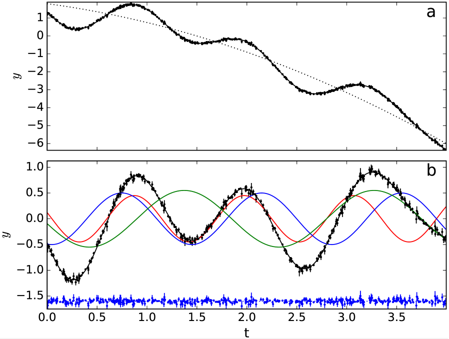

(a) Black dots = data = y_i

(a) Black curve $= g(t)$

(a) Dotted curve $= p(t)$

(b) **Removing** $p(t)$ trend

(b) Black dots = $y_i - p(t_i)$

(b) Black curve $= g(t) - p(t)$

(b) Red curve $= h_1(t)$ having period $1/f_1 = P_1 = 1.1$

(b) Blue curve $= h_2(t)$ having period $1/f_2 = P_2 = 1.4$

(b) Green curve $= h_3(t)$ having period $1/f_3 = P_3 = 1.9$

(b) Blue dots = Residuals $= \epsilon_i = y_i - g(t_i) =$ Data - model

Model (Paper I)

- **Problem:** If you only had **data**, black dots = y_i, **how** could you **unambiguously detect** $p(t)$ **trend** and three $h_i(t)$ **signals**?
- **DCM** succeeds in this!

Model (Paper I)

- DCM searches for combination of two patterns in data
- **Periodic** pattern $h(t)$ **repeating** itself
- **Aperiodic** pattern $p(t)$ **not repeating** itself
- **Sum of K_1 harmonic signals** $= h_i(t)$

  $f_i =$ signal frequency

  $K_2 =$ signal order
- **Polynomial K_3 order trend** $= p(t)$
- **Free parameters** of model

$$\begin{aligned}\bar{\beta} &= [\beta_1, \beta_2, ..., \beta_p] \\ &= [B_{1,1}, C_{1,1}, f_1, ..., B_{K_1,K_2}, C_{K_1,K_2}, f_{K_1}, M_0, ..., M_{K_3}]\end{aligned}$$

- **Number of free parameters**

$$p = K_1 \times (2K_2 + 1) + K_3 + 1 \qquad (6)$$

Linear and non-linear models

- **Main problem:** **Solution of best free parameter** $\bar{\beta}$ values for analysed data $y_i \pm \sigma_i$?

  Definition: Model $g(t)$ has p free parameters $[\bar{\beta} = \beta_1, \beta_2, ..., \beta_p]$. This model is **linear**, **if all** $i = 1, ..., p$ model partial derivatives

$$\frac{\partial g(t)}{\partial \beta_i}$$

  do not contain any free parameter $\beta_1, ..., \beta_p$. The model is **non-linear**, **if any** of these partial derivatives contains any free parameter $\beta_1, ..., \beta_p$.

Linear and non-linear models

- Crucial difference between **linear** and **non-linear** models is
  - **Solution of free parameters** $\bar{\beta}$ is **ambiguous**, if the model is **non-linear**, because this solution depends on the chosen trial value $\bar{\beta}_{\mathrm{trial}}$. The final value $\bar{\beta}_{\mathrm{final}}$ is obtained from an iteration beginning from $\bar{\beta}_{\mathrm{trial}}$.
  - **Solution of free parameters** $\bar{\beta}$ is **unambiguous**, if the model is **linear**. No trial value $\bar{\beta}_{\mathrm{trial}}$ is required.
- **Conclusion:** If possible, analyse data with a **linear** model. Then all results are **unambiguous**. If a **non-linear** model is necessary, then some, or maybe even all, results are **ambiguous**.

Model (Paper I)

- DCM model $g(t)$ has p free parameters
  $\bar{\beta} = [B_{1,1}, C_{1,1}, f_1, ..., B_{K_1,K_2}, C_{K_1,K_2}, f_{K_1}, M_0, ..., M_{K_3}]$
- They belong to **two groups**

1st group = $\bar{\beta}_I = [f_1, ..., f_{K_1}]$

2nd group = $\bar{\beta}_{II} = [B_{1,1} C_{1,1}, ..., B_{K_1,K_2}, C_{K_1,K_2}, M_0, ..., M_{K_3}]$

- **1st group** $\bar{\beta}_I$ make model **non-linear**
- **If** $\bar{\beta}_I$ are fixed to constant known numerical values
  $\rightarrow$ Model becomes **linear**
  $\rightarrow$ Solution for remaining $\bar{\beta}_{II}$ free parameters becomes **unambiguous**
- This is explained thoroughly Here: 05.09.2023
  ExerciseLinearNonlinear ☠ **(A2022)**
  where linear and non-linear models are identified.

Model

What causes nonlinearity?

- **Simple answer:** All trigonometric terms, like $B_{i,j} \cos(2\pi j f_i t)$. Its partial derivatives

$$\frac{\partial [B_{i,j} \cos(2\pi j f_i t)]}{\partial B_{i,j}} = \cos(2\pi j f_i t)$$

$$\frac{\partial [B_{i,j} \cos(2\pi j f_i t)]}{\partial f_i} = -B_{i,j} (\sin(2\pi j f_i t))(2\pi j t)$$

  contain free parameters f_i and $B_{i,j}$
- **If frequency f_i is fixed to a constant value**, frequencyf_i is no longer a free parameter
  $\rightarrow$ The first partial derivative $\cos(2\pi j f_i t)$ no longer contains any free parameters, and there is no need for the second partial derivative
  $\rightarrow$ Model becomes **linear**
  $\rightarrow$ $B_{i,j}$ solution becomes **unambiguous**

Model (Exercise)

- Simulating data using model **"Trend + Signal"**

ExerciseTrendSine ☠ (A2023)

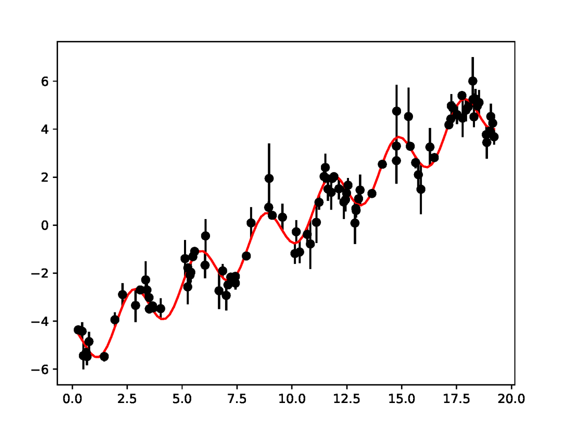

Model (Paper I)

- **Paper I** statement
  "The first group of free parameters, the frequencies $\bar{\beta}_I = [f_1, ..., f_{K_1}]$, make this $g(t)$ model **non-linear**. *If these $\bar{\beta}_I$ are fixed to constant known numerical values, the model becomes* **linear**, *and the solution for the remaining second group of free parameters, $\bar{\beta}_{II} = [B_{1,1} C_{1,1}, ..., B_{K_1,K_2}, C_{K_1,K_2}, M_0, ..., M_{K_3}]$, is* **unambiguous**.*"*
  should now be clear.
- In other words, **if** we test a frequency grid, where every tested frequency combination $\bar{\beta}_I = [f_1, ..., f_{K_1}]$ has fixed numerical constant values, then all these DCM models are **linear** and all results are **unambiguous**.

Model (Paper I)

- **Residuals**

$$\epsilon_i = y(t_i) - g(t_i) = y_i - g_i \qquad (7)$$

  are differences between **data** and **model**

- Residuals ϵ_i can be positive (**data** y_i above **model** g_i) or negative (**data** y_i below **model** g_i)
- **Good model**
  - **Mean** of ϵ_i residuals close to zero = Data at both sides of model = Model goes through data
  - **Standard deviation** of ϵ_i residuals equal to σ_i errors of data
  - **Absolute values** of individual ϵ_i residuals equal to errors of individual data $= |\epsilon_i| \approx \sigma_i =$ more accurate data closer to model

Model (Paper I)

- **Chi-square**

$$\chi^2 = \sum_{i=1}^{n} \frac{\epsilon_i^2}{\sigma_i^2} \tag{8}$$

  is sum of squared residuals divided by errors σ_i
- **Test statistic** χ^2 can be computed only if errors σ_i are **known**
- **Good** model has **small** χ^2
- **Bad** model has **large** χ^2
- **Reasonable** model has

$$\chi^2 \approx n,$$

  because $|\epsilon_i| \approx \sigma_i \Rightarrow \epsilon_i^2/\sigma_i^2 \approx 1$

Model (Paper I)

- **Sum of squared residuals**

$$R = \sum_{i=1}^{n} \epsilon_i^2. \qquad (9)$$

- **Test statistic** R can be computed even when errors σ_i are **unknown**
- **Good** model has **small** R
- **Bad** model has **large** R
- **Least Squares Fit (LSF)** method gives **solution for free parameters** $\bar{\beta}$. This method solves $\bar{\beta}$ values that
  - **Minimize** χ^2 when errors σ_i are **known**
  - **Minimize** R when errors σ_i are **unknown**

Least Squares Fit = LSF

ExerciseSineFit ☠ **(A2022)** and **ExerciseTrendSineFit** ☠ **(A2023)** show how Least Squares Fit (LSF) is done in **python**.

- **Both** can be solved without presenting **the other exercise!**
  - **scipy** subroutine **optimize.leastsq** is **numerical** $\rightarrow$ No need to code model $g(t)$ partial derivatives
  - Only three subroutines are needed

    Model(T,BETA)
    Funct(BETA,T,Y,EY)
    LSF(T,Y,EY)

  - Many models can be applied in the same program by simply changing names of these three subroutines
  - Code **Model** $\rightarrow$ **Funct** always same $\rightarrow$ Only dimensions of **BETA** must be adjusted in **LSF**

Least Squares Fit = LSF

Memorize: **Least Squares Fit = LSF**

- Download **dcm.py**, **dcm.dat** and **TestData.dat** from **Zenodo**
- Edit **only** **dcm.dat**. Do **NOT** edit **dcm.py**. Mistakenly edited? No worries, just download all files again.

ExampleDCMmodels

- Explains **dcm.py** **linear** and **non-linear** model codes
- **Advice:** **Re-read** this example several times during this course → At this first time, you do not have to understand everything about this example → Print all seven pages of this example, **reread, reread, ...**

LSF of dcm.py in a nutshell

- Six **subroutines**: Two three **subroutine** models.
- Three free parameter groups:
  - **Frequencies**
  - **Signal amplitudes**
  - **Polynomial coeffients**

LinearLSF **Lfunct** **LinearModel**	**NonLinearLSF** **Nfunct** **NonLinearModel**
Frequencies: **Not free** fixed tested values	Frequencies: **Free** parameters
Signal amplitudes: **Free** parameters	Signal amplitudes: **Free** parameters
Polynomial coefficients: **Free** parameters	Polynomial coeffients: **Free** parameters

- Any K_1, K_2 and K_3 combination: All six subroutines work.

Model (Paper I)

- **Parameters** of $h_i(t)$ signals

  $P_i = 1/f_i =$ Period
  $A_i =$ Peak to peak amplitude
  $t_{\mathrm{i,min,1}} =$ Deeper primary minimum epoch
  $t_{\mathrm{i,min,2}} =$ Secondary minimum epoch (if present)
  $t_{\mathrm{i,max,1}} =$ Higher primary maximum epoch
  $t_{\mathrm{i,max,2}} =$ Secondary maximum epoch (if present)

- **Paper I** colour code in all figures (Examples from Table 1)

  $f_1 \equiv$ **red** circle
  $h_1(t) \equiv$ **red** continuous line
  $A_3 \equiv$ **green** circle

- **Colour code** saves a lot of work in figure captions and improves readabiliy

Method (Paper I)

- **Note:** From Model section to Method section
- Frequencies $\bar{\beta}_I = [f_1, f_2, ..., f_{K_1}]$ fixed to constant tested numerical values $\rightarrow$ Model $g(t)$ becomes **linear**!
  - If data errors σ_i **known** $\rightarrow \chi^2$ minimized $\Rightarrow$ Period finding method **test statistic**

$$z = z(f_1, f_2, ..., f_{K_1}) = \sqrt{\frac{\chi^2}{n}}, \qquad (10)$$

  - If data errors σ_i **unknown** $\rightarrow R$ minimized $\Rightarrow$ Period finding method **test statistic**

$$z = z(f_1, f_2, ..., f_{K_1}) = \sqrt{\frac{R}{n}}. \qquad (11)$$

  - **dcm.py** minimizes $z \equiv$ minimizes χ^2 or $R \equiv$ minimizes distance between data (y_i) and model (g_i)

Method (Paper I)

- Impossible to code all possible K_1, K_2 and K_3 combinations into **dcm.py**
- Chosen combinations

$$1 \leq K_1 \leq 6 \equiv \text{From one to six periodic } h_i(t) \text{ signals}$$
$$1 \leq K_2 \leq 2 \equiv \text{Harmonic signal orders}$$
$$0 \leq K_3 \leq 6 \equiv \text{Polynomial trend } p(t) \text{ orders}$$

- **Statement:** *"Any arbitrary pair, $g_1(t)$ and $g_2(t)$, of these nested models can be compared."*
- **Definition of nested models:** "Two models are nested if one model contains all the terms of the other, and at least one additional term. The larger model is the **complex** (or full) model, and the smaller is the **simple** (or restricted) model."

Method (Paper I)

- **Paper I** notation

  Complex model is model $g_2(t)$ having **more** free parameters p_2

  Simple model is model $g_1(t)$ having **less** free parameters p_1

- **Example 1.** Models
  $g_2(t) = At + B, \bar{\beta} = [A, B]$
  $g_1(t) = Ct, \bar{\beta} = [C]$
  are **nested**, because $g_1(t)$ is a special case of $g_2(t)$ where $B = 0$.

- **Example 2.** Any DCM model $g_2(t, K_1 = 2, K_2, K_3)$ becomes model $g_1(t, K_1 = 1, K_2, K_3)$ when $f_1 \rightarrow f_2$, because two signal $f_1 \neq f_2$ model becomes one signal $f_1 = f_2$ model, i.e. these models are **nested**.

Method (Paper I)

- **Problem:** Which one of two **nested** $g_1(t)$ and $g_2(t)$ models is a better model for data
  - Number of free parameters ($p_1 < p_2$)
  - Chi-squares (χ_1^2, χ_2^2)
  - Sums of squared residuals (R_1, R_2)
- **Solution:** Compute Fisher **test statistic**
  - If errors σ_i **known**

$$F_\chi = \left(\frac{\chi_1^2}{\chi_2^2} - 1\right)\left(\frac{n - p_2 - 1}{p_2 - p_1}\right) \quad (12)$$

  - If errors σ_i **unknown**

$$F_R = \left(\frac{R_1}{R_2} - 1\right)\left(\frac{n - p_2 - 1}{p_2 - p_1}\right) \quad (13)$$

Here: 12.09.2023

Method (Paper I)

- Null hypothesis H_0:
  "Complex model $g_2(t)$ does not provide a significantly better fit to the data than simple model $g_1(t)$."
- F_χ and F_R have Fisher F-distribution with (ν_1, ν_2) degrees of freedom
  $\nu_1 = p_2 - p_1$
  $\nu_2 = n - p_2$
- Probability for $F = F_\chi$ or $F = F_R$ reaching a fixed level $F_0 = P(F \geq F_0)$ = **Critical level** $= Q_F$
- Hypothesis H_0 **rejected, if**

$$Q_F < \gamma_F = 0.001 \quad (14)$$

γ_F is **pre-assigned significance level**

Method (Paper I)

- Understanding F **test statistic**

$$F_\chi = \left(\frac{\chi_1^2}{\chi_2^2} - 1\right)\left(\frac{n - p_2 - 1}{p_2 - p_1}\right)$$

- F large $\rightarrow$ Complex model better than simple model
- **Increasing** free parameters from p_1 to p_2 **increases**

$$\left(\frac{\chi_1^2}{\chi_2^2} - 1\right)$$

because χ_2^2 becomes smaller, but this **decreases**

$$\left(\frac{n - p_2 - 1}{p_2 - p_1}\right)$$

penalty term. In other words, more complex models must have sufficiently smaller χ^2 or R

Method **(Paper I)**

- Let us assume that two signal ($K_1 = 2$) model is used. This leads to test statistic **symmetry**

$$z(f_1, f_2) = z(f_2, f_1)$$

- If tested frequency range is between $f_{\min} = P_{\max}^{-1}$ and $f_{\max} = P_{\min}^{-1}$, one could test combinations of **all**

  f_1 values in this range

  f_2 values in this range,

  which are inside a two-dimensional **square**.
- **Symmetry** $\rightarrow$ z values with respect to **square** diagonal same $\rightarrow$ Only **triangle** $f_1 > f_2$ pair combinations need to be tested
- **Note:** Why can $f_1 = f_2$ not be tested?

Method (Paper I)

Graphical presentation of $z(f_1, f_2) = z(f_2, f_1)$ **symmetry**, as well as **model break down** $f_1 \rightarrow f_2$

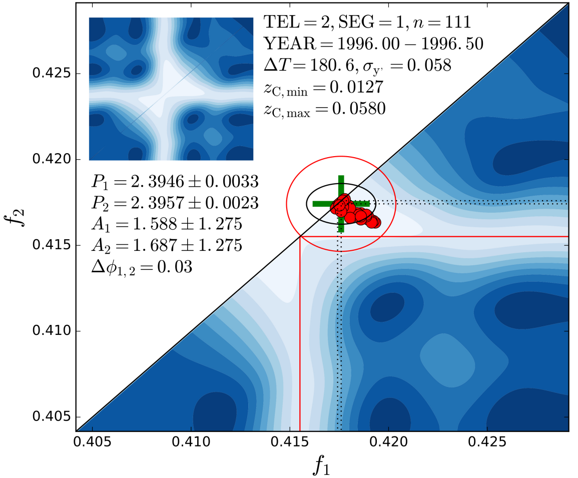

Method (Paper I)

- Next three pages: **evince paperi.pdf** (**Paper I**, Fig. 1)
- Three signal model has six $K_1! = 3! = 6$ respective **symmetries** $z(f_1, f_2, f_3) = z(f_1, f_3, f_2) = z(f_2, f_1, f_3) = z(f_2, f_3, f_1) = z(f_3, f_1, f_2) = z(f_3, f_2, f_1) \rightarrow$
  DCM tests only $f_1 > f_2 > f_3$ combinations
- **dcm.py** tests only $f_1 > f_2 > f_3 > f_4 > f_5 > f_6$ combinations, not all possible $6! = 720$ combinations
- **Long** tested frequency grid between $f_{\mathrm{min}} = P_{\mathrm{max}}^{-1}$ and $f_{\mathrm{max}} = P_{\mathrm{min}}^{-1}$ (Figs. 1a-f: higher longer rows)
  n_{L} evenly spaced tested frequencies
- **Long search** gives best frequency **candidates** $f_{1,\mathrm{mid}}, ..., f_{\mathrm{K}_1,\mathrm{mid}}$ at the z minimum = Mid points for denser **short search** grids (Fig. 1: diamonds)

Method (Paper I)

- **Short** tested frequency grid ranges are

$$[f_{\rm i,mid} - a, f_{\rm i,mid} + a]. \quad (15)$$

  - Suitable values $a = c\,(f_{\rm max} - f_{\rm min})/2$, $5\% \equiv 0.05 \leq c \leq 0.20 \equiv 20\%$
  - Evenly spaced $n_{\rm S}$ tested frequencies (Fig. 1a-f: lower shorter rows).
  - Short search grid denser than long search grid: **Why?**
- **Definition: Periodogram** is test statistic z plotted as a function of tested frequencies.
- Best frequencies at periodogram **global minimum**

$$z_{\rm min} = z(f_{1,\rm best}, f_{2,\rm best}, ..., f_{\rm K_1,best}). \quad (16)$$

Method (Paper I)

- Fig. 1 **Long and short** tested frequency grids
  (a) Six signal frequency grids
  red circles $= f_1$
  blue circles f_2
  green ...
  (b) Five signal ...
  (c) Four signal ...
  (d) Three signal ...
  (e) Two signal ...
  (f) One signal ...

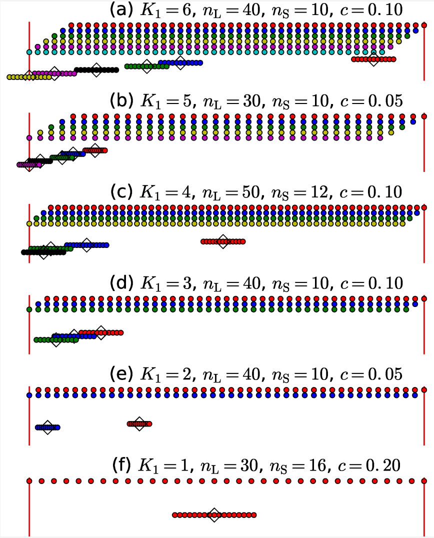

DCM → DFT Figure: @www.quotemaster.org

- Next two slides about

Discrete Fourier Transform (DFT)

Discrete Fourier Transform

- **Discrete Fourier Transform (DFT)** is also known as **Power Spectrum Method**
- **DFT** is most cited period finding method in Astronomy
- **DFT** searches for **one pure sinusoid** in the data
- **DFT** is **one-dimensional** period finding method = Searches for **one signal at the time**
- **DFT** requires **detrending**: removal of trends
- **DCM** is **many-dimensional** period finding method = Searches for **many signal at the time**
- **DCM** solves **signals and trends** simultaneously
- We will compare performance of **DFT** and **DCM** in several **Exercises** and **Examples**

Discrete Fourier Transform

- **First** **DFT** application example is given in
ExerciseScargle ☠ **(A2022)**
which applies **DFT** method to data file **Scargle.dat**
  - Analysed **Scargle.dat** data contains **no trend**

- **Second** **DFT** application example is given in
ExerciseTrendDFT ☠ **(A2023)**
which applies **DFT** method to data file **TrendDFT.dat**
  - Analysed data contains **a trend**
  - It is difficult to solve this second **ExerciseTrendDFT**, if the solution for **first** **ExerciseScargle** not presented

$\rightarrow$ The solution for **ExerciseScargle** is python program **ExerciseScargle.py**
This solution is shown and explained **here!**

DFT → DCM Figure: @www.quotemaster.org

- Next slides about

Discrete Chi-square Method (DCM)

Method (Paper I)

- Next two pages: **evince paperi.pdf** (**Paper I**, Fig. 2)
- How can K_1 dimensional periodograms $z(f_1, ..., f_{K_1})$ be **plotted**?

  $K_1 = 1$ signals: (f_1) gives z **curve**
  - Plot **possible**

  $K_1 = 2$ signals: (f_1, f_2) give z **plane**
  - Plot **possible**, like map of z as height or colour

  $K_1 = 3$ signals: (f_1, f_2, f_3) give z **cube**
  - Plot **impossible** in four dimensions (f_1, f_2, f_3) give z

  $K_1 \geq 4$ signals
  - Plot **impossible** also in five or more dimensions

Solution: Plot one-dimensional slices that intersect **global minimum** $z_{\min} = z(f_{1,\mathrm{best}}, f_{2,\mathrm{best}}, ..., f_{\mathrm{K}_1,\mathrm{best}})$

Method (Paper I)

- **Definition**: One-dimensional slices are

$$
\begin{aligned}
z_1(f_1) &= z(f_1, f_{2,\mathrm{best}}, ..., f_{\mathrm{K}_1,\mathrm{best}}) \\
z_2(f_2) &= z(f_{1,\mathrm{best}}, f_2, f_{3,\mathrm{best}}, ..., f_{\mathrm{K}_1,\mathrm{best}}) \\
z_3(f_3) &= z(f_{1,\mathrm{best}}, f_{2,\mathrm{best}}, f_3, f_{4,\mathrm{best}}, ..., f_{\mathrm{K}_1,\mathrm{best}}) \\
z_4(f_4) &= z(f_{1,\mathrm{best}}, f_{2,\mathrm{best}}, f_{3,\mathrm{best}}, f_4, f_{5,\mathrm{best}}, f_{\mathrm{K}_1,\mathrm{best}}) \\
z_5(f_5) &= z(f_{1,\mathrm{best}}, f_{2,\mathrm{best}}, f_{3,\mathrm{best}}, f_{4,\mathrm{best}}, f_5, f_{\mathrm{K}_1,\mathrm{best}}) \\
z_6(f_6) &= z(f_{1,\mathrm{best}}, f_{2,\mathrm{best}}, f_{3,\mathrm{best}}, f_{4,\mathrm{best}}, f_{5,\mathrm{best}}, f_6)
\end{aligned}
\quad (17)
$$

- When these one-dimensional slices are overplotted
  $\rightarrow f_{\mathrm{i,best}} > f_{\mathrm{i+1,best}}$, because tested frequencies fulfill
  $f_1 > f_2 > f_3 > f_4 > f_5 > f_6$
  $\rightarrow$ Periodogram slice $z_i(f_i)$ ends at minimum of next slice $z_{i+1}(f_{i+1})$ (**Paper I**: Fig. 2, upper panel)

Method (Paper I)

- **Fig. 2** Long and short search periodograms of three signal $K_1 = 3$ model: $z_1(f_1) \equiv$ red line, $z_2(f_2) \equiv$ blue line and $z_2(f_3) \equiv$ green line

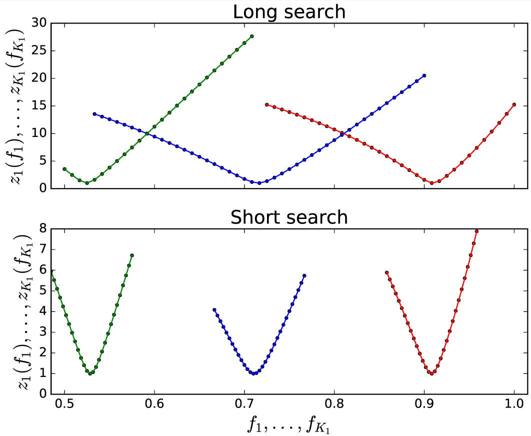

Method (Paper I)

- [13] (Jetsu 2019: his Fig. 1)
  - Two-dimensional $z(f_1, f_2)$ periodogram
  - White colour at $z(f_1, f_2)$ minima
  - Blue colour at $z(f_1, f_2)$ maxima
  - Green cross: global $z(f_1, f_2)$ minimum
  - $z_1(f_1) = z(f_1, f_2 = f_{2,\mathrm{best}})$ is one-dimensional **horizontal** slice through green cross ($f_{2,\mathrm{best}}$ constant)
  - $z_2(f_2) = z(f_1 = f_{1,\mathrm{best}}, f_2)$ is one-dimensional **vertical slice** through green cross ($f_{1,\mathrm{best}}$ constant)

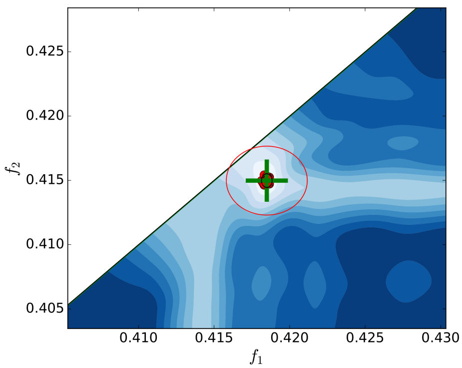

Questions (Paper I)

- The following three questions are presented in **ExerciseSymmetry** (A2022)

1. The DCM test statistic is symmetric.
   For two signals ($K_1 = 2$), this symmetry for tested frequencies is

$$z(f_1, f_2) = z(f_2, f_1).$$

   For three signals ($K_1 = 3$), this symmetry for tested frequencies is

$$\begin{aligned} z(f_1, f_2, f_3) &= z(f_1, f_3, f_2) = z(f_2, f_1, f_3) = \\ z(f_2, f_3, f_1) &= z(f_3, f_1, f_2) = z(f_3, f_2, f_1). \end{aligned}$$

   Can you explain what causes this symmetry?

2. DCM tests only frequency combinations that fulfill $f_1 > f_2 > f_3 > f_4 > f_5 > \ldots > f_{K_1}$.
   Can you explain why?

3. Assume that the DCM model $g(t)$ frequencies are equal ($f_1 = f_2$), or they approach each other ($f_1 \rightarrow f_2$). Can you explain why this $g(t)$ model makes no sense?

Method (Paper I)

- **Global** $z_{\min} = z(f_{1,\mathrm{best}}, f_{2,\mathrm{best}}, ..., f_{\mathrm{K}_1,\mathrm{best}})$ minimum gives

$$\bar{\beta}_{\mathrm{I,Initial}} = [f_{1,\mathrm{best}}, f_{2,\mathrm{best}}, ..., f_{\mathrm{K}_1,\mathrm{best}}]$$

- **Linear** model with these frequencies also gives

$$\bar{\beta}_{II,initial} = [B_{1,1} C_{1,1}, ..., B_{K_1,K_2}, C_{K_1,K_2}, M_0, ..., M_{K_3}]$$

- Best trial value are $\bar{\beta}_{\mathrm{Initial}} = [\bar{\beta}_{\mathrm{I,Initial}}, \bar{\beta}_{\mathrm{II,Initial}}]$
- **Non-linear** LSF iteration gives final best free parameter values

$$\bar{\beta}_{\mathrm{Initial}} \rightarrow \bar{\beta}_{\mathrm{Final}} \tag{18}$$

Method (Paper I)

- **Problem**: What are the **Errors** of model parameters $f_i, A_i, t_{\mathrm{min,1,i}}, \ldots$
- **Solution**: **Bootstrap** procedure

  $g_i = g(t_i)$ = Best model for **original** data $y_i = y(t_i)$
  $\epsilon_i^* =$ Random sample from residuals ϵ_i of best g_i model for **original** data y_i

- *"Any ϵ_i value can enter into this random sample $\bar{\epsilon}^*$ as many times as the random selection happens to favour it."*
- **Artificial** bootstrap data samples

$$y_i^* = g_i + \epsilon_i^* \tag{19}$$

Method (Paper I)

- Create many, S, **artificial** bootstrap samples $\bar{y}^*$
- Analyse each **artificial** bootstrap sample $\bar{y}^*$ with DCM using same short frequency intervals as for **original** data
- Each **artificial** random data bootstrap sample $\bar{y}^*$ gives **one** estimate for every model parameter $f_i, A_i, t_{\mathrm{min,1,i}}, \ldots$
- **Error estimate** for each particular model parameter $f_i, A_i, t_{\mathrm{min,1,i}}, \ldots$ is **standard deviation** of **all** its S bootstrap estimates
- **python** program **ExampleBootstrap.py** gives one detailed example of bootstrap. It is explained in **ExampleBootstrap** Here: 19.09.2023

One simulated model (Paper I)

- **Note:** New Section 4.1: "One simulated model"
- Observations simulated from **known** $g_{\mathrm{S1}}(t)$ model

$$
\begin{aligned}
g_{\mathrm{S1}}(t) &= h(t) + p(t) = \sum_{i=1}^{K_1} h_i(t) + \sum_{k=0}^{K_3} p_k(t) \quad (20) \\
h_i &= (A_i/2)\sin\left[2\pi f_i(t - T_i)\right] \\
p_k(t) &= M_k \left[\frac{2t}{\Delta T}\right]^k,
\end{aligned}
$$

$K_1 = 3 =$ three $h_i(t)$ signals

$K_2 = 1 =$ signals $h_i(t)$ are pure sinusoids

$K_3 = 2 =$ quadratic (parabola) trend $p(t)$

One simulated model (Paper I)

- Simulating $n^{\star} = 500$ random data of **TestData.dat**
- **Time points** $t_i^{\star}$ of simulated data drawn from uniform random distribution between 0 and $\Delta T = 4$

$$U(0, \Delta T, n^{\star}) \qquad (21)$$

- Data y_i evenly spaced in t_i coincide with a **sinusoid** $g_i = a \sin 2\pi t_i$
  $\Rightarrow y_1 = g_i \Rightarrow$ Both have same standard deviation s_y
  $\Rightarrow a = 2^{3/2} s_y$ [21](Jetsu et al. 2013)
  $\Rightarrow A = 2a = 2^{5/2} s_y =$ peak to peak amplitude
- Simulated data mean error $\sigma_m \Rightarrow$ Signal to noise ratio

$$\mathrm{SN} = A/\sigma_m = 2^{5/2} s_y^{\star}/\sigma_m$$

One simulated model (Paper I)

- This SN relation holds for cosines, double sinusoids and double cosines, i.e. for both orders $K_2 = 1$ and 2.
- Standard deviation of sum $h(t_i^\star)$ of all h_i signals = $s_y^\star$
- SN of simulated data fixed $\Rightarrow$ Error of simulated data

$$\sigma_m = 2^{5/2} s_y^\star / \mathrm{SN} \tag{22}$$

- **Errors** $\sigma_i^\star$ of simulated data drawn from Gaussian distribution

$$N(m^\star, s^\star, n^\star), \tag{23}$$

where $m^\star = 0$ and $s^\star = \sigma_m$.
- **Simulated data**

$$y_i^\star = g(t_i^\star, \bar{\beta}^\star) + \sigma_i^\star. \tag{24}$$

TestData.dat (Paper I)

- Observations simulated with model $g_{S1}(t)$ of Eq. 20

  Column 1: $t_i^\star =$ **T**
  Column 2: $y_i^\star =$ **Y**
  Column 3: $\sigma_i^\star =$ **EY**

- Four first lines of all $n = 500$ lines of **TestData.dat**

```
0.001954782    1.285584396    0.053913136
0.008301549    1.222326656    0.082413098
0.011958311    1.257181220    0.027658351
0.013231162    1.275299902    0.002635674
```

- Any data analysed with **dcm.py** must have this format

- If errors $\sigma_i =$ **EY** are unknown
  $\rightarrow$ Give all errors same arbitrary constant value
  $\rightarrow$ Use **TestStat$\neq$1**
  $\rightarrow$ Test statistic computed from R

One simulated model (Paper I)

- Periods and amplitudes of three $h_i(t)$ signals are
  $P_1 = 1.1$ and $A_1 = 0.9$
  $P_2 = 1.4$ and $A_2 = 1.0$
  $P_3 = 1.9$ and $A_3 = 1.1$
  during $0 \leq t \leq 4\Delta T = 4$.
- Other model parameters are given in **Table 2**
- DCM period analysis of **TestData.dat** between
  $P_{\mathrm{min}} = 1$ and $P_{\mathrm{max}} = 2$
- Test statistic

$$z = z(f_1, f_2, f_3) = \sqrt{\frac{\chi^2}{n}}$$

computed for model (“model 19” in **Table 4**)

$$g(t, K_1 = 3, K_2 = 1, K_3 = 3)$$

Method (Paper I)

$z_1(f_1)$, $z_2(f_2)$ and $z_3(f_3)$ periodograms again (**Fig. 2**)

Minima a clearly separated = All periodicities clear

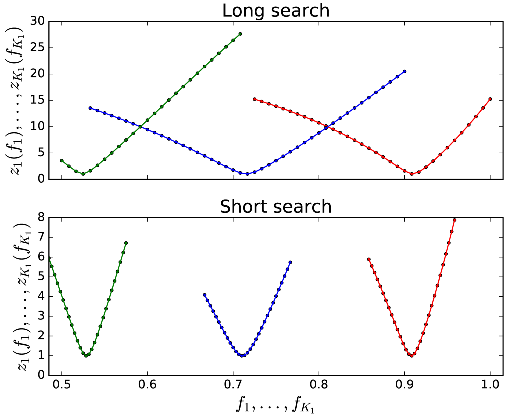

- **Table 2**: Simulated and Detected agree perfectly

Table 2	Simulated	Detected	
Parameter	$g_{S1}(t)$	Model 19	Model 20
$1/f_1 = P_1$	1.1	1.100 ± 0.001	1.104 ± 0.003
A_1	0.9	0.90 ± 0.01	0.95 ± 0.03
$t_{1,\mathrm{min}}$	0.325	0.325 ± 0.001	0.322 ± 0.002
$t_{1,\mathrm{max}}$	0.875	0.875 ± 0.001	0.874 ± 0.001
$1/f_2 = P_2$	1.4	1.40 ± 0.01	1.50 ± 0.04
A_2	1.0	1.00 ± 0.02	1.8 ± 0.3
$t_{2,\mathrm{min}}$	0.050	0.50 ± 0.01	1.441 ± 0.003
$t_{2,\mathrm{max}}$	0.75	0.7500 ± 0.006	0.69 ± 0.02
$1/f_3 = P_3$	1.9	1.90 ± 0.01	1.73 ± 0.07
A_3	1.1	1.10 ± 0.03	1.94 ± 0.3
$t_{3,\mathrm{min}}$	0.425	0.426 ± 0.008	0.54 ± 0.05
$t_{3,\mathrm{max}}$	1.375	1.375 ± 0.002	1.41 ± 0.01
M_0	1.8	1.800 ± 0.002	1.74 ± 0.02
M_1	-1.5	-1.500 ± 0.003	-1.1 ± 0.2
M_2	-1.2	-1.201 ± 0.001	-1.8 ± 0.2
M_3	-	-	0.21 ± 0.08

One simulated model (Paper I)

- **Fig. 3 Perfect!!!**

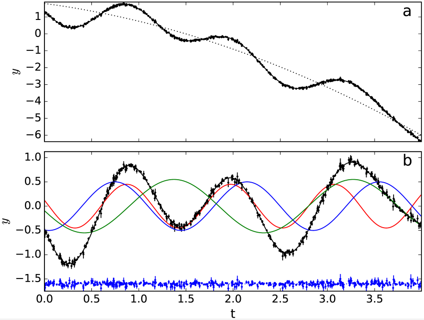

(a) Black dots = data = y_i

(a) Black curve $= g(t)$

(a) Dotted curve $= p(t)$

(b) **Removing** $p(t)$ trend

(b) Black dots = $y_i - p(t_i)$

(b) Black curve $= g(t) - p(t)$

(b) Red curve $= h_1(t)$ period $1/f_1 = P_1 = 1.100 \pm 0.001$

(b) Blue curve $= h_2(t)$ period $1/f_2 = P_2 = 1.40 \pm 0.01$

(b) Green curve $= h_3(t)$ period $1/f_3 = P_3 = 1.90 \pm 0.01$

(b) Blue dots = Residuals = Data - model $= y_i - g(t_i)$ are stable and show no trends

One simulated model (Paper I)

Fig 4.: Bootstrap

- Frequencies f_1, f_2, f_3
- Amplitudes A_1, A_2, A_3
- Original data: blue
- Bootstrap data: red
- Dotted lines $\pm 1\sigma, \pm 2\sigma, \pm 3\sigma$ error limits

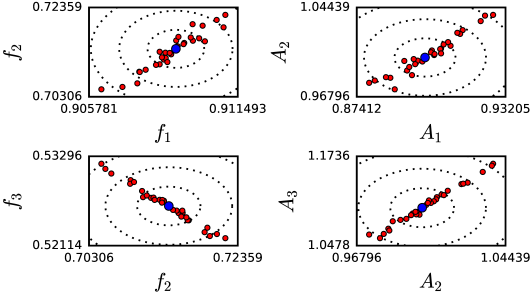

- **Linear correlations**: **Any** shift away from correct frequency or amplitude is compensated by shifts of **all** other frequencies and amplitudes
- **Note**: Frequency errors far from $f_1 = f_2$ and $f_2 = f_3$
- **Note**: Amplitudes A_1, A_2, A_3 do not disperse

DCM → DFT Figure: @www.quotemaster.org

- Next four slides about

Discrete Fourier Transform

Discrete Fourier Transform

- You will get model solution **ExerciseTrendDFT.py**, **but only after** completing **ExerciseTrendDFT**

- Now lessons learned from **ExerciseTrendDFT.py** are presented here in **ExampleTrendDFT** ☠ **(Always)**

- Can **DFT** detect **many frequencies** f_k $(k = 1, 2, ...)$?
  - **Yes**, but **only if**
    - No trend(-s)
    - If trend(-s), they can be removed
    - Signals are pure sinusoids
    - Frequencies f_k are not too close to each other
    - Data time span ΔT is larger than periods $P_k = 1/f_k$
    - Adequate sample size (n)
    - Adequate signal to noise ratio (A/σ_i)

Pre-Whitening: First example

"Frequency analysis of Cepheids ..."

[29] (Moskalik & Kolaczkowski, 2009, Fig. 3)

- DFT to **original data** gives frequency f_1
- Frequency f_1 sine fit to **original data** gives **1st rediduals**
- DFT to **1st residuals** gives frequency f_2
- Frequency $f_1 + f_2$ sine fit to **original data** gives **2nd residuals**
- Continues until no significant periodicity ...

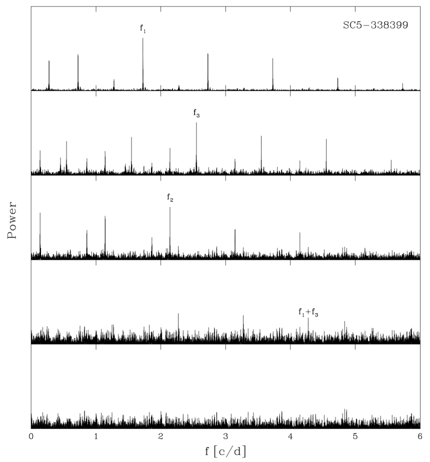

Pre-whitening: Second example

"... RR-Lyrae ..." [6] (Duan et al. 2021, Fig. 10)

- Same pre-whitening technique ... much more frequencies!

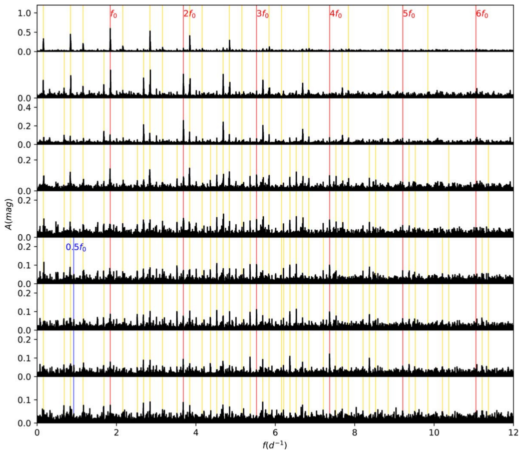

Discrete Fourier Transform

- **DFT** searches for the frequency f of the best sinusoidal model for the data

- Hence, there must be a connection between **DFT** and **direct** sinusoidal **DCM** fit to the data

- This **DFT** and **DCM** connection is illustrated in

ExerciseSineZ ☠ **(A2023)**

where DCM periodogram

$$z(f) = \sqrt{\chi^2/n}$$

for **DCM** model having $K_1 = 1, K_2 = 1, K_3 = 0$ is compared to **DFT** periodogram $z_{\mathrm{LS}}(f)$

Discrete Fourier Transform

- **DFT** pre-whitening technique exercise in **ExerciseSinesDFT** ☠ **(A2022)**
  - Analysed **TestData.dat** data contains **a trend**
  - Trend is not removed before applying DFT!
  - This exercise requires that model solution programs **ExerciseSineFit.py** of **ExerciseSineFit** and **ExerciseScargle.py** of **ExerciseScargle** have been explained earlier during the course

Discrete Fourier Transform

- DFT pre-whitening technique exercise in

ExercisePreWhiten ☠ **(A2023)**

1. Remove cubic polynomial trend $\rightarrow$ Detrended data
2. DFT for Detrended data $\rightarrow$ First P_1 period
3. Period P_1 Sine fit to detrended data $\rightarrow$ 1st residuals
4. DFT for 1st residuals $\rightarrow$ Second P_2 period

Note: In this particular case, detection of both periods P_1 and P_2 **succeeds!**

Uncertainties in real data

- Is trend (K_3) correct?
- Is number of signals (K_1) correct? $\equiv$ Should pre-whitening continue, or stop earlier?
- Are sinusoids correct signal models?

Discrete Fourier Transform

- Next DFT

ExerciseFailWhiten ☠ **(A2023)**

shows two cases, where pre-whitening fails or succeeds

- DFT detection criterion for f_1 and f_2 is

$$
\begin{aligned}
|f_1 - f_2| &> f_0 \\
f_0 &= 1/\Delta T \\
\Delta T &= t_n - t_1
\end{aligned}
$$

- In other words, the difference in completed rounds for f_1 and f_2 during ΔT must be larger than one.
- If frequencies are nearly the same, the required time span for their detection is longer.

DFT $\rightarrow$ DCM Figure: @www.quotemaster.org

- Next slides about

Discrete Chi-square Method

Appendix (Paper I)

- **Note**: New section Appendix
- **Appendix = Instructions** for using **dcm.py**
- Create your DCM test directory **mkdir DCMtest**
- Go to your DCM test directory **cd DCMtest**
- Download following four files to **.../DCMtest** directory

  dcm.py

  dcm.dat

  TestData.dat

  fisher.py
- Note that there were problems in downloading **python** programs from Zenodo to Helsinki University computers. From the above links, you can download these files directly from course home-page.

Appendix (Paper I)

- We will try to turn this statement into an advantage

  "The main idea is that the user **never edits** *the* **dcm.py** *program, but* **only executes** *it with the* **python dcm.py** *command. The user edits* **only the last right hand column** *of the control file* **dcm.dat**. *This control file* **dcm.dat** *is shown in the end of this appendix."*

- **Actually true?!!!!? Left behind: Raise your voice!**
- We test one **dcm.dat** combination at the time.
- **TestData.dat** analysis requires understanding of fifteen first lines 1-15 parameters in **dcm.dat**

Appendix (Paper I)

- **dcm.dat** is **control file**
- **dcm.dat** parameters control what **dcm.py** does
- When editing **dcm.dat**
  1. **DO NOT** remove or add any **"="** character
  2. **DO NOT** change any first column number **1, 2, ..., 24**
  3. **USE** integer values for variables **K1**, **K2**, **K3**, **nL**, **nS**, **Rounds**, **SimN** and **SimRounds**
- Edit mistake! $\rightarrow$ Load new **dcm.dat** from home-page
- **dcm.py** analyses/creates data in three modes

SimMany $\neq$ **1**	**RealData = 1**	Mode 1: One sample of *real* data of **file1**
SimMany $\neq$ **1**	**RealData** $\neq$ **1**	Mode 2: One sample of *simulated* data
SimMany = 1	Any **RealData** value	Mode 3: Many samples of *simulated* data

- Analysis of **TestData.dat** is performed in **Mode 1**
  SimMany $\neq$ **1**, **Realdata=1**, **file1=TestData.dat**

Appendix (Paper I)

- **Aim of this course:** You learn to use **DCM**
- **Achieving this aim:** You learn best by using DCM
- **Next page screenshot** displays my **desktop icons**

  Left white box: **emacs dcm.dat &**
  K1=3 edited to **K1=1** in **dcm.dat**
  Rounds=30 edited to **Rounds=2** in **dcm.dat**
  Middle black box: **python dcm.py**
  Right box above: **evince Dec2019gdet.eps &**
  Right box below: **evince Dec2019z.eps &**

- We try to use similar box locations when possible
- **Solution: dcm.dat** always shown first left

DCM practice

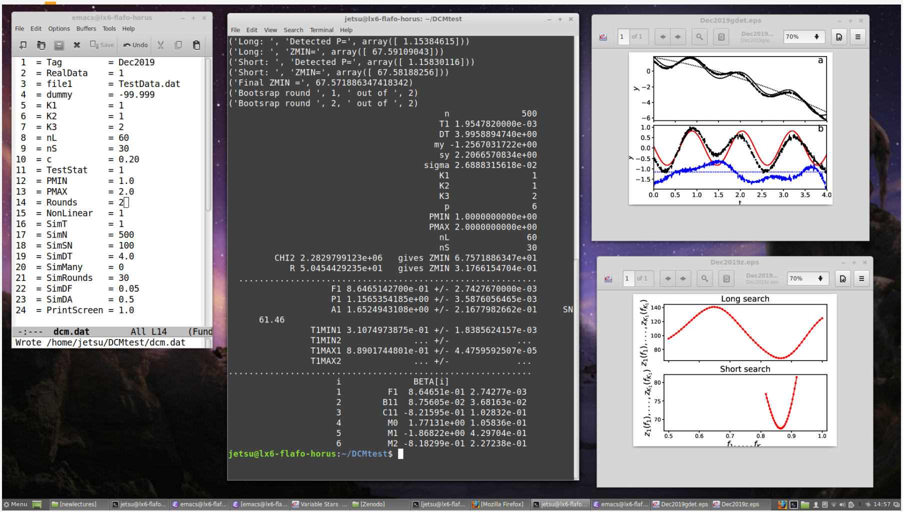

Appendix (Paper I) Here: 03.10.2023

- Numbers highlighted inside **Orange squares** refer to line numbers in **dcm.dat**
- For example, **RealData** on line 2 in **dcm.dat** gets 2

1 **Tag** determines beginning of names of **all output** figures and files. This gives following advantages

- **Different output file names** can be specified
- **Different analyses** can be easily coded: separated from each other
- **Results of different analyses** can be studied separately **after** DCM analysis
- For example, **Tag = Dec2019** $\rightarrow$ periodogram figure named **Dec2019z.eps** (**Paper I**, Fig. 2)

- Exercise of how to use **Tag, K1, K2, K3**

ExerciseTag ☠ **(A2022)**

Appendix (Paper I)

2 **RealData** determines analysed data

- Combination **RealData=1** and **SimMany** $\neq$ **1** analyses **one real data sample**
- Combination **RealData** $\neq$ **1** and **SimMany** $\neq$ **1** creates and analyses **one simulated data sample**
- Combination of **any** **RealData** value and **SimMany=1** creates and analyses **many simulated data samples**
- **Simulations can be used to**
  - Test reliability of DCM, like in Fig. 11 of **Paper I**
  - Simulations use real data $t_i =$**T**, if **SimT** $\neq$ **1**
- Here is one exercise of how to use **RealData**

ExerciseSimulatedData ☠ **A2022**

Appendix (Paper I)

3 **file1** is real data file analysed **when RealData=1**

- Allows DCM analysis of **any** file of real data
- **Sect. 4.1** One simulated model
  Confirms that DCM works: **file1=TestData.dat**
- **Sect. 4.2** Identifying the best model
  Confirms that DCM indentifies the best model among many models: **file1=TestData.dat**
- **Sect. 4.3** Searching for too many signals
  Identifies too complex models: **file1=TestData.dat**
- **Sect. 4.4** Finding too few signals
  Identifies too simple models: **file1=TestData.dat**
- **Sect. 4.5** Many simulated models
  Confirms that DCM works: **file1 $\neq$ TestData.dat** because many data samples are simulated/analysed

Appendix (Paper I)

4 **dummy** means "no value". This exact value should not occur in **data** or in **model parameters**

- **dcm.py discards and/or removes dummy** values
- **dcm.dat** has **dummy=-99.999** because
  - Data file **TestData.dat** contains no such values
  - Sensible $g_{\mathrm{S1}}(t)$ model (Eq. 20) free parameters and other parameters have no such values
- For example, another value than **dummy=-99.999** would be better when analysing **data** $y_i =$ **Y of temperatures** between -300 and 300 degrees
- Probability for data or model value **being exactly equal to dummy** is low. For example, values like **-99.99900001**, **-99.99899999** are treated as real data values, or as real model parameter values

Appendix (Paper I)

- **dcm.py** can analyse **all combinations of following** $g(t)$ model orders

  5 **K1**$= K_1 = 1, 2, 3, 4, 5$ or 6 signals $h_i(t)$ (Eq. 1)

  6 **K2**$= K_2 = =$ signal order (Eq. 1)
  1 = sum of one sine & one cosine waves
  2 = sum of one sine & one cosine,
  and double sine & double cosine waves

  7 **K3**$= K_3 = 0, 1, 2, 3, 4, 5$ or 6 order polynomial trend $p(t)$ (Eq. 1)

- When **Realdata $\neq$ 1** or **SimMany=1** program **dcm.py**
  - **Creates** simulated data having these model orders **K1**, **K2** and **K3**
  - **Analyses** simulated data using DCM models having **the same** orders **K1**, **K2** and **K3**

Appendix (Paper I)

- **Next two dcm.dat** control file parameters determine **number** of long and short search tested frequencies
  - 8 **nL** $= n_{\mathrm{L}} =$ tested frequencies in **long search**
  - 9 **nS** $= n_{\mathrm{S}} =$ tested frequencies in **short search**
- **Too few** tested $\rightarrow$ Best frequencies **not detected**
- **Increase** n_{L} and n_{S} $\rightarrow$ Best frequencies **detected**
- **Computing time** proportional to $\propto n_{\mathrm{L}}^{K_1}$ and $\propto n_{\mathrm{S}}^{K_1}$
- **Linear computing time** increase for **one signal**
- **Exponential computing time** increase of number of tested frequency combinations for **many signals**
- Typical **TestData.dat** analysis: $K_1 = 1$ (seconds), $K_1 = 2$ (minutes), $K_1 = 3$ (hours), $K_1 = 4$ (days), ...

Appendix (Paper I)

- **Next dcm.dat** control file parameter
  10 **c**$=c=$ determines relative width of **short** search frequency interval
- **Long** search frequencies between $f_{\max}$ and $f_{\min}$
- **Long** search best frequency **candidates** $f_{1,\mathrm{mid}}, ..., f_{\mathrm{K}_1,\mathrm{mid}}$ (**Paper I**, Fig. 1: diamonds)
- **Short** search tested intervals

$$[f_{\mathrm{i,mid}} - a, f_{\mathrm{i,mid}} + a]$$

- Suitable values are $a = c\,(f_{\max} - f_{\min})/2$ where $5\% \equiv 0.05 \le c \le 0.20 \equiv 20\%$
- **Short** search tested **frequency grid denser** than **long** search tested **frequency grid**
  $\rightarrow$ Gives **more accurate** best frequency estimates

Appendix (Paper I)

- **Eleventh dcm.dat** control file parameter

  11 **TestStat** selects **which** test statistic **z**$=z$ is used in DCM analysis

  - If **TestStat=1**, z is computed from χ^2 (Eq. 10)
    - **Requires** that data errors are **known**
  - If **TestStat** $\neq$ **1**, z is computed from R (Eq. 11)
    - **Does not require** that data errors **known**

- **Next two dcm.dat** control file parameters are

  12 **PMIN**$=P_{\mathrm{min}}=$ smallest **long search** period

  13 **PMAX**$=P_{\mathrm{max}}=$ largest **long search** period

- **Real data**: Period search minimum and maximum
- **Simulated data**: Minimum and maximum of **random periods** when creating/analysing simulated data

Appendix (Paper I)

- **Fourteenth dcm.dat** control file parameter

14 **Rounds** = Number of bootstrap rounds

- **Higher Rounds** $\rightarrow$ **Longer** computation time
- Model parameter **results same for any Rounds**
- Bootstrap gives **only parameter error estimates**
- **Rounds=2** $\rightarrow$ Results for model parameters

$\rightarrow$ Make sense? $\rightarrow$ Errors with higher **Rounds**

- **Next dcm.dat** control file parameter

15 **NonLinear** determines, if **non-linear iteration** from β_{initial} to β_{final} (Eq. 18) **is performed:**

NonLinear$= 1$ = Yes; **NonLinear**$\neq 1$ = No

- Latter alternative may cause error messages, when best frequencies in tested grids are the same during all bootstrap rounds

Appendix (Paper I)

- Analysis of **real data** in data file **file1** requires understanding/use of **only** control file **dcm.dat** parameters 1 - 15
- Analysis of **simulated data** requires understanding/use of **other** control file **dcm.dat** parameters 16 - 24
- **Possible code improvements for "beginners"**
    - **Simple dcm.py** version for **real data analysis**
    - Uses **only** real data parameters 1 - 15
    - Simulated data parameters 16 - 24 **removed**
    - Detailed **manual for users only in Zenodo**
    - **Perhaps add** predictions formulated in **Paper II**
    - **dcm.dat** parameter numbers **can not change**. **Why!**

Appendix (Paper I)

- **Next dcm.dat** control file parameters

16 - **23** determine analysis of **simulated data**

- All these parameters begin with letters **Sim**

16 **SimT** determines **simulated data** time points $t_i^\star$

- **SimT=1** means that
  $t_i^\star$ drawn from uniform random distribution of Eq. 21
- **SimT$\neq$1** means that
  $t_i^\star = t_i$ from real data file **file1**
- Latter **SimT$\neq$1** alternative allows simulation of data that resembles analysed real data

17 **SimN** determines number $n^\star$ of **simulated data**

18 **SimSN** determines **simulated data** signal to noise ratio SN of Eq. 22.

Appendix (Paper I)

- **Nineteenth dcm.dat** control file parameter

  19 **SimDT** determines **simulated data** time span ΔT in uniform random distribution $U(0, \Delta T, n^{\star})$ defined in Eq. 21

  - Simulated $t_i^{\star}$ are **drawn** from this distribution

  20 **SimMany** de-activates or activates Mode 3

  - Mode 1: **SimMany** $\neq$ **1** and **RealData=1** $\rightarrow$ **dcm.py** analyses **one real** data sample
  - Mode 2: **SimMany** $\neq$ **1** and **RealData** $\neq$ **1** $\rightarrow$ **dcm.py** creates/analyses **one simulated** sample
  - Mode 3: **SimMany = 1** $\rightarrow$ **dcm.py** creates/ analyses **many simulated** samples
  - For any **Tag=***, results are figure ***Many.eps** (e.g. **Paper I**, Fig. 11), and free parameter file ***AllBeta.dat**

Appendix (Paper I)

- **Next** **dcm.dat** control file parameters are

21 **SimRounds** determines number of created and analysed **simulated data** samples when **SimMany=1** (Mode 3)

22 **SimDF** $= f_{\rm crit}$ of Eq. 28 (e.g. Fig. 11: diamonds)
- Distance between two best frequencies is below $f_{\rm crit}$
$\rightarrow$ Model may suffer from **“intersecting frequencies”**
$\rightarrow$ Model may be unstable

23 **SimDA** $= A_{\rm crit}$ of Eq. 29 (e.g. Fig. 11: circles)
- Amplitude of at least one signal is $1/A_{\rm crit}$ times weaker than amplitude of strongest signal
$\rightarrow$ This weak signal may not be detected

- Description of **simulated data** parameters
16 - **23** of control file **dcm.dat** completed!

Appendix (Paper I)

Last dcm.dat control file parameters

24 **PrintScreen** controls printing to screen

- **Problem**: Computing many signal models takes time: seconds ($K_1 = 1$), minutes ($K_1 = 2$), hours ($K_1 = 3$), days ($K_1 = 4$), ...
- **Solution**: Jobs to computer queue (batch)
  $\rightarrow$ **New problem:** Printing may need to be prevented
  $\rightarrow$ Use **PrintScreen**$\neq 1 \rightarrow$ **New problem solved!**

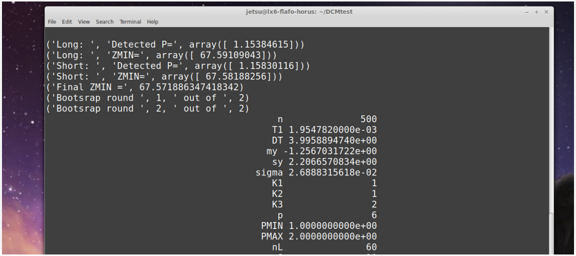

Appendix (Paper I)

Analysis results file

- Printed to screen if **PrintScreen=1**
- Always printed to file in same format

- **Tag=*** $\rightarrow$ ***Params.dat**
- For example, Model 18 analysis results file for three signals

n,T1,DT	$n, t_1, \Delta T$
my,sy,SN	m_y, s_y, SN
K1,K2,K3	K_1, K_2, K_3
p	p
PMIN,PMAX	$P_{\min}, P_{\max}$
nL,nS	$n_{\mathrm{L}}, n_{\mathrm{S}}$
CHI2,R	χ^2, R
F1,P1,A1,T1MIN1,T1MIN2,T1MAX1,T1MAX2	$f_1, P_1, A_1, t_{1,\min,1}, t_{1,\min,2}, t_{1,\max,1}, \ldots$
F2,P2,A2,T2MIN1,T2MIN2,T2MAX1,T2MAX2	$f_2, P_2, A_2, t_{2,\min,1}, t_{2,\min,2}, t_{2,\max,1}, \ldots$
F3,P3,A3,T3MIN1,T3MIN2,T3MAX1,T3MAX2	$f_3, P_3, A_3, t_{3,\min,1}, t_{3,\min,2}, t_{3,\max,1}, \ldots$
BETA[i]	$\bar{\beta}$

DCM $\rightarrow$ DFT Figure: @www.quotemaster.org

- Next slides about

Discrete Fourier Transform (DFT)

DCM versus DFT pre-whitening

- Sect 4.1, **Main result**: DCM can detect $P_1 = 1.1$, $P_2 = 1.4$ and $P_3 = 1.9$ signals from **TestData.dat**
- **Paper I**: **Introduction**
    - *"The Discrete Fourier Transform (DFT), also called the power spectrum method, is one of the most frequently applied period analysis methods in natural sciences ..."*
    - *"DFT versions rely on the assumption that the data contains no trends, and the correct model is one sinusoidal signal."*
    - *"Systematic trends in the data must be removed before DFT analysis, ..."*
    - *"... removal of trends is not trivial, and it can seriously mislead the period analysis ..."*

DCM versus DFT Pre-whitening

- **Paper I**: **Introduction** (continues...):
  - *"Since DFT searches for one period at the time, we call it a* **one-dimensional** *period finding method."*
  - *"After ... detrending, the DFT search for* **many** *pure sinusoidal signals usually relies on* **pre-whitening.**"

1. *"... highest DFT periodogram peak gives the* **best period** *for the detrended* **original data**.*"*
2. *"... sinusoidal model with this* **best period** *is subtracted from these detrended data."*
3. *... next* **second best period** *is determined with the DFT analysis of the* **residuals**.*"*
4. *"This* **second best period** *gives the sinusoidal model for the* **residuals**, *and the* **next residuals** *for DFT analysis."*

DCM versus DFT pre-whitening

- **DFT pre-whitening** is applied to two different samples in **ExerciseFailWhiten**
  - 1st sample: **Fails** to detect P_1 or P_2
  - 2nd sample: **Succeeds** to detect P_1 and P_2

ExerciseOneDCM ☠ **(A2023)**

- One important difference between DFT and DCM
  - DFT **can not** detect two frequencies f_1 and f_2, **if** $|f_1 - f_2| \leq f_0 = 1/\Delta T$
  - DCM **can** detect two frequencies f_1 and f_2, **even if** $|f_1 - f_2| \leq f_0 = 1/\Delta T$
  - ΔT **limits** DFT performance for any sample size (n) or any accuracy (σ_i) [27](Loumos & Deeming 1978)
  - ΔT **does not limit** DCM performance, only sample size (n) and/or accuracy (σ_i) do

DFT → DCM Figure: @www.quotemaster.org

- Next slides about

Discrete Chi-square Method (DCM)

Identifying the best model (Paper I)

Note: New section 4.2

- Previous Sect. 4.1
  - Data **simulated** with $K_1 = 3$, $K_2 = 1$, $K_3 = 2$ model
  - Data **analysed** with $K_1 = 3$, $K_2 = 1$, $K_3 = 2$ model
  - **Correct** model was **known**
    $\rightarrow$ **Correct** simulated model parameters retrieved

Problem: How to proceed, if **correct** model **unknown**?

Assumption: **TestData.dat** represents real data, but correct model **unknown**.

Solution: Test numerous alternative models. Fisher-test identifies best one of those models.

Identifying the best model (Paper I)

- **Test all 32 model** combinations

  $1 \leq K_1 \leq 4$
  $1 \leq K_2 \leq 2$
  $0 \leq K_3 \leq 3$

- Each combination has
  $p = K_1 \times (2K_2 + 1) + K_3 + 1$
  free parameters (Eq. 6).
- Each combination gives χ^2, F_χ and Q_F.
- Fisher-test results given in Table 4 of **Paper I**
- **Correct** "model 19" has $p = 12$ free parameters
- **Alternative 31 models** are

  A: Models 1-13, 17-18: Less free parameters ($p_2 = 12$)
  B: Model 14: Same number of free parameters
  C: Other models: More free parameters ($p_1 = 12$)

Identifying best the model **(Paper I)**

A: Models 1-13, 17-18 have $Q_F < 10^{-16}$
$\rightarrow$ Model 19 is better

B: Model 14 χ^2 **larger** than Model 19 χ^2
$\rightarrow$ Model 19 is better

C: Models 15, 21, 25 and 26 χ^2 **larger** than Model 19 χ^2
$\rightarrow$ Model 19 is better

C: Models 16, 22, 22-24 and 27-32 χ^2 **smaller** than Model 19 χ^2, **but** these models have $Q_F > 0.001$
$\rightarrow$ Model 19 is better

- Above, **only** Model 19 compared to other models
- Here is one exercise of how to compare all alternative models to each other, and to identify the best model: **ExerciseFisher** ☠ **(A2022)**

DCM → DFT Figure: @www.quotemaster.org

- Next slide compares

Discrete Fourier Transform (DFT) to
Discrete Chi-square Method (DCM)

DFT limitations

- **1st limitation**
  $|f_1 - f_2| < f_0 = 1/\Delta T \rightarrow$
  DFT periodogram peaks merge $\rightarrow$
  Both periods $P_1 = 1/f_1$ and $P_2 = 1/f_2$ **not detected!**
- **2nd limitation**
  $P > \Delta T \rightarrow$
  Period P **not detected!**
- **Other limitations**
  Trends, only sinusoids, one signal at the time, pre-whitening, ...
- One re-assuring DCM **detection example**
  ExerciseTwoDCM ☠ **(A2023)**

DFT → DCM Figure: @www.quotemaster.org

- Next slides about

Discrete Chi-square Method (DCM)

Identifying the best model (Paper I)

- Model 19 ($K_1 = 3$, $K_2 = 1$, $K_1 = 2$)

  Correct periods $P_1 = 1.1$, $P_2 = 1.4$ and $P_3 = 1.9$

- Model 20 is second best model

  $Q_F = 0.078 > 0.001 = \gamma_F$

  $K_1 = 3$ and $K_2 = 1$ is correct

  $K_3 = 3$ is not correct

  $\rightarrow$ **Additional cubic trend**

  $\rightarrow$ Period search fails

  1st period $P_1 = 1.104$ **nearly correct**

  2nd period $P_2 = 1.50$ **not correct**

  3rd period $P_3 = 1.73$ **not correct**

Conclusion: Even a minor deviation from correct $p(t)$ trend can seriously mislead DCM analysis.

Search... too many signals (Paper I)

- **Note**: New Sect. 4.3.
- **TestData.dat** contains three signals

  Problem: What happens, if DCM searches for **too many**, e.g. four signals?
- Four signal model 27 ($K_1 = 4$, $K_2 = 1$, $K_3 = 2$)
  - $Q_F = 0.168$ (**Paper I**, Table 4)$\rightarrow$ Model 19 is better!
  - Periodograms shown on next page (**Paper I**, Fig. 5)
  - Red $z_1(f_1)$, blue $z_2(f_2)$ and green $z_3(f_3)$ periodograms low and stable, and their minima shallow
  - Only yellow $z_4(f_4)$ periodogram has clear minimum
  - $P_1 = 1.16$, $P_2 = 1.19$, $P_3 = 1.25$, $P_4 = 1.97$ not correct

"Shallow periodograms" Fig. 5 (Paper I)

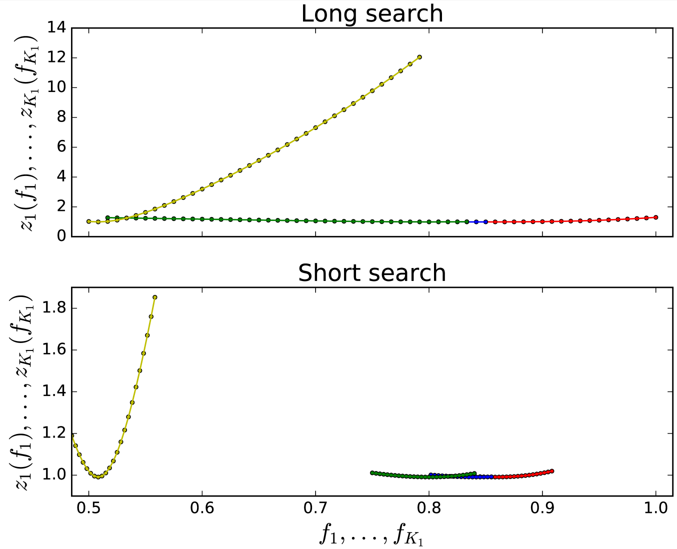

Search... too many signals (Paper I)

- Four signal model 27 “explodes”
  - Four signals (**Paper I**, Fig. 6)
  - Red $h_1(t)$, blue $h_2(t)$ and green $h_3(t)$ signal amplitudes disperse
  - Only yellow $h_4(t)$ signal amplitude stable
  - red $h_1(t)$, blue $h_2(t)$ and green $h_3(t)$ signals “cancel each other out”

Instability: **“Dispersing amplitudes”**

  - Bootstrap error estimates (**Paper I**, Fig. 7)
  - Dotted frequency error lines intersect thick green continuous $f_1 = f_2$ and $f_2 = f_3$ diagonal lines

Instability: **“Intersecting frequencies”**

- Both instabilities in **all** four signal models (**Paper I**, Table 4) $\rightarrow$ DCM does not “detect” too many signals

“Dispersing amplitudes” Fig. 6 (Paper I)

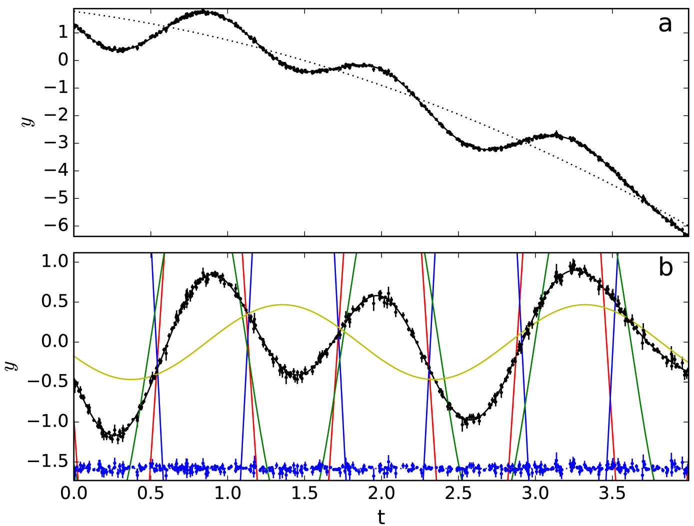

“Intersecting frequencies” Fig. 7 (Paper I)

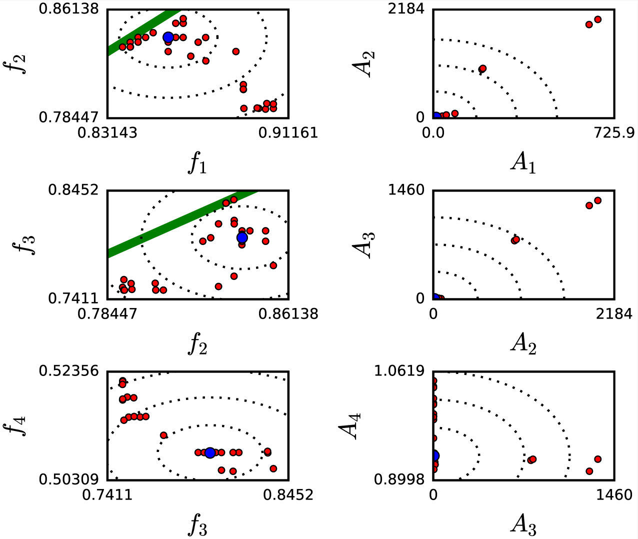

Finding too few signals (Paper I)

- **Note**: New Sect. 4.4.
- **TestData.dat** contains **three sinusoidal signals** ($K_1 = 3, K_2 = 1$) and a **quadratic** trend ($K_3 = 2$)
  $\rightarrow$ **Model 19** is correct model for **TestData.dat**

  Problem: What happens, if DCM searches for **too few** signals from **TestData.dat**?
- **Test case: Model 9** applied to **TestData.dat**
  - Two signals ($K_1 = 2$): **Wrong**
  - Sinusoids ($K_2 = 1$): **Correct**
  - Constant trend ($K_3 = 0$): **Wrong**
- **Before test:**
  - Fisher test comparison of **Model 19** and **Model 9** gives $Q_F < 10^{-16}$ (**Paper I**, Table 4)
    $\rightarrow$ **Model 19** is certainly better!

Finding too few signals (Paper I)

- **Model 9** results in nut shell:
  - Red $z_1(f_1)$ and blue $z_2(f_2)$ periodograms merge (**Paper I**, Fig. 8)
  - Red $h_1(t)$ and blue $h_2(t)$ signals have **"dispersing amplitudes"** (**Paper I**, Fig. 9)
  - f_1 and f_2 bootstrap estimates show **"intersecting frequencies"** (**Paper I**, Fig. 10)
- **Conclusion: Model 9** search for too few signals fails
- **All** two, three and four signal models having constant trend $K_3 = 0$ **fail** (**Paper I**, Table 4: Models 9, 13, 17, 21, 25 and 29)

"Periodograms merge" Fig. 8 (Paper I)

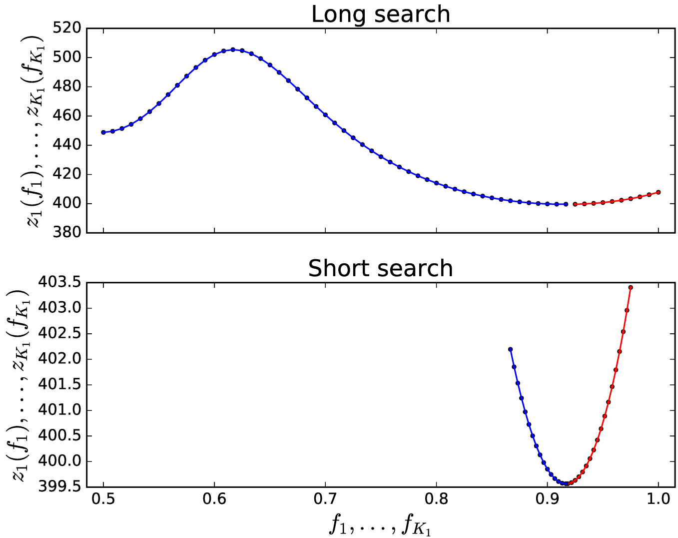

ExerciseOneDCM Fig. 2: “Long merge, Short not!”

- Long search merge → Not necessarily failed model!

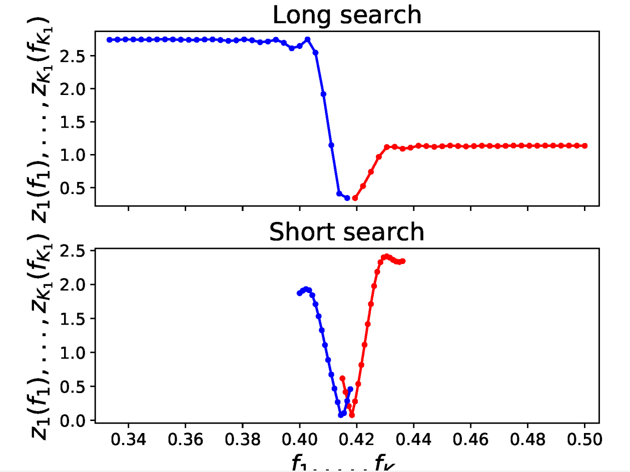

“Amplitudes disperse” Fig. 9 (Paper I)

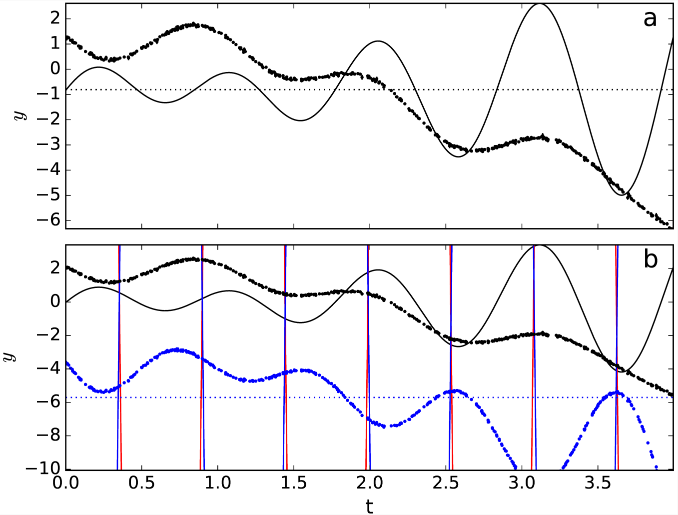

“Frequencies intersect” Fig. 10 (Paper I)

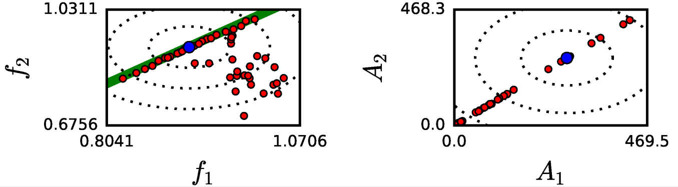

- Following regularities prevail in Table 4 (**Paper I**)
  - **Too many** signals → Models unstable
  - **Too few** signals → Models stable or unstable
  - → There may be more signals
  - **Wrong** $p(t)$ trend → Models unstable
  - **Failures**: 2 signals (2/8=25%), 4 signals (8/8=100%)
- **Conclusion**: *“false detection of too few signals is more probable than false detection of too many signals’* **Here: 17.10.2023**

Many simulated models (Paper I)

- **Note**: New Sect. 4.5. (Testing DCM performance)
- **SimMany=1** activates simulation of many samples

  SimN $= n^* =$ sample size
  SimDT $= \Delta T =$ sample time span
  SimSN = S/N = sample signal to noise (Eq. 22)
  SimRounds = Number of simulated samples
  SimDF and **SimDA** = Frequency and amplitude highlighting criteria (Eqs. 28 and 29)
  K1, **K2** and **K3** = Simulation model orders, K_1, K_2, K_3.
  PMIN, **PMAX** = Minimum and maximum simulation model periods

  - Let's run some **live tests**

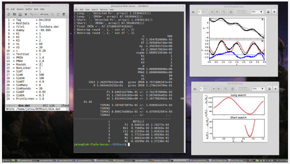

Many simulated models (Paper I)

- **Many simulated models** having random signal frequencies
  $\rightarrow$ Used to create artificial **simulated data**
- **Test**: Can DCM analysis of **simulated data** retrieve known **simulation model** input parameters?
- K_1 simulated $f_i^{\star}$ frequencies drawn from a uniform random distribution

$$U(f_{\mathrm{min}}, f_{\mathrm{max}}, K_1) \tag{25}$$

between $f_{\mathrm{min}} = 1/P_{\mathrm{max}}$ and $f_{\mathrm{max}} = 1/P_{\mathrm{min}}$, where $P_{\mathrm{min}} = 1$ and $P_{\mathrm{max}} = 2$.

Many simulated models (Paper I)

- Rearranged into decreasing order $f_1^\star > f_2^\star ... > f_{K_1}^\star$
  $\rightarrow \bar{\beta}_I^\star = [f_1^\star, f_2^\star ..., f_{K_1}^\star]$ **for simulated $g(t)$ model**
- **Other free parameters** of simulated $g(t)$ model drawn from a uniform random distribution

$$U(-0.5, +0.5, K_1 \times 2K_2 + K_3 + 1) \qquad (26)$$

  - **Random values** of $K_1 \times 2K_2$ amplitudes $B_{1,1}^\star$, $C_{1,1}^\star$, ..., $B_{K_1,K_2}^\star$, $C_{K_1,K_2}^\star$ of simulated $h_i(t)$ signals
  - **Random values** of $K_3 + 1$ values for $M_0^\star, ..., M_{K_3}^\star$ of coefficients of simulated $p_k(t)$
  - The above two give $\bar{\beta}_{II}^\star$ **for simulated $g(t)$ model**
- **All simulated $g(t)$ model free parameters are**

$$\bar{\beta}^\star = [\bar{\beta}_I^\star, \bar{\beta}_{II}^\star]$$

Many simulated models (Paper I)

- $n^\star = 500$ **time points of simulated data** $t_i^\star$ drawn from uniform random distribution $U(0, \Delta T, n^\star)$ between 0 and $\Delta T = 4$ (see Eq. 21)
- Chosen signal to noise ratio $\mathrm{SN} = 100$ gives **accuracy of simulated data** $\sigma_m = 2^{5/2} s_y^\star / \mathrm{SN}$ of simulated data, where $s_y^\star$ is standard deviation of all $g(t_i^\star)$ (see Eq. 22).
- $n^\star = 500$ **errors of simulated data** $\sigma_i^\star$ drawn from Gaussian distribution $N(m^\star, s^\star, n^\star)$, where $m^\star = 0$ and $s^\star = \sigma_m$ (see Eq. 23)
- **Simulated data** are

$$y_i^\star = g(t_i^\star, \bar{\beta}^\star) + \sigma_i^\star. \quad (27)$$

Many simulated models (Paper I)

- Thirty samples of simulated simulates data created with three signal model 18 ($K_1 = 3, K_2 = 1, K_3 = 1$)
- Sample size $n^\star = 500$, signal to noise ratio is $\mathrm{SN} = 100$
- **Diamonds** highlight frequencies and amplitudes

$$f_{\mathrm{i,sim}} - f_{\mathrm{i+1,sim}} < f_{\mathrm{crit}}(f_{\mathrm{max}} - f_{\mathrm{min}}), \quad (28)$$

  where $f_{\mathrm{crit}} = 0.05$ (i.e. differ less than $\pm 5\%$)
- These models may suffer from
  Dispersing amplitudes
  Intersecting frequencies
  $\rightarrow$ Simulated frequencies **more difficult to detect**
- This effect seen in Fig. 11 of **Paper I**

Many simulated models **(Paper I)**

- **Circles** highlight frequencies and amplitudes

$$A_i/A_{\mathrm{max}} < A_{\mathrm{crit}}, \tag{29}$$

  where $A_{\mathrm{crit}} = 0.5$ and A_{max} is highest of all signal amplitudes A_i ($i = 1, 2, 3$).
- At least one signal two times weaker than strongest signal
- Weak signals difficult to detect
- This effect also seen in Fig. 11 of **Paper I**

30 three signal simulations **Fig. 11** (Paper I)

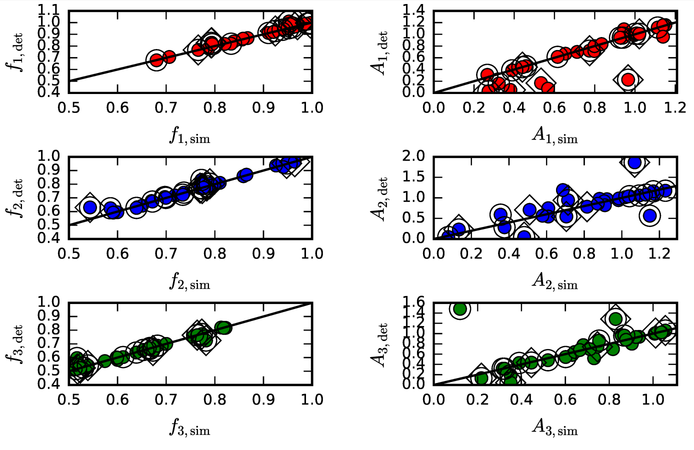

- Simulated frequencies (x-axis), Detected frequencies (y-axis), Equal values (diagonal line) **Perfect!**

Many simulated models (Paper I)

Relative error **between simulated and detected**

$$\sigma_{f_i,\mathrm{rel}} = |f_{\mathrm{i,det}} - f_{\mathrm{i,sim}}|/f_{\mathrm{i,sim}}. \quad (30)$$

Detection error of $f_{\mathrm{i,det}}$ relative to simulated $f_{\mathrm{i,sim}}$

Paper I, Table 5: 100 simulated three signal models

		$n^\star = 500, \mathrm{SN} = 100$			
Line	Samples	$\sigma_{f_1,\mathrm{rel}}$	$\sigma_{f_2,\mathrm{rel}}$	$\sigma_{f_3,\mathrm{rel}}$	m
1	All	0.012	0.029	0.0090	100
2	Eq. 28	0.0085	0.013	0.0065	69
3	Eqs. 28 and 29	0.0030	0.011	0.0051	48
		SN doubled: $n^\star = 500, \mathrm{SN} = 200$			
Line	Samples	$\sigma_{f_1,\mathrm{rel}}$	$\sigma_{f_2,\mathrm{rel}}$	$\sigma_{f_3,\mathrm{rel}}$	m
4	All	0.0039	0.014	0.011	100
5	Eq. 28	0.0036	0.0083	0.0082	76
6	Eqs. 28 and 29	0.0019	0.0036	0.0032	37
		$n^\star$ doubled: $n^\star = 1000, \mathrm{SN} = 100$			
Line	Samples	$\sigma_{f_1,\mathrm{rel}}$	$\sigma_{f_2,\mathrm{rel}}$	$\sigma_{f_3,\mathrm{rel}}$	m
7	All	0.010	0.019	0.0050	100
8	Eq. 28	0.0064	0.015	0.0049	77
9	Eqs. 28 and 29	0.0034	0.0077	0.0041	40

Many simulated models (Paper I)

Conclusion: DCM detects **correct frequencies** when

1. Signal frequencies are **not too close** (Eq. 28).
2. **None** of the signal amplitudes is **too weak** (Eq. 29).
3. Sample **size** n and **signal to noise ratio** SN are **sufficient** (Table 5).

- **If correct frequencies** are detected
  $\rightarrow$ Remaining other model parameters also correct, because **linear modelling** is always **unambiguous**
- Failing to detect even **one correct frequency**
  $\rightarrow$ Period analysis fails

DCM $\rightarrow$ DFT **Figure: @www.quotemaster.org**

- Next slide about **Discrete Fourier Transform**

DFT sinusoid parameters

- DFT model is a pure sinusoid ($K_2 = 1$)
- **Analytical solutions** for sinusoid amplitude, minimum and maximum, as well as error estimates, are **relatively tedious!**
  ExerciseCosineOne ☠ **(A2023)**
- **Numerical Monte Carlo or bootstrap solutions** for sinusoid amplitude, minimum and maximum, as well as error estimates, are **easy!**
  ExerciseCosineTwo ☠ **(A2023)**
- Solutions for amplitudes, minima and maxima for higher $K_2 > 1$ orders would be **extremely tedious!**
  $\rightarrow$ **Numerical bootstrap solutions** are **easy!**

DFT → DCM Figure: @www.quotemaster.org

- Back to **Discrete Chi-square Method (DCM)**

Real use case (Paper I)

Note: New Sect. 5. “Real use case”

- **Data**: Observed (O) minus Computed (C) primary eclipse epochs of binary XZ And
- **Preliminary results**
- Two clear periodogram minima (**Paper I**: Fig. 12)
- Two periods $P_1 = 13418^{\mathrm{d}} = 37^{\mathrm{y}}$ and $P_2 = 32192^{\mathrm{d}} = 88^{\mathrm{y}}$ (**Paper I**: Fig. 13)
- More detailed **final analysis** O-C data of XZ And was published in [14]Jetsu (2020, **submitted**)
  $\rightarrow$ The above detailed analysis not presented here.

Real use case Paper I

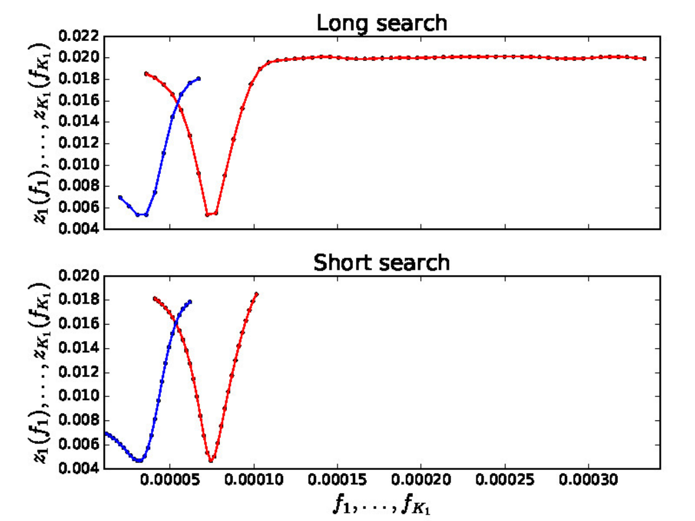

Real use case Paper I

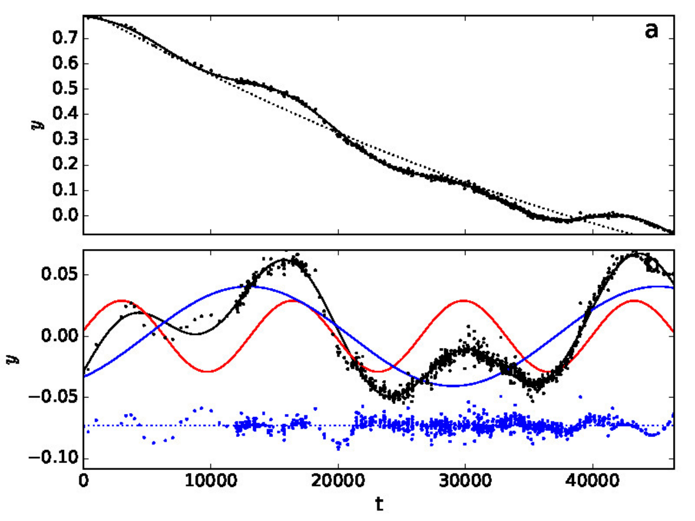

Discussion **(Paper I)**

- **Note**: New Sect. 6. “Discussion”

1. Main point of DCM

- Periodic **non-linear** models become **linear** when grid of constant tested frequencies are fixed

$\rightarrow$ All analysis results become unambiguous

$\rightarrow$ DCM success “full proof”

$\rightarrow$ General numerical **solution for any** non-linear $g(t, \bar{\beta})$ model

$\rightarrow$ **General** means that **non-linear model** may be

- periodic
- aperiodic
- combination of periodic and aperiodic

Discussion (Paper I)

Simple recipe for solving **any non-linear model**

1. **Divide** free parameters $\bar{\beta}$ to two parts:

   a: Those that make model **nonlinear** = $\bar{\beta}_I$
   b: Rest of free parameters = $\bar{\beta}_{II}$

2. **Fix** tested $\bar{\beta}_I$ grid.
3. **Test all** reasonable linear models.
4. **Identify** best model among these models.
5. **Solve** model parameter errors with **bootstrap**

- DCM **in particular**
  Free parameters $\bar{\beta}_I =$ Frequencies
  Free parameters $\bar{\beta}_{II} =$ Rest of free parameters
  Best model identified with Fisher-test

Discussion (Paper I)

2. Main point of DCM

Idea: *"Whatever the correct real frequency values may be, they can always be rearranged into a decreasing order."*

- **Symmetry** of z in K_1-dimensional frequency space
  $\rightarrow$ For many signals, **symmetry** eliminates **"search for a needle in a haystack"** effect (e.g. Six signals have $K_1! = 6! = 720$ symmetries = identical solutions)
  $\rightarrow$ **symmetry** allows testing of **only** $f_1 > f_2 > ... > f_{K_1}$ frequency combinations
  $\rightarrow$ $K_1! - 1$ **other** alternative combinations irrelevant

Problem: **Plotting** $K_1 > 2$ periodograms?

Solution: **Plot one-dimensional slices** crossing solution for **all best frequencies**.

Discussion (Paper I)

Other points of DCM

Steep periodogram minima (e.g. **Paper I**: Fig 2)

- If tested frequency grid **adequately dense**
  $\rightarrow$ Accurate best frequency values obtained even **before** non-linear iteration of Eq. 18.
  $\rightarrow$ No need for **too dense** tested grid!

No sudden jumps in periodograms

- **Strong correlation** between χ^2 and R values for tested frequencies close to each other
  $\rightarrow$ **Linear models** give stable, smooth and unambiguous $z_i(f_i)$ periodograms
  $\rightarrow$ **"No escape"**(No alternative best frequency solutions) from these continuous periodograms
  $\rightarrow$ Again, no need for **too dense** tested grid!

Discussion (Paper I)

Non-linear iterations

- **Dense** tested frequency grids give **accurate** results for best frequencies

  $\rightarrow$ **Non-linear iteration** of Eq. 18 not always needed

  $\rightarrow$ **Non-linear iteration** not done if **NonLinear** $\neq$ **1**

- Letter “D”=”Discrete” in **DCM** abbreviation

  - Method is **Discrete** only when **NonLinear** $\neq 1$

  - Method is **Continuous** when **NonLinear** $= 1$

  $\rightarrow$ “C”=”Continuous” Chi-square Method = **CCM**?

Parameter correlations

- **Correct model** bootstrap shows signal frequency and amplitude estimate **correlations** (Fig. 4)

  $\rightarrow$ **If one** estimate shifts away from correct value, **then other** estimates compensate this shift

Discussion (Paper I)

Too sparse tested frequency grid

- **Shifts** may mislead DCM analysis

Dense tested frequency grid

- DCM detects correct best frequencies
- **Computation time** proportional to number of tested frequency combinations: $n_{\mathrm{L}}^{K_1}$ and $n_{\mathrm{S}}^{K_1}$
  $\rightarrow$ Detecting many signals takes long **computation time** (e.g. **Paper I**: Figs. 5-7: three days)
  $\rightarrow$ **"Wasted" computation time** irrelevant if **correct** frequencies detected (e.g. **expensive** satellite data)
  $\rightarrow$ **Unambiguous correct** results for all other model parameters

Discussion (Paper I)

Correct model identication: Fisher-test

- **Correct model 19** has $p = 12$ free parameters
- **All fifteen models** having less than $p = 12$ free parameters have Fisher-test $Q_F < 10^{-16}$
  $\rightarrow$ Data must contain **at least three signals**
- **All remaining sixteen $p \geq 12$ models** have χ^2 and/or Q_F values confirming that model 19 is the best
- **Fifteen failed models** having
  "Intersecting frequencies" (**Paper I**: Eq. 28)
  "Dispersing amplitudes" (**Paper I**: Eq. 29)
  could have been rejected **without**
  even comparing their χ^2 and/or Q_F
  $\rightarrow$ All four signal models fail
  $\rightarrow$ Data must contain **less than four signals**

Discussion (Paper I)

Argument missing from Paper I

- Data must contain **at least three signals**
- Data must contain **less than four signals**
- Only possible case: Data **contains three signals**

Problems with double waves $K_2 = 2$

- Spare you from unnecessary details

1a,1b. **Correct** period P and/or $P/2$

1c. **Correct** model period P and/or $P/2$

2. **Single** model analysis probably fails. Must compare **many** models.
3. **Quality** (σ_i) and **quantity** (n) of data
4. **Computational aspect**: $K_2 > 2$ bootstrap minimum and maximum epoch estimates complicated

Discussion (Paper I)

Cases that DCM solves more directly than DFT

1. **One** signal data **without trends**

   DFT: **Finds** correct period. **Models** data with a sinusoid having this period.

   DCM: **Directly** models data with $g(t, 1, 1, 0)$.

2. **One** signal data **with trends**

   DFT: **Remove** trend. **Find** correct period. **Model** detrended data with a sinusoid having this period.

   DCM: **Directly** models $g(t, 1, 1, K_3)$ for any K_3:th order polynomial trend.

3. **Many** signal data **with trends**

   DFT: **Remove** trend. **Pre-whitening** gives periods. **Model** detrended data with these periodic sinusoids.

   DCM: **Directly** models any number of signals superimposed on any arbitrary trend.

Discussion

- Additional discussion from **Paper II** (Sects. 3 and 6.6)
  - DCM is designed for **periodicity detection**
    $\rightarrow$ DCM gives no **direct** S significance estimates for detected periods and models
    $\rightarrow$ This may lead to **overfitting**
    $\rightarrow$ DCM does not account for this *"Look-elsewhere Effect"* ([28]Miller 1981, [3]Bayer & Seljak 2020)
- *"Look-elsewhere Effect"*:
  - *"DCM searches for the correct model over a vast free parameter space. This increases the probability for finding apparently significant signals."*
    $\rightarrow$ Detected signals and models may be **spurious**
  - DCM gives no **direct** S significance estimates, like e.g. the method by [3]Bayer & Seljak 2020)

Paper II discussion continues ...

- DCM can not address *"Look-elsewhere Effect"*, **but** this **does not mislead** DCM analysis results:
  1. Fisher-test **prevents overfitting** and **gives indirect** Q_F significance estimates
     $\rightarrow$ **Correct number of signals** detected with $\gamma_F = 0.001 = 1/1000$ pre-assigned significance
     $\rightarrow$ Most signals detected at $Q_F < 10^{-16}$ level
     $\rightarrow$ Their detection is **absolutely certain!**
  2. DCM periodograms show **no sudden "jumps"**
     $\rightarrow$ **Number of tested periods** does not alter detected periods or models (No trial factor effect)
  3. **Paper II**: After exploring numerous alternative models, the simplest alternative $K_3 = 1$ is the best
  4. **Paper II**: DCM **predictions succeed**
     $\rightarrow$ Periods and models can not be **spurious**

Paper II (Fig. 2: DCM prediction)

- **Model** for 1782-2007 data **predicts** 2008-2018 data
- **Model** is linear trend and five signals

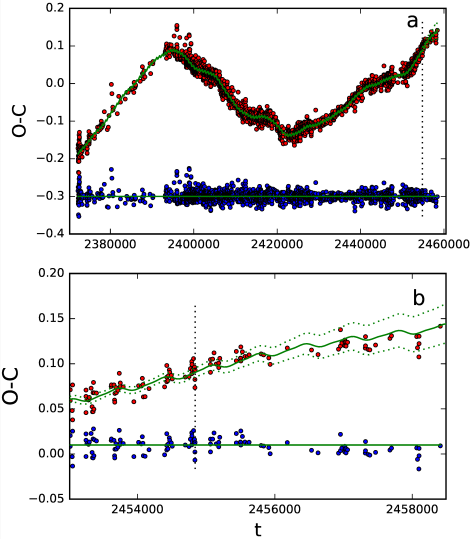

Conclusions (Paper I)

Note: New Sect. 7 "Conclusions"

- **DFT** signal detection **unambiguous** only if
  1. Correct model is a **sinusoid**.
  2. Data contains **no trend**.
- **DCM** **unambiguously** detects **any** number of **signals** superimposed on **any** arbitrary **trend**.
- **DCM** model $g(t) = h(t) + p(t)$

  Periodic $h(t)$ contains signals, **repeats itself**

  Aperiodic $p(t)$ contains trend, **does not repeat itself**
- **DCM** model **non-linear**

  Tested frequencies fixed.

  $\rightarrow$ Model becomes **linear**

  $\rightarrow$ Linear models give **unambiguous** results.

Conclusions (Paper I)

- **DCM** based on **brute numerical approach**.

1. **Tests** all possible free parameter values for all reasonable linear models
2. **Identifies** best model among all alternative models
3. **Detects** correct frequencies

   When frequencies not too close (Eq. 28)
   When none of signals is too weak (Eq. 29)
4. **Correct frequencies** $\rightarrow$ Rest is **unambiguous**.

- **Free** DCM python code **dcm.py** in Xenodo
- **DFT** most frequently applied period finding method $\rightarrow$ Tedious comparison between **DCM** and **DFT** left **to next studies** (Diplomatic decision: No controversy)

Paper I completed!

Future

- Tedious **DFT and DCM** comparison
- Before entering this swamp, maze, mountain, ...
  $\rightarrow$ Cristal clear plan required. Preliminary version:
  - Detrending
  - Frequencies f_1 and f_2 detection limit f_0
  - One frequency f detection limit $\Delta T = f_0^{-1}$
  - Combinations of above three
  - More than two frequencies
- **Absurd work dilemma**
  "The Myth of Sisyphus"
  (Albert Camus)

How would you apply DCM?

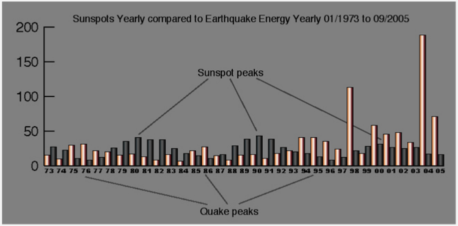

Left: @depositphotos.com, Right: @jupitersdance.com

How would you apply DCM to any phenomenon? What kind of data file and test statistic would you use?

- If you had observing times t_i and observations y_i, but you would **not have error estimates** σ_i.
- If you had observing times t_i, observations y_i, and you would **also have error estimates** σ_i.

Abstract (Paper II)

Say hello to Algol's new companion candidates

Constant orbital period ephemerides of eclipsing binaries give the computed eclipse epochs (C). These ephemerides based on the old data can not accurately predict the observed future eclipse epochs (O). Predictability can be improved by removing linear or quadratic trends from the O-C data. Additional companions in an eclipsing binary system cause light-time travel effects that are observed as strictly periodic O-C changes. Recently, Hajdu et al. estimated that the probability for detecting the periods of two new companions from the O-C data is only 0.00005. We apply the new Discrete Chi-square Method (DCM) to 236 years of O-C data of the eclipsing binary Algol (β Persei). We detect the tentative signals of at least five companion candidates having periods between 1.863 and 219.0 years. The weakest one of these five signals does not reveal a "new" companion candidate, because its 680.4 ± 0.4 days signal period differs only 1.4σ from the well-known 679.85 ± 0.04 days orbital period of Algol C. We detect these same signals also from the first 226.2 years of data, and they give an excellent prediction for the last 9.2 years of our data. The orbital planes of Algol C and the new companion candidates are probably co-planar, because no changes have been observed in Algol's eclipses. The 2.867 days orbital period has been constant since it was determined by Goodricke.

Introduction (Paper II)

Short modern history of variable stars

1. **Mira**
   Fabricius 1596: variability
   Holwarda 1638: 11 months period
   Pulsations: **expands and contracts**
2. **Algol**
   Montanari 1669: variability
   Goodricke 1783: 2.867 days period
   Eclipsing binary
   - 10h **primary eclipse**: observable with **naked eyes**
   - **Secondary eclipse**: observable only with telescope

We have revised this history: Ancient Egyptians **detected Algol's variability and periodicity** three millennia earlier.

Introduction (Paper II)

John Goodricke (17 September 1764 - 20 April 1786)

Introduction (Paper II)

- In 3 hours, Algol becomes **dimmer** than all six ∗ & •
- For 4 hours, Algol the **dimmest**
- In 3 hours, Algol becomes **brighter** than all six ∗ & •
- **Goodricke's** discovery:
  - **Tabulated** eclipse epochs

  → Epochs **multiples** of 2.867^{d}

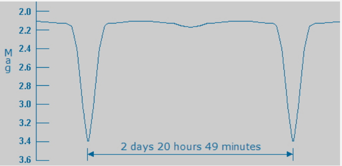

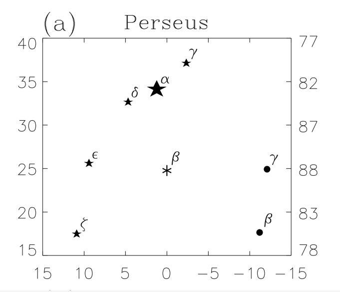

★	α Per	$1.^{\mathrm{m}}79$
∗	β Per	$2.^{\mathrm{m}}12 \leftrightarrow 3.^{\mathrm{m}}37$
⋆	ζ Per	$2.^{\mathrm{m}}85$
⋆	ϵ Per	$2.^{\mathrm{m}}88$
⋆	γ Per	$2.^{\mathrm{m}}93$
⋆	δ Per	$3.^{\mathrm{m}}01$
•	γ And	$2.^{\mathrm{m}}26$
•	β Tri	$3.^{\mathrm{m}}00$

(Upper figure: @nightskyinfo.com)

- **Whole 10h eclipse** observed **only** every 19th night.

Introduction **(Paper II)**

Ancient Egyptian **"Calendar of Lucky and Unlucky days"** in Papyrus Cairo 86637

- **Written** by Ancient Egyptian **scribes**
- **Dated** to 1271-1163 B.C.
- **Prognoses**: **Lucky** = Good and **Unlucky** = Bad
- **One year**: **Three prognoses** for each day
- Additional prognosis **descriptive texts**
- **"Hour-watchers"** measured **time from stars** for religious purposes
  → **Describe** astronomical and mythological events
  → **Thousands of years**: 300 clear nights every year
- **Descriptions** of other events: Flood of Nile, weather, seasons, human activity, animals, ...

Periods: 29.6 days (Moon) and 2.850 days (Algol)

Introduction (Paper II)

- Daytime and night-time: **12 hours**
- Scribes called **“hour-watchers”** measured night-time with **hour-stars**
- This required at least **three stars in 24 hour-patterns** (72 stars)
- **Algol** 51st brightest star in Ancient Egypt
- **Algol** was an hour-star or belonged to an hour-star pattern

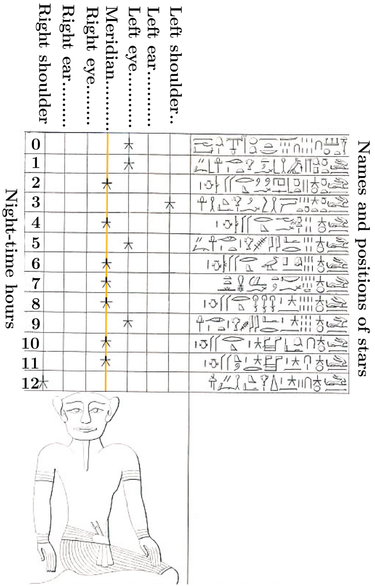

Introduction (Paper II)

Algol was called "Horus" (inside small rectangle)

Introduction (Paper II)

Details of Algol's 2.850 days period discovery:

- [31] **Porceddu et al. (2008),** "Evidence of Periodicity in Ancient Egyptian Calendars of Lucky and Unlucky Days", **Cambridge Archaeological Journal**
- [21] **Jetsu et al. (2013),** "Did the Ancient Egyptians Record the Period of the Eclipsing Binary Algol—The Raging One?", **The Astrophysical Journal**
- [20] **Jetsu & Porceddu (2015),** "Shifting Milestones of Natural Sciences: The Ancient Egyptian Discovery of Algol's Period Confirmed", **Plos One**
- [30] **Porceddu et al. (2018),** "Algol as Horus in the Cairo Calendar: The Possible Means and the Motives of the Observations", **Open Astronomy**

Introduction **(Paper II)**

Light time effect

- Computed times of eclipsing binary (EB) eclipses
  $C = t_0 + i\, P_{\mathrm{orb}},$
  where t_0 is zero epoch and i is an integer
- **Third body:**
  $\rightarrow$ Eclipses occur **earlier** when EB **approaches**
  $\rightarrow$ Eclipses occur **later** when EB **recedes**
  $\rightarrow$ O = Observed eclipse epochs differ from C = Computed epochs
  $\rightarrow$ O-C data may reveal **third, fourth, ... bodies**

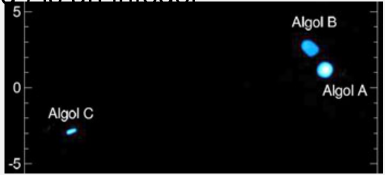

- **Figure: CHARA interferometer image of Algol**
- Algol C was detected from Algol A-B **radial velocity changes**, not from Algol A-B **puzzling O-C changes**.

Introduction (Paper II)

- Ancient Egyptians discovered **Algol A** and **Algol B**
- Goodricke (1783)[9] re-discovered Algol's period

  Data: Visual photometric observations

  Period: 2.867 days
- [5] Curtiss (1908) discovered **Algol C**

  Data: Radial velocities of Algol A-B system

  Period: 1.9 years
- **Paper II**: Jetsu (2021)[16] **discovers Algol D, Algol E, Algol F, Algol G and Algol H** companion candidates, and **re-discovers Algol C**

  Data: Observed minus Computed (O-C) eclipse epochs of Algol during past 237 years

  Periods: 1.9, 20.0, 27.8, 33.7, 66.4 and 219.0 years

Introduction (Paper II)

- Most probable causes for **periodic O-C** in **Eclipsing Binaries (EBs)**
  - A third body, e.g. Li et al. 2018)[26]
  - A magnetic activity cycle, e.g. Applegate 1992)[1]
  - An apsidal motion, e.g. Borkovits et al. (2005)[4]
- **Direct** interferometric images of Algol A, Algol B and Algol (Zavala et al. (2010)[39], Baron et al. (2012)[2])

  $\rightarrow$ **Presence of third body** (Algol C) in eclipsing binary Algol AB certainly confirmed

  $\rightarrow$ **Accurate known period** for Algol C
- **Detection of third and fourth body** in O-C **sample of other 80 000 EBs** (Hajdu et al. 2019)[10]
  - 992 third body systems
  - only 4 fourth body systems ($4/80\,000 = 0.00005$)

Introduction (Paper II)

Paper I: Preliminary DCM analysis of O-C data of **XZ And**: Discovery of **third and fourth body**

$\rightarrow$ 3rd, 4th, ... bodies more common than 0.00005

- **Mass transfer** from less massive Algol B ($0.8 m_{\odot}$) to more massive Algol A ($3.7 m_{\odot}$)

  $\rightarrow$ **Should** cause $P_{\rm orb}$ **period increase**

  - **No clear** long-term $P_{\rm orb}$ increase in Algol since 1783!

  $\rightarrow$ **Should** cause **quadratic** long-term O-C changes

  - **No clear** quadratic O-C changes in Algol since 1783!

- Algol in Cairo Calendar (Jetsu et al. 2013)[21]
  - Algol's period 2.850 days **1224 B.C.**
  - Algol's period 2.867 days **today**
  - Could **mass transfer** explain 0.017 days **period increase** during past three thousand years?

Introduction (Paper II)

- Equation of **mass transfer** (Kwee 1958)[23]

$$\frac{\dot{P}_{\mathrm{orb}}}{P_{\mathrm{orb}}} = -\frac{3\dot{m}_B\left(m_A - m_B\right)}{m_A m_B}$$

$\dot{P}_{\mathrm{orb}}$ = period change
$\dot{m}_B$ = mass transfer from Algol B to Algol A

- Constant **period increase** from 2.850 days to 2.867 during three thousand years gives period change $\dot{P}_{\mathrm{orb}}$ $\rightarrow$ **mass transfer** $\dot{m}_B = -2.2 \times 10^{-7} M_{\odot}\mathrm{yr}^{-1}$
- Best evolutionary model by Sarna (1993)[33] **predicted!** $\dot{m}_B = -2.9 \times 10^{-7} M_{\odot}\mathrm{yr}^{-1}$
- **Main result:** **Mass transfer** could explain 0.017 days increase of Algol's period during past three millennia

Introduction (Paper II)

Modern observations since Goodricke (1783)[9]

- Only negative and positive **alternating** O-C changes
  → **Irregular** small period **increase** and **decrease**
- **Algol C**
  → **Low amplitude** 1.9 year O-C changes
- **Quasiperiodic** activity cycles (Applegate 1992)[1]
  → **High amplitude** 30 and 200 years O-C changes
- **Past century**: Presence of **more than three members** in Algol system claimed in many studies
  → **Only three stars** (Friesboes-Conde et al. (1970)[8]

Main conclusion: Since Goodricke (1783), no one has explained Algol's puzzling O-C changes

→ **Mixture** of unknown **signals** and arbitrary **trends**
→ Ideal case for DCM analysis!

Data (Paper II)

Note: New section 2. "Data" (**O-C** observations)

C = Computed epochs

- **Ephemeris**

$$\mathrm{HJD}\ 2445641.5135 + 2.86730431\mathrm{E}. \qquad (1)$$

- **Predicts** primary eclipses at multiples $\mathrm{HJD}\ 2445641.5135 + E \times P_{\mathrm{orb}}$
- Orbital period $= P_{\mathrm{orb}} = 2.^{\mathrm{d}}86730431$
- Integer number $= E$

O = Observed primary and **secondary** minimum epochs from TIDAK database ($n = 2238$)

- November 12th, 1782 - October 18th, 2018
- All 14 **secondary** minima rejected ($n \rightarrow 2224$)
- Many techniques (visual, plates, fotometer, CCD, ...)
- Accuracy increases towards modern times

Data (Paper II)

Algol's puzzling O-C changes (TIDAK database)

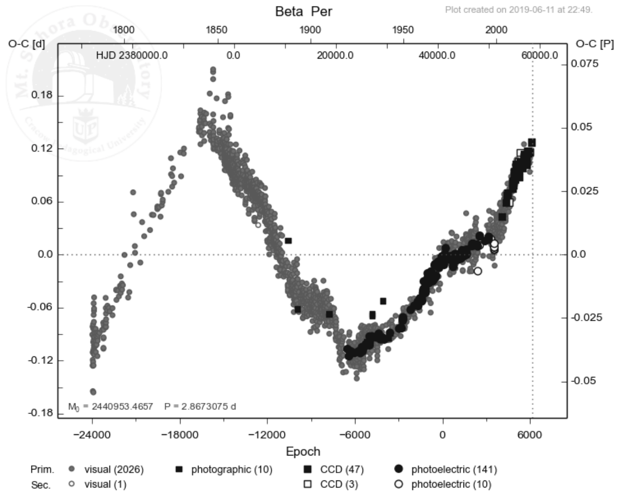

Data (Paper II)

- Epheremeris (Eq. 1) prediction is quite **accurate**
  - During 236 years the difference between observed and computed eclipse epochs has been $-0.^{\mathrm{d}}24 < \mathrm{O} - \mathrm{C} < +0.^{\mathrm{d}}15$
- **Errors unknown** for **all** individual O-C values

  $\rightarrow$ Data file: **Arbitrary** errors $\sigma_i = 0.^{\mathrm{d}}00010$ in third column of **file1**

  $\rightarrow$ DCM **test statistic** z computed from **sum of squared residuals** R (**Paper I**: Eqs. 9 and 11)

  $\rightarrow$ All observations have same weight

  $\rightarrow$ Presented DCM analysis results for Algol **do not depend on** O-C data errors

  - **Referee comment**: Test some case, where accuracy increases towards modern times

    $\rightarrow$ "Can do": Detected periods remained the same

Method (Paper II)

- **Note**: New Sect. 3 "Method"
- Time span $\Delta T = t_n - t_1$ mid point $t_{\mathrm{mid}} = t_1 + \Delta T/2$
- Model $g(t) = h(t) + p(t)$ **aperiodic** polynomial part

$$p(t) = p(t, K_3) = \sum_{k=0}^{K_3} p_k(t)$$

Paper I, Eq. 20: $T(t) = \frac{2t}{\Delta T}$, where $T(t) \geq 0$

$$p_k(t) \;=\; M_k T^k(t) = M_k \left[\frac{2t}{\Delta T}\right]^k$$

Paper II, Eq. 6: $T(t) = \frac{2(t - t_{\mathrm{mid}})}{\Delta T}$, where $-1 \leq T(t) \leq 1$

$$p_k(t) \;=\; M_k T^k(t) = M_k \left[\frac{2(t - t_{\mathrm{mid}})}{\Delta T}\right]^k$$

Method (Paper II)

- **Paper I** (Eq. 20) formulation of $p_k(t)$
  $\rightarrow$ For **all** k values, $p_k(t)$ can **only increase or decrease monitonically** inside ΔT interval
- **Paper II** (Eq. 6) formulation of $p_k(t)$
  $\rightarrow$ For all **uneven** k values, $p_k(t)$ can **only increase or decrease monitonically** inside ΔT interval
  $\rightarrow$ For all **even** k values, $p_k(t)$ **both increase and decrease** inside ΔT interval
  $\rightarrow$ Greater model flexibility!
- **Check:** Both $p(t)$ formulations give the same results for **TestData.dat**, but the latter is more flexible

Method (Paper II)

- DCM formulation practically the same as in **Paper I**
  $\rightarrow$ **Method not explained** here again
- **Minor improvements** of **dcm.py** code
  1. **Notes:** Prints and stores notes, like

     ```
     Long search: 1 period at edge
     Long search: 2 period at edge
     1 and 2 frequencies intersect
     ```
  2. **Figures:** No need to add back zero epoch t_0
  3. **Figures:** Signals separately, in time and in phase
  4. **Figures:** Marks minima, expands outside long search interval, if necessary (edges).
  5. **Files:** new ones: data, model, curves, ...
- This improved version is **dcm2.py** (Home-page)

Method (Paper II)

- **Unstable models** denoted with "Um" in text and tables of **Paper II**
- **Reasons** for **unstable** models denoted in text and tables of **Paper II**

  "Ad" = Dispersing amplitudes = Amplitudes and/or amplitude errors disperse

  "If" = Intersecting frequencies = At least two model frequencies are too close to each other
- **... period at edge**
  - DCM searches for periods slightly below P_{min} or above P_{max} long search limits
  - These cases denoted with "Lp"
  - Such DCM models are not unstable ("Um")

Third body O-C Changes (Paper II)

Geometry of third body orbit (New section 4)

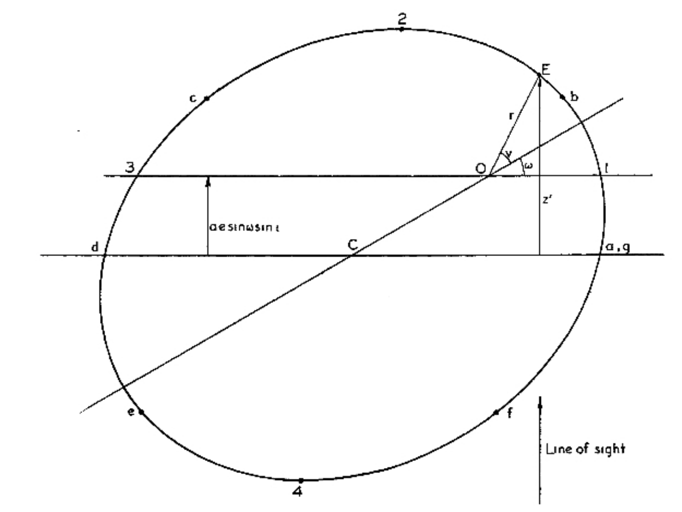

Third body O-C Changes (Paper II)

- **Third body** light time effect [12](Irwin 1952)

$$(\mathrm{O}-\mathrm{C}) = K \frac{1}{\sqrt{(1-e^2\cos^2\omega)}}\left[\frac{1-e^2}{1+e\cos\nu}\sin(\nu+\omega)+e\sin\omega\right] \quad (13)$$

$$K = \frac{a\ \sin i\sqrt{1-e^2\cos^2\omega}}{173.15} \quad (14)$$

- Third body orbit **semimajor axis** ($[a] = \mathrm{AU}$)
- **Inclination** of third body orbital plane ($[i] = \mathrm{rad}$)
- **Eccentricity** of third body orbit (e)
- Third body **periastron longitude** ($[\omega] = \mathrm{rad}$)
- Third body **true anomaly** ($[\nu] = \mathrm{rad}$)
- **Amplitude** of light time effect ($[K] = \mathrm{d}$)

$$K = A/2 \quad (15)$$

- **Peak to peak amplitude** of O-C changes ($[A] = \mathrm{d}$)

Third body O-C Changes (Paper II)

- Computation of $t \rightarrow \nu(t)$ **time dependence**

True anomaly (**uneven** pace in time) computed from Fourier expansion

$$\nu(t) = M(t) + (2e - \frac{1}{4}e^3)\sin M(t) + \frac{5}{4}e^2 \sin 2M(t) + \frac{13}{12}e^3 \sin 3M(t) + O(e^4), \quad (16)$$

where $O(e^4)$ refers to omitted fourth order terms

Mean anomaly (**even** pace in time) computed from

$$M(t) = \frac{2\pi(t - t_p)}{P_{\mathrm{orb}}}, \quad (17)$$

where t_p is pericentre epoch

Third body O-C Changes (Paper II)

$A =$ Peak to peak amplitude of O-C changes **in days**

$p =$ Period of these changes **in days**

- **If** third body orbit is **circular** $(e = 0)$, the mass function is

$$f(m_3) = \frac{(m_3 \sin i)^3}{(m_1 + m_2 + m_3)^2} = \frac{[173.15(A/2)]^3}{p^2}, \quad (18)$$

where m_1 and m_2 are the masses of EB

- For such circular orbits, **semi-major axis** of m_3

$$a_3 = a\frac{(m_1 + m_2)}{m_3}, \quad (19)$$

where $a = 173.15(A/2)/\sin i$ **Here: 14.11.2022**

- Here is one exercise of how A and p give m_3

ExerciseMasses ☠ **(A2022)**

Third body O-C changes

- **Submitted** Algol paper to ApJ (**Paper II**)
  - Based on **circular** orbit $e = 0 \equiv K_2 = 1$ **assumption**
  - Referee did not question this assumption
- A bit later, **submitted** XZ And paper to JAAVSO
  - Based on **circular** orbit $e = 0 \equiv K_2 = 1$ **assumption**
  - $\rightarrow$ Referee: If orbit **eccentric** $e > 0$, what would be DCM analysis results?
  - $\rightarrow$ Decided to solve this problem already in **Paper II**, although the referee did not ask about this
  - $\rightarrow$ Results more general in **Paper II**, and it will be easier to get JAAVSO paper published
- Subject of many next slides
  - Are **circular** and **eccentric** analyses connected?
  - What are those logical connections?
  - Can both analyses show that results are correct?

Appendix (Paper II)

- O-C changes **when** $e > 0$

$$(\mathrm{O}-\mathrm{C})_{e>0} = K \frac{1}{\sqrt{(1-e^2\cos^2\omega)}} \left[\frac{1-e^2}{1+e\cos\nu} \sin(\nu+\omega) + e\sin\omega \right]$$

- For these **eccentric** $e > 0$ orbits, suitable DCM model order is $K_2 = 2$ (Hoffman et al. 2006)[11]
- O-C changes **when** $e = 0$

$$(\mathrm{O}-\mathrm{C})_{e=0} = K\sin(\nu+\omega)$$

- For these **circular** $e = 0$ **purely sinusoidal** orbits, suitable DCM model order is $K_2 = 1$
- Both $(\mathrm{O}-\mathrm{C})_{e>0}$ and $(\mathrm{O}-\mathrm{C})_{e=0}$ have **the same peak to peak amplitude** $A = 2K$

Appendix (Paper II)

- **Eccentric** and **circular** orbit O-C curve **difference**

$$(\mathrm{O}-\mathrm{C})_{\mathrm{diff}} = (\mathrm{O}-\mathrm{C})_{e>0} - (\mathrm{O}-\mathrm{C})_{e=0}$$

  has a **peak to peak amplitude** A_{diff}

- **Amplitude ratio** is

$$\Delta A = A_{\mathrm{diff}}/A$$

- Two first minimum ($t_{\mathrm{1st.min}}$,$t_{\mathrm{2nd.min}}$) and maximum ($t_{\mathrm{1st.max}}$,$t_{\mathrm{2nd.max}}$) epochs of $(\mathrm{O}-\mathrm{C})_{\mathrm{diff}}$ curve give **phase differences**

$$\Delta\phi_{\mathrm{min}} = (t_{\mathrm{2nd.min}} - t_{\mathrm{1st.min}})/p$$
$$\Delta\phi_{\mathrm{max}} = (t_{\mathrm{2nd.max}} - t_{\mathrm{1st.max}})/p,$$

  where p is the detected period

Appendix (Paper II)

- Studied three cases of simulated data
- **Case I**: **One eccentric** orbit signal having **period** p and **amplitude** A

  Correct DCM model analysis:

  $K_1 = 1 \equiv$ **one** signal
  $K_2 = 2 \equiv$ **eccentric** $e > 0$ orbit
- Tested numerous e and ω combinations
- Results given in Table A2 and Fig. A1 (next page)
  - Using **correct** DCM model **always** gave **correct** period p and **correct** amplitude A
  - When $e \to 0$, O-C curve approaches a pure sinusoid, and **"correct"** period can be p or $2p$.
- **Conclusion**: DCM can detect period p and amplitude A of **eccentric** O-C orbits

Appendix (Paper II: Fig. A1)

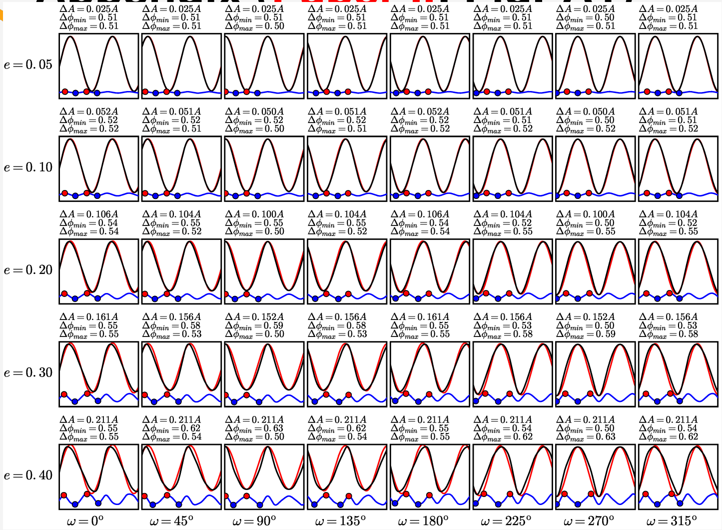

Appendix (Paper II)

- **Case I**: **One eccentric** orbit signal having **period** p and **amplitude** A

  Wrong DCM model analysis:

  $K_1 = 2 \equiv$ **two** signals

  $K_2 = 1 \equiv$ **circular** $e = 0$ orbits

- Tested numerous e and ω combinations
- Results given in Table A3
  - Using **wrong** DCM model **always** gave **correct** period p and **wrong** half period $p/2$
  - Using **wrong** DCM model still gave slightly weaker, **correct**, amplitude A for p signal
- **Conclusion**: If **wrong two circular** orbit DCM model is applied to **eccentric one** p signal orbit, the detected periods will be p and $p/2$.

Appendix (Paper II)

- **Case II**: **Two circular** orbit signals having **periods** p_1 and p_2, and **amplitudes** A_1 and A_2. Stronger p_2 signal **dominates!**

  Correct DCM model analysis:

  $K_1 = 2 \equiv$ **two** signals
  $K_2 = 1 \equiv$ **circular** $e = 0$ orbits

- Results
  - Using **correct** DCM model gave **correct** periods p_1 and p_2, as well as **correct** amplitudes A_1 and A_2
- **Conclusion**: If **correct two circular** orbit DCM model is applied to the sum of **two circular** orbits, where one signal **is dominating**, the **correct** p_1 and p_2 periods, as well as **correct** amplitudes A_1 and A_2, are detected.

Appendix (Paper II)

- **Case II**: **Two circular** orbit signals having **periods** p_1 and p_2, and **amplitudes** A_1 and A_2. Stronger p_2 signal **dominates!**

  Wrong DCM model analysis:

  $K_1 = 1 \equiv$ **one** signals

  $K_2 = 2 \equiv$ **eccentric** $e > 0$ orbit
- Results
  - **Wrong** DCM model gave **nearly correct** period for stronger signal. **Interference** prevented detection of weaker signal (see next page).
- **Conclusion**: If **wrong one eccentric** orbit DCM model is applied to the sum of **two circular** orbits, **nearly correct dominating** stronger signal period p_2 may be detected. **One dimensional-period** search can not detect both periods p_1 and p_2.

Appendix (Paper II: Fig. A2)

Case II: Simulated two circular orbit signals $p_1 = 12295^{\mathrm{d}}$ and $p_2 = 46159^{\mathrm{d}}$. Longer $p_2 = 46159^{\mathrm{d}}$ period signal **dominates**. **Wrong** one eccentric orbit DCM model detects $P_1 = 46122^{\mathrm{d}}$ signal. Note curve dispersion, especially at minima and maxima.

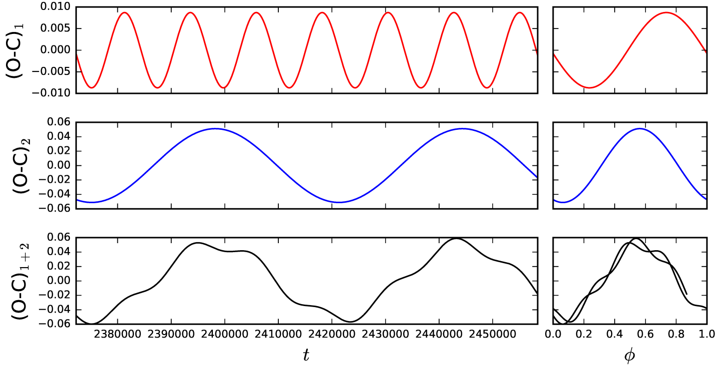

Appendix (Paper II)

- **Case III**: **Two circular** orbit signals having **periods** p_1 and p_2, and **amplitudes** A_1 and A_2. Signals are **equally strong**

  Correct DCM model analysis:

  $K_1 = 2 \equiv$ **two** signals
  $K_2 = 1 \equiv$ **circular** $e = 0$ orbits

- Results
  - Using **correct** DCM model gave **correct** periods p_1 and p_2, as well as **correct** amplitudes A_1 and A_2
- **Conclusion**: If **correct two circular** orbit DCM model is applied to the sum of **two circular** orbits, where both signal are **equally strong**, the **correct** p_1 and p_2 periods, as well as **correct** amplitudes A_1 and A_2, are detected.

Appendix (Paper II)

- **Case III**: **Two circular** orbit signals having **periods** p_1 and p_2, and **amplitudes** A_1 and A_2. Signals are **equally strong**

  Wrong DCM model analysis:

  $K_1 = 1 \equiv$ **one** signal

  $K_2 = 2 \equiv$ **eccentric** $e > 0$ orbit
- Results
  - **Wrong** DCM model gave **wrong** interference period

$$p' = k(p_1^{-1} - p_2^{-1})^{-1},$$

where $k = \pm 1, \pm 2, ...$

- **Conclusion**: If **wrong one eccentric** orbit DCM model is applied to the sum of **two circular** orbits, where both signal are **equally strong**, wrong interference period p' is detected.

Appendix (Paper II: Fig. A3)

Case III: Simulated two circular orbit signals $p_1 = 12304^{\mathrm{d}}$ and $p_2 = 25274^{\mathrm{d}}$. These signals are **equally strong**. **Wrong** one eccentric orbit DCM model detects $P_1 = 24771^{\mathrm{d}}$ signal. Note phase curve dispersion, especially at minima and maxima.

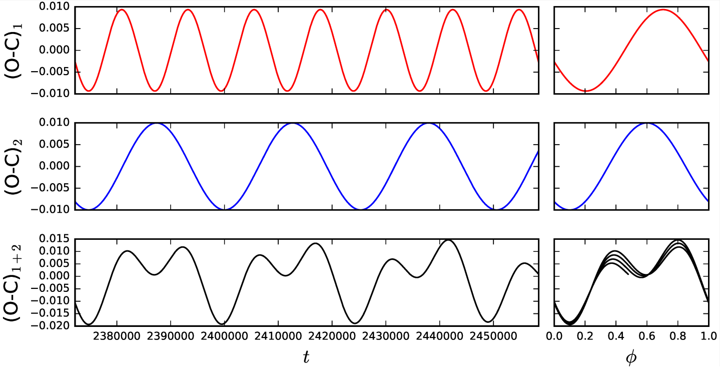

Results (Paper II)

- **Note**: New Sect. 5 "Results"
  - All data
  - First 226^{y}-data
  - First 185^{y}-data
  - Can DCM analysis of First 226^{y}-data predict Last 9^{y}-data observations?
  - Can DCM analysis of First 185^{y}-data predict Last 50^{y}-data observations?

	n	t_1	t_n	ΔT	
Sample	-	[HJD]	[HJD]	[d]	[y]
All data	2224	2372238.351	2458409.7612	86171.4102	235.9
First226^{y}-data	2174	2372238.351	2454839.9189	82601.5679	226.2
Last9^{y}-data	50	2455063.566	2458409.7612	3346.1952	9.2
First185^{y}-data	1731	2372238.351	2439918.358	67680.007	185.3
Last50^{y}-data	493	2440144.8771	2458409.7612	18264.8841	50.0

Results (All data: Trend)

- **Trend** determined from **all data**
  - **Twelve** separate DCM models $\mathcal{M}$=1, $\mathcal{M}$=2, ..., $\mathcal{M}$=12 for searching periodicity between $P_{\mathrm{min}} = 6000^{\mathrm{d}}$ and $P_{\mathrm{max}} = 80000^{\mathrm{d}}$
  - **Eccentric** third body orbits ($K_2 = 2 \equiv e > 0$).
  - **Three** alternatives signal models ($K_1 = 1, 2$ or 3)
  - **Four** alternatives $p(t)$ trends ($K_3 = 0, 1, 2$ or 3)
  - **Four** unstable models: "Um" ($\mathcal{M}$= 3, 5, 8 and 9)
  - **Three** leaking models: "Lp" ($\mathcal{M}$= 2, 3 and 7)
- **Fisher test** shows that $\mathcal{M}$=10 **best** (Table A6)
  - **Three signals** ($K_1 = 3$)
  - **Eccentric** orbits ($K_2 = 2$)
  - **Linear trend** ($K_3 = 1$)
- Not mentioned: Three strongest signals determine trend, because other detected signals much weaker

Results (All data: Eccentric orbits)

- **All analysis of all original data** is hereafter based on **linear trend** assumption $K_3 = 1$
- Meaning of linear trend discussed separately later
- **All data**: Search for **long period eccentric orbits** between 8000 and 80000 days (Table A7)
  - Four signal alternatives ($K_1 = 1, 2, 3, 4$)
  - Eccentric ($K_2 = 2$)
  - Linear trend ($K_3 = 1$)

  $\rightarrow$ Four models $\mathcal{M}$ = 1, 2, 3 and 4
- Fisher test: **Three signal model $\mathcal{M}$ = 3 best**
  - One and two signal models $\mathcal{M}$ = 1 and 2 **rejected with absolute certainty** $Q_F < 10^{-16}$
  - Four signal **unstable** model $\mathcal{M}$ = 4 **is rejected**

  $\rightarrow$ All data contains **only three long period signals**

Results (All data: Eccentric orbits)

Fig. A4: **Unstable** four signal eccentric orbit model **periodograms** for all data (Table A7: $\mathcal{M}$ = 4).

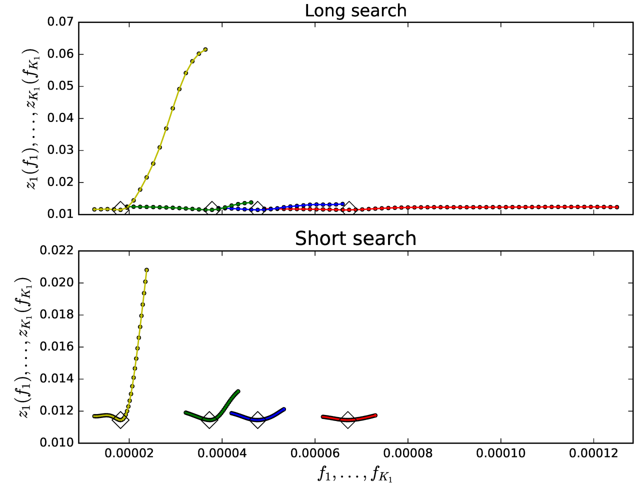

Results (All data: Eccentric orbits)

Fig. A5: **Unstable** four signal eccentric orbit **model** for all data (Table A7: $\mathcal{M} = 4$).

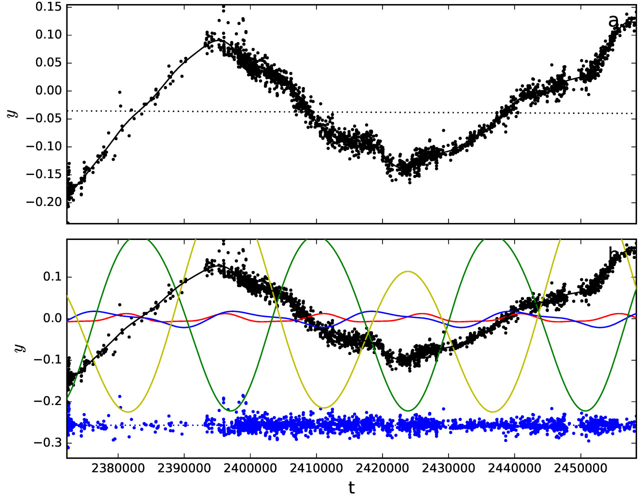

Results (All data: Eccentric orbits)

- **All data**: **Best model** for **longer periods** between 8000 and 80000 days is **three signal model** $\mathcal{M}$= 3 $(K_1 = 3, K_2 = 2, K_3 = 1)$
- Signal **periods** and **amplitudes**

$$P_1 = 20358^{\mathrm{d}} = 55.7^{\mathrm{y}} \quad A_1 = 0.013^{\mathrm{d}}$$
$$P_2 = 24742^{\mathrm{d}} = 67.7^{\mathrm{y}} \quad A_2 = 0.029^{\mathrm{d}}$$
$$P_3 = 79999^{\mathrm{d}} = 219.0^{\mathrm{y}} \quad A_3 = 0.287^{\mathrm{d}}$$

- Strong P_3 signal **dominates**: about 10 and 20 times stronger than P_2 and P_1 signals

→ Strong P_3 signal dominates sum of residuals R in **periodogram figure** (Fig. A6: green line)

→ Strong P_3 signal dominates in sum of signals $h(t)$ in **model figure** (Fig. A7: green line)

Results (All data: Eccentric orbits)

Fig. A6: **Stable** three signal **longer period** eccentric orbit **best model periodograms** for all data (Table A7: $\mathcal{M} = 3$).

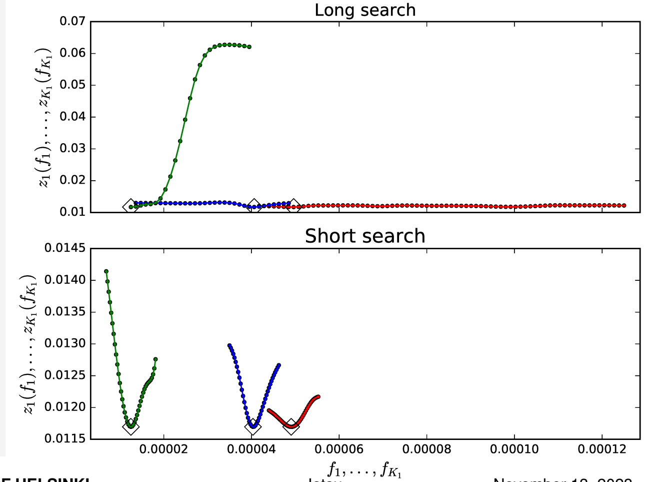

Results (All data: Eccentric orbits)

Fig. A7: **Stable** three signal **longer period** eccentric orbit **best model** for all data (Table A7: $\mathcal{M}$ = 3).

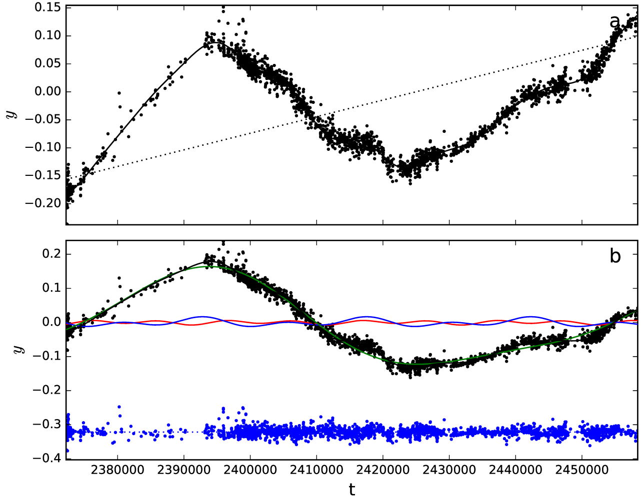

Results (All data: Eccentric orbits)

Fig. A8: **Stable** three eccentric **longer period** orbit **best model** signals separately (Table A7: $\mathcal{M} = 3$).

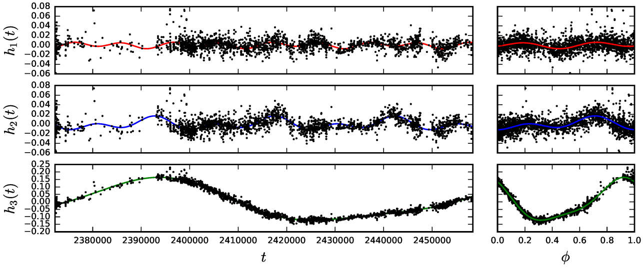

- P_1 signal looks like a **double period** curve

$\rightarrow$ can not be circular or eccentric orbit period

- P_2 signal looks like an **interference** curve

$\rightarrow$ can not be circular or eccentric orbit period

- P_3 signal looks like a **real eccentric orbit** curve

Results (All data: Eccentric orbits)

- All **three longer periods** between 8000 and 80000 days have been detected (Table A7: $\mathcal{M}$= 3)

→ Search for **shorter periods** below 8000 days from **$\mathcal{M}$= 3 model residuals**

- DCM search between 500 and 8000 days
  - $K_2 = 2 \equiv e > 0 \equiv$ **eccentric** orbits
  - $K_0 = 0 \equiv$ **no trend** in residuals
- **All data**: **Best model** for **shorter periods** between 500 and 8000 days is **two signal model $\mathcal{M}$= 6** $(K_1 = 2, K_2 = 2, K_3 = 0)$
- Signal **periods** and **amplitudes**
  $P_1 = 680.4^{\mathrm{d}} = 1.86^{\mathrm{y}}$ $A_1 = 0.0064^{\mathrm{d}}$
  $P_2 = 7290^{\mathrm{d}} = 20.0^{\mathrm{y}}$ $A_2 = 0.007^{\mathrm{d}}$
- Signals 45 and 41 times weaker than dominating 219 years signal

Results (All data: Eccentric orbits)

- **Reason for rejecting** three signal $\mathcal{M}$ = 7 model for **shorter periods** not based on Fisher test (Table A7)!
  - Periods $P_2 = 7124^{\mathrm{d}}$ and $P_3 = 7698^{\mathrm{d}}$ fulfil

$$p' = [P_2^{-1} - P_3^{-1}]^{-1} = 95541^{\mathrm{d}} \pm 13902^{\mathrm{d}}$$

  → This time interval p' equal to time span $\Delta T = 86171^{\mathrm{d}}$ of all data

  → Difference between **real** $P_2 = 7124^{\mathrm{d}}$ and **spurious** $P_3 = 7698^{\mathrm{d}}$ period is **one round during** ΔT

  → **spurious** $P_3 = 7698^{\mathrm{d}}$ period rejected

  → three signal $\mathcal{M}$ = 7 model **rejected**

- Such **spurious = unreal** periods denoted with "Sp"

Results (All data: Eccentric orbits)

Fig. A9: Two eccentric **shorter period** orbit model
$\mathcal{M} = 6$ **periodograms** for $\mathcal{M} = 3$ model residuals

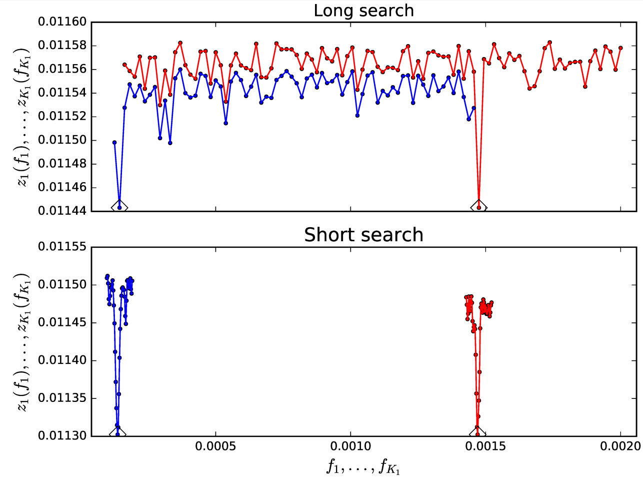

Results (All data: Eccentric orbits)

Fig. A10: Two eccentric **shorter period** orbit $\mathcal{M}$ **= 6 model** for $\mathcal{M}$ = 3 model residuals

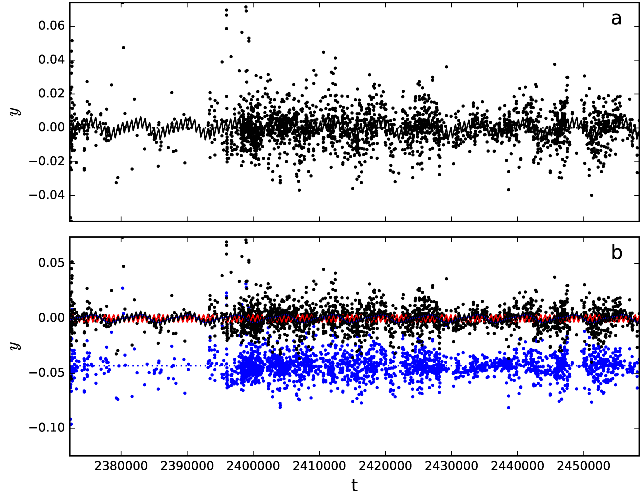

Results (All data: Eccentric orbits)

Fig. A11: Two eccentric **shorter period** orbit $\mathcal{M}$ **= 6 model signals** detected from $\mathcal{M}$ = 3 model residuals

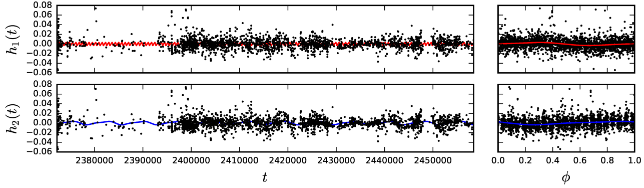

- $P_1 = 1.86^{\mathrm{y}}$ signal looks like a **real eccentric orbit**
- $P_2 = 20.0^{\mathrm{y}}$ signal looks like a **real eccentric orbit**
- **Regularity**: Periods detected earlier are always **re-detected** when searhing for the next signal
- Best model for **all** Algol's O-C data is **sum** of $\mathcal{M}$**=3 model for original data**, and $\mathcal{M}$**=6 model for residuals** of original data: "$\mathcal{M}$= 3 + 6" (five signals)

Results (All data: Eccentric orbits) Here: 21.11.2022

Fig. 1, upper part: Best five-signal $\mathcal{M} = 3 + 6$ model for all data. **Prediction** for next ten years begins from dotted vertical line.

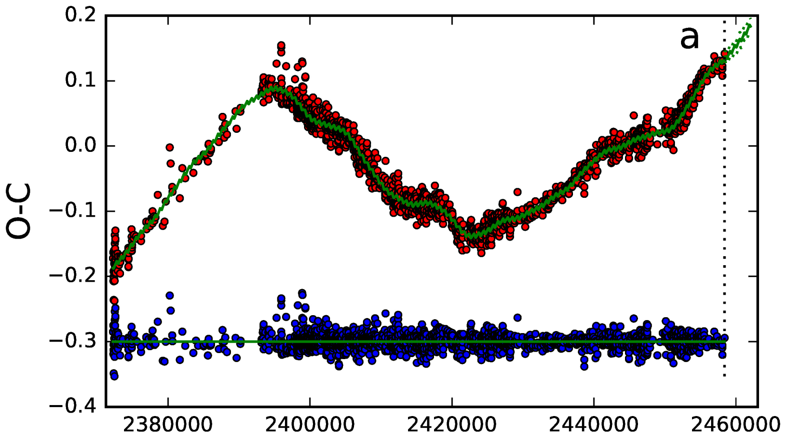

Results (All data: Eccentric orbits)

Fig. 1, lower part: Five-signal model **prediction** for next ten years begins from dotted vertical line.

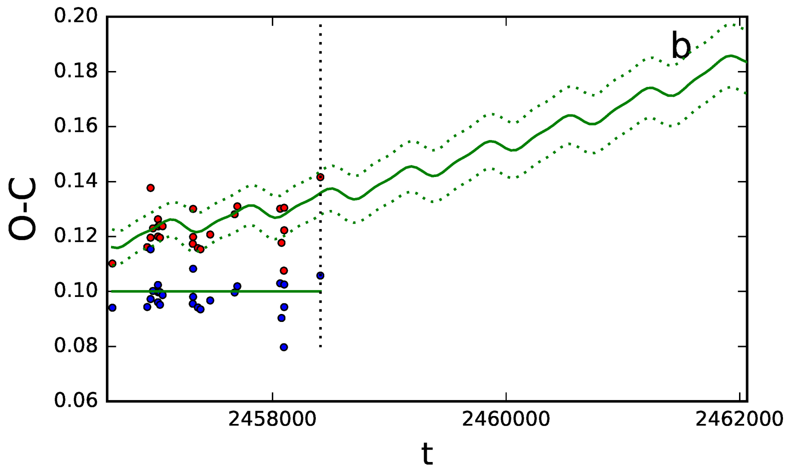

How would you solve this?

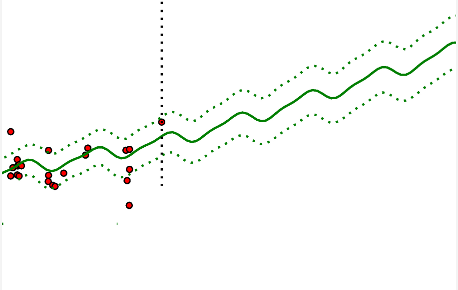

@depositphotos.com

How would you solve this five-signal DCM prediction (continuous green line) and prediction error (dotted dotted line)?

1. **Mathematical theory?**
2. **Computational program?**

Results (All data: Eccentric orbits)

Open questions

- 219 years signal looks like a **real eccentric orbit**
- 67.7 years signal looks like **interference**

$\rightarrow$ can not be **circular** or **eccentric** orbit period

- 55.7 years signal looks like a **double period**

$\rightarrow$ can not be **circular** or **eccentric** orbit period

- 20.0 years signal looks like a **real eccentric orbit**
- 1.86 years signal looks like a **real eccentric orbit**

$\leftrightarrow$ Is this **weakest** 1.86 years signal that of **Algol C**?

$\leftrightarrow$ Does this confirm that stronger four signals are real?

Possible solutions

- Can **circular orbit analysis** clarify this mess?
- Can O-C data be predicted? No one has been able to do that! **Shorter samples** First 226^{y}-data and First 185^{y}-data can be used to **test predictablity.**

Results (All data: Circular orbits)

- Section changes from **eccentric** orbits (Sect. 5.1.2) to **circular** orbits (Sect. 5.1.3)
- **Appendix**: If an **eccentric** orbit O-C curve has a **period** p, then this curve is a sum of **two circular** orbit O-C curves having **periods** p **and** $p/2$

$\rightarrow$ **Circular orbit** results can be used to **eccentric orbit** results, and vice versa

$\rightarrow$ **Two alternative circular orbit** analyses performed

- **1st alternative circular orbit** results in Table A8
  - **1st alternative DCM circular orbit analysis** for **longer periods** between 8000 and 80000 days
  - $K_1 = 1, 2, 3, 4, 5 \equiv \mathcal{M}$ = 1, 2, 3, 4, 5 models
  - $K_2 = 1 \equiv e = 0 \equiv$ circular orbit
  - $K_3 = 1 \equiv$ linear trend

Results (All data: Circular orbits)

Original data

- Four-signal $\mathcal{M}$ = 4 model **periods** and **amplitudes**

  $P_1 = 12352^{\mathrm{d}} = 33.80^{\mathrm{y}}$ $A_1 = 0.0118^{\mathrm{d}}$

  $P_2 = 24773^{\mathrm{d}} = 67.8^{\mathrm{y}}$ $A_2 = 0.018^{\mathrm{d}}$

  $P_3 = 42610^{\mathrm{d}} = 116.7^{\mathrm{y}}$ $A_3 = 0.088^{\mathrm{d}}$

  $P_4 = 145456^{\mathrm{d}} = 398.2^{\mathrm{y}}$ $A_3 = 0.9^{\mathrm{d}}$

- One-signal $\mathcal{M}$ = 5 model **period** and **amplitude** for **$\mathcal{M}$ = 4 model residuals**

  $P_1 = 10175^{\mathrm{d}} = 27.8^{\mathrm{y}}$ $A_1 = 0.0087^{\mathrm{d}}$

- **1. Problem**: Models $\mathcal{M}$ = 2, 3 and 4 are unstable ("Um"), because longest 398.2 year period exceeds 236 year time span of data ("Lp")

$\rightarrow$ This signal suffers from amplitude dispersion ("Ad")

- **2. Problem**: $K_1 = 5$ analysis would take "an eternity"

$\rightarrow$ Fifth 27.8 year signal detected from **residuals**

Results (All data: Circular orbits)

Residuals

- **1st alternative DCM circular orbit analysis** for **shorter periods** between 500 and 8000 days performed for **$\mathcal{M}$ = 5 model residuals**
  - $K_1 = 1, 2, 3 \equiv \mathcal{M}$ = 7, 8 ,9 models
  - $K_2 = 1 \equiv e = 0 \equiv$ circular orbit
  - $K_3 = 0 \equiv$ no trend
- Three-signal $\mathcal{M}$ = 9 model **periods** and **amplitudes**

  $P_1 = 680.7^{\mathrm{d}} = 1.86^{\mathrm{y}}$ $\quad A_1 = 0.0057^{\mathrm{d}}$

  $P_2 = 2986^{\mathrm{d}} = 8.2^{\mathrm{y}}$ $\quad A_2 = 0.0031^{\mathrm{d}}$

  $P_3 = 7360^{\mathrm{d}} = 20.9^{\mathrm{y}}$ $\quad A_3 = 0.0056^{\mathrm{d}}$

1st alternative DCM circular orbit analysis results

- Algol C signal 1.86 year detected again
- Best $\mathcal{M}$ = 4 + 5 + 9 model is sum of 8 circular orbits
- Will **2nd alternative DCM circular orbit analysis** confirm these orbits?

Results (All data: Circular orbits)

1st alternative circular orbit analysis period grids

$n_{\mathrm{L}} = 80$ in long search

$n_{\mathrm{S}} = 40$ in short search

$\rightarrow$ Eliminates "trial factor" error: correct period(s) missed

- Computation time proportional to $\propto n_{\mathrm{L}}^{K_1}$ and $\propto n_{\mathrm{S}}^{K_1}$

$\rightarrow$ Four-signal model computation takes one month

$\rightarrow$ Five-signal model takes "an eternity"

$\rightarrow$ Fifth signal **indirectly from residuals**

$\rightarrow$ **2nd alternative circular orbit** analysis period grids

$n_{\mathrm{L}} = 30$ in long search

$n_{\mathrm{S}} = 8$ in short search

$\rightarrow$ Six-signal model computation takes one week

$\rightarrow$ 5th and 6th signal **directly from original data**

- **2nd alternative circular orbit** results in Table A9

Results (All data: Circular orbits)

2nd alternative circular orbit analysis for **longer periods** between 8000 and 80000 days (Table A9)

- $K_1 = 4, 5, 6 \equiv \mathcal{M}$ = 1, 2, 3 models
- $K_2 = 1 \equiv e = 0 \equiv$ circular orbit
- $K_3 = 1 \equiv$ linear trend
- Strongest signal period of four-, five- and six-signal models exceeds time span of data (Table A9: $"\mathrm{Lp}"$)

$\rightarrow$ These models suffer from amplitude dispersion (“Ad”)

$\rightarrow$ These models are unstable (“Um”)

- **Fisher test**: Five-signal model is best
- Five-signal $\mathcal{M}$ = 2 model **periods** and **amplitudes**

$P_1 = 10144^{\mathrm{d}} = 27.8^{\mathrm{y}}$ $A_1 = 0.0097^{\mathrm{d}}$

$P_2 = 12294^{\mathrm{d}} = 33.7^{\mathrm{y}}$ $A_2 = 0.018^{\mathrm{d}}$

$P_3 = 24247^{\mathrm{d}} = 66.4^{\mathrm{y}}$ $A_3 = 0.018^{\mathrm{d}}$

$P_4 = 42422^{\mathrm{d}} = 116.1^{\mathrm{y}}$ $A_3 = 0.08^{\mathrm{d}}$

$P_5 = 120740^{\mathrm{d}} = 330.6^{\mathrm{y}}$ $A_3 = 0.6^{\mathrm{d}}$

Results (All data: Circular orbits)

Fig. A12: **2nd alternative circular orbit** five-signal **periodogram** for all data (Table A9: $\mathcal{M}$ = 2)

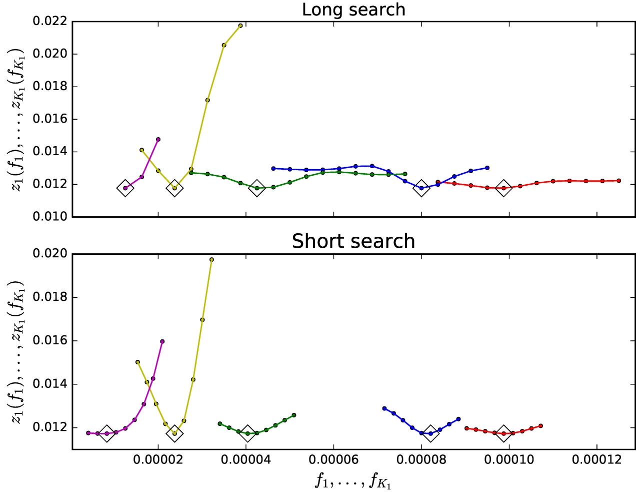

Results (All data: Circular orbits)

Fig. A13: **2nd alternative circular orbit** five-signal **model** for all data (Table A9: $\mathcal{M}$ = 2)

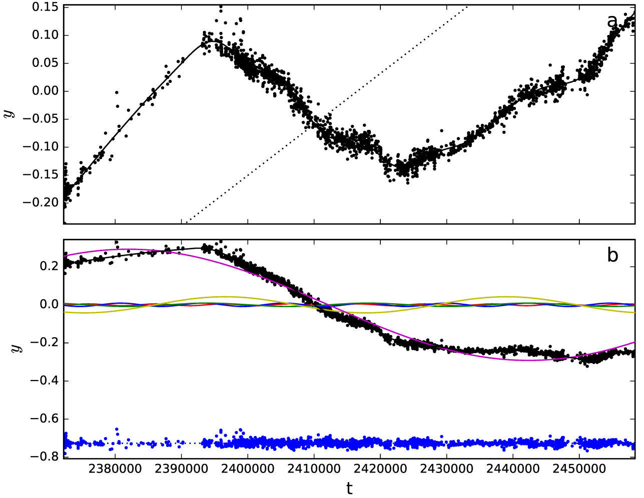

Results (All data: Circular orbits)

2nd alternative **circular orbit** analysis for **shorter periods** between 500 and 8000 days (Table A9)

- Analysis of $\mathcal{M}$ = 2 **five-signal model residuals**
  - $K_1 = 1, 2, 3 \equiv \mathcal{M}$ = 4, 5, 6 models
  - $K_2 = 1 \equiv e = 0 \equiv$ circular orbit
  - $K_3 = 0 \equiv$ no trend
  - Two-signal $\mathcal{M}$ = 5 model is **best**
    $P_1 = 680.7^{\mathrm{d}} = 1.86^{\mathrm{y}}$ $A_1 = 0.0057^{\mathrm{d}}$
    $P_2 = 7395^{\mathrm{d}} = 20.2^{\mathrm{y}}$ $A_2 = 0.0009^{\mathrm{d}}$
  - Three-signal model $\mathcal{M}$ = 6 **no Fisher test rejection!**

  $\rightarrow$ Third period $P_3 = 7034$ spurious ("*Sp*"), Intersecting frequencies ("If")

  $\rightarrow$ Three-signal model unstable ("Um")
- **2nd alternative** **circular orbit** analysis best model is $\mathcal{M}$ = 2 + 5 model of 7 circular orbits

Results (All data: Circular orbits)

- Comparison of **1st and 2nd alternative circular orbit** analysis results (Table A12)
  - **1st alternative**: First four longer signals from **original data** → one longer signal from **residuals** → two shorter signals from **next residuals**
  - **2nd alternative**: First five longer signals from **original data** → two shorter signals from **residuals**
  - **All results are consistent**
  - All seven signals have **same** amplitudes and periods
  - Results for **longer periods same**
  - Results for **shorter periods same**, including Algol C
  - Unstable models, leaking periods and dispersing amplitudes do not mislead this analysis
  - **Minor difference**: weakest 2986 days 8th signal detected only in **1st alternative** (real or spurious?)

Results (First 226^{y}-data)

- **New section** "First 226^{y}-data"
- First 226 years **subsample** (Results in Table A10)
- **Original data**: **Longer periods** between 8000 and 80000 days
  - $K_1 = 1, 2, 3, 4 \equiv \mathcal{M}$ = 1, 2, 3, 4 models
  - $K_2 = 2 \equiv e > 0 \equiv$ **eccentric** orbit
  - $K_3 = 1 \equiv$ **linear** trend
  - One- and two-signal models $\mathcal{M}$ = 1 and $\mathcal{M}$ = 2 suffer from **leaking periods** ("Lp") longer than ΔT
  - Three signal **stable** $\mathcal{M}$ = 3 best
  - Four-signal $\mathcal{M}$ = 4 model **unstable**

$$P_1 = 20592^{\mathrm{d}} = 56.4^{\mathrm{y}} \qquad A_1 = 0.014^{\mathrm{d}}$$
$$P_2 = 24870^{\mathrm{d}} = 68.1^{\mathrm{y}} \qquad A_2 = 0.030^{\mathrm{d}}$$
$$P_3 = 78589^{\mathrm{d}} = 215.2^{\mathrm{y}} \qquad A_3 = 0.282^{\mathrm{d}}$$

- **Subsample** periods&amplitudes **same** as in **all data**

Results (First 226^{y}-data)

- First 226 years **subsample** (Results in Table A10)
- **Residuals of $\mathcal{M}$ = 3 model for original data**:
  Shorter periods between 500 and 8000 days
  - $K_1 = 1, 2, 3 \equiv \mathcal{M}$ = 5, 6, 7 models
  - $K_2 = 2 \equiv e > 0 \equiv$ **eccentric** orbit
  - $K_3 = 0 \equiv$ **no** trend
  - **Stable** two-signal model $\mathcal{M}$ = 6 best
  - Three-signal $\mathcal{M}$ = 7 model: **no** Fisher test rejection!

  $\rightarrow$ $P_3 = 7757^{\mathrm{d}}$ spurious = unreal, P_2 and ΔT connection
  - Two-signal $\mathcal{M}$ = 5 model **periods** and **amplitudes**

    $P_1 = 7887^{\mathrm{d}} = 21.6^{\mathrm{y}}$ $\quad A_1 = 0.007^{\mathrm{d}}$

    $P_2 = 680.3^{\mathrm{d}} = 1.86^{\mathrm{y}}$ $\quad A_2 = 0.0063^{\mathrm{d}}$
- **Subsample** periods&amplitudes **same** as in **all data**
- First 226^{y}-data **best $\mathcal{M}$ = 3 + 6 five-signal model**

Results (Adataone: Eccentric orbits)

Fig. 2, upper part: Best five-signal $\mathcal{M} = 3 + 6$ model for First 226$^{\mathrm{y}}$-data. **Prediction** for Last 9$^{\mathrm{y}}$-data begins from dotted vertical line.

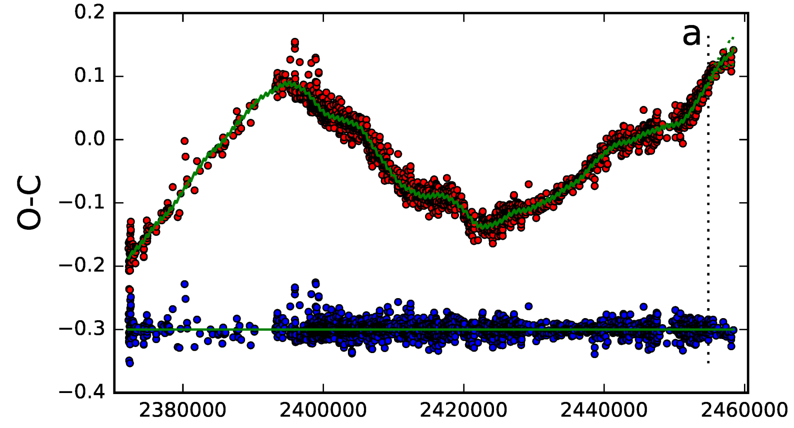

Results (First 226^{y}-data: Eccentric orbits)

Fig. 2, lower part: Five-signal model **prediction** for Last 9^{y}-data begins from dotted vertical line.

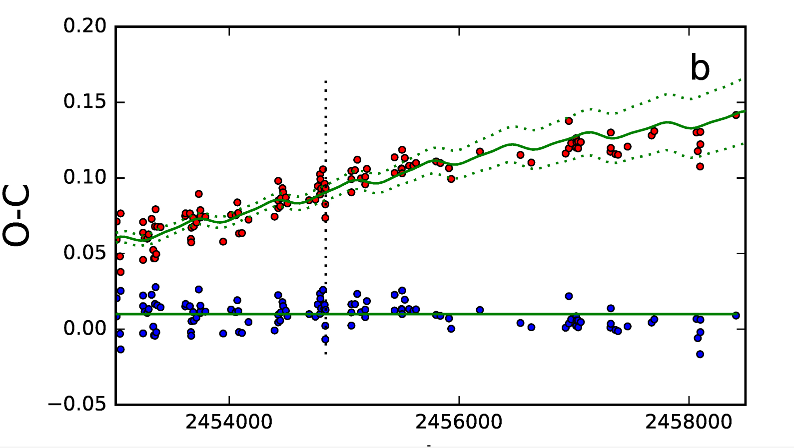

What does this mean?

@depositphotos.com

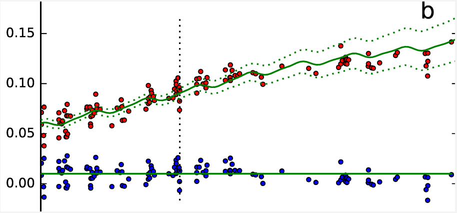

- Standard deviation of predictive $\mathcal{M}$ = 3+6 model $n = 2174$ residuals is $0.^{\mathrm{d}}011$
- Standard deviation of $n = 50$ prediction residuals is $0.^{\mathrm{d}}0078$ is **smaller!** (New data more accurate)

Prediction succeeds. What does this mean?

Results (First 185^{y}-data: Eccentric orbits)

- **New section** "First 185^{y}-data"
- Second 185 years **subsample** (Results in Table A11)
- **Original data**: **Longer periods** between 8000 and 80000 days
  - $K_1 = 1, 2, 3, 4 \equiv \mathcal{M}$ = 1, 2, 3, 4 models
  - $K_2 = 2 \equiv e > 0 \equiv$ **eccentric** orbit
  - $K_3 = 1 \equiv$ **linear** trend
  - One-signal $\mathcal{M}$ = 1 model **stable**
  - Two- and three-signal $\mathcal{M}$ = 2 and 3 model **unstable**
  - Four-signal $\mathcal{M}$ = 1 model **stable** and **best** having **periods** and **amplitudes**

$$P_1 = 12370^{\mathrm{d}} = 33.9^{\mathrm{y}} \qquad A_1 = 0.018^{\mathrm{d}}$$
$$P_2 = 15429^{\mathrm{d}} = 42.2^{\mathrm{y}} \qquad A_2 = 0.008^{\mathrm{d}}$$
$$P_3 = 20037^{\mathrm{d}} = 54.8^{\mathrm{y}} \qquad A_3 = 0.015^{\mathrm{d}}$$
$$P_4 = 62992^{\mathrm{d}} = 172.5^{\mathrm{y}} \qquad A_3 = 0.25^{\mathrm{d}}$$

Results (First 185^{y}-data)

- First 185 years **subsample** (Results in Table A10)
- **Residuals of $\mathcal{M}$ = 4 model for original data**:
  Shorter periods between 500 and 8000 days
  - $K_1 = 1, 2, 3 \equiv \mathcal{M}$ = 5, 6, 7 models
  - $K_2 = 2 \equiv e > 0 \equiv$ **eccentric** orbit
  - $K_3 = 0 \equiv$ **no** trend
  - One-signal model **stable**
  - **Stable** two-signal model $\mathcal{M}$ = 6 **best**
  - Three-signal $\mathcal{M}$ = 7 model **unstable**
  - Two-signal $\mathcal{M}$ = 6 model **periods** and **amplitudes**
    $P_1 = 3387^{\mathrm{d}} = 9.3^{\mathrm{y}}$ $A_1 = 0.0051^{\mathrm{d}}$
    $P_2 = 679.6^{\mathrm{d}} = 1.86^{\mathrm{y}}$ $A_2 = 0.0074^{\mathrm{d}}$
  - Again, Algol C period detected
- First 185^{y}-data **best $\mathcal{M}$ = 4 + 6 six-signal model**

Results (First 185^{y}-data: Eccentric orbits)

Fig. 3, upper part: Best six-signal $\mathcal{M}$ = 4 + 6 model for First 185^{y}-data. **Prediction** for Last 50^{y}-data begins from dotted vertical line.

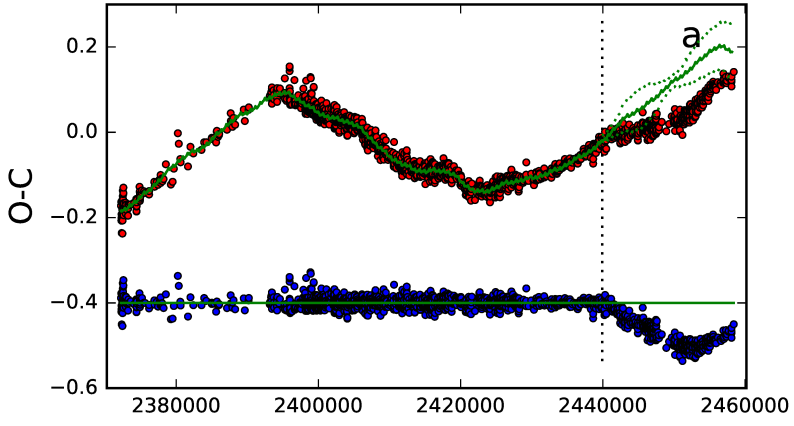

Results (First 185^{y}-data: Eccentric orbits)

Fig. 3, lower part: Six-signal model **prediction** for Last 50^{y}-data begins from dotted vertical line.

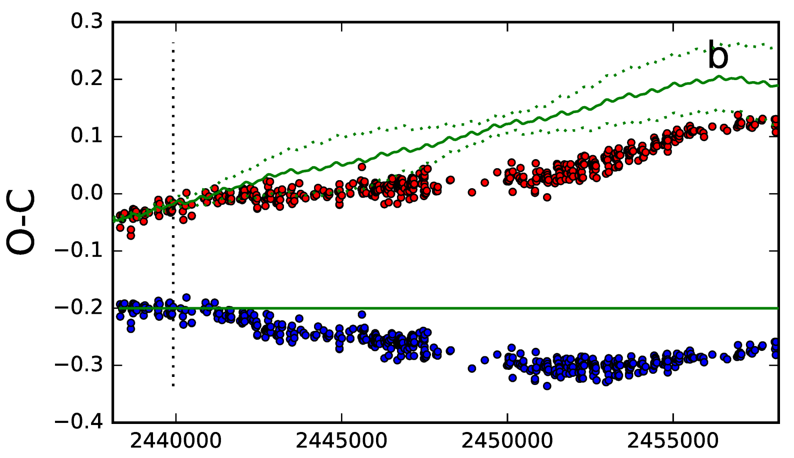

Results (First $185^{\rm y}$-data: Eccentric orbits)

- First $185^{\rm y}$-data **prediction** for Last $50^{\rm y}$-data **fails**
  - Predictive data **time span** $\Delta T = 67680^{\rm d} = 185^{\rm y}$
  - $\rightarrow$ **Strongest** predictive signal $P_4 = 62992^{\rm d} = 172^{\rm y}$
  - $\rightarrow$ This signal determines long-term **prediction trend**
  - $\rightarrow$ **Correct** period would be $219^{\rm y}$ already detected from all data and First $226^{\rm y}$-data
  - $\rightarrow$ **Wrong** $172^{\rm y}$ period detected from First $185^{\rm y}$-data
  - $\rightarrow$ Trend **fails**
  - $\rightarrow$ Prediction **fails**

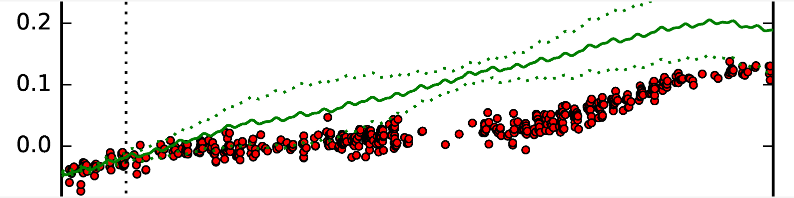

Results (First 185^{y}-data: Eccentric orbits)

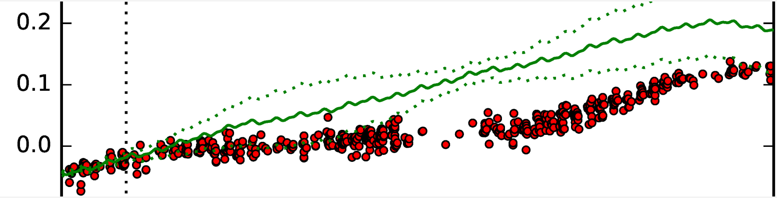

- First 185^{y}-data **prediction** for Last 50^{y}-data seems to **defy laws of statistics**
  - **First**, prediction $\pm 3\sigma$ error **increases**, as expected
  - **Then**, prediction $\pm 3\sigma$ error **decreases**, and prediction becomes very accurate. **This is not expected!!!**
  - **Then**, prediction $\pm 3\sigma$ error **increases**, as expected
- What explains this **peculiarity** in six-signal interference curve?

Results (First 185^{y}-data: Eccentric orbits)

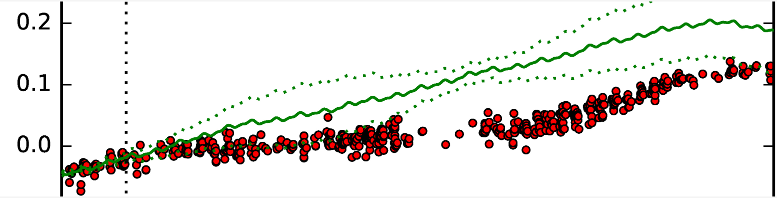

Data shows

- After vertical line: Positive slope, but slope **decreases**

$\rightarrow$ Suitable model $\dot{g}(t) > 0$ and $\ddot{g}(t) < 0$

- After gap in data: Positive slope, but slope **increases**

$\rightarrow$ Suitable model $\dot{g}(t) > 0$ and $\ddot{g}(t) > 0$

- **Turning point** $\dot{g}(t) = 0$ close to HJD 2450000 epoch, where $\ddot{g}(t)$ sign changes from negative to positive
    - Second derivative sign change of **any function** $g(t)$ **forces** this function to **change its direction twice!**

Results (First 185^{y}-data: Eccentric orbits)

Fig. A14: Green line denotes $g(t)$ model $\mathcal{M}$=4+6. Dotted red lines show models for 20 bootstrap samples. Prediction begins from dotted vertical line. Continuous vertical line at **data turning point**.

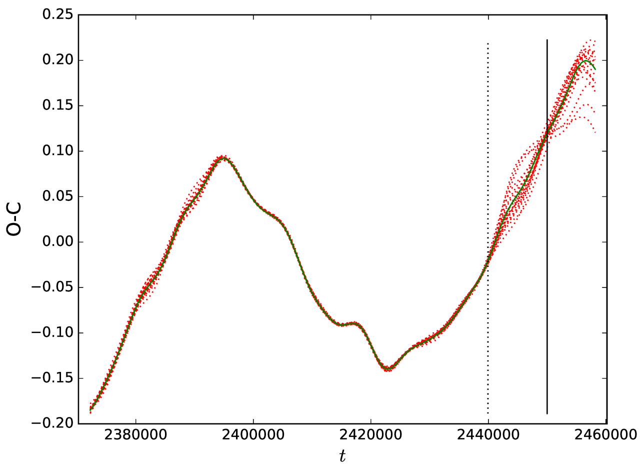

Results (First 185^{y}-data: Eccentric orbits)

$\mathcal{M}$=4+6 model **turning point** at continuous vertical line **forces** bootstrap model solutions to converge. This simple effect explains why **prediction error** **increases**, **decreases**, and again **increases**.

- **Note**: We **can not** predict **long-term trend** of Last 50^{y}-data, **but** we **can** predict **turning point epoch** of Last 50^{y}-data

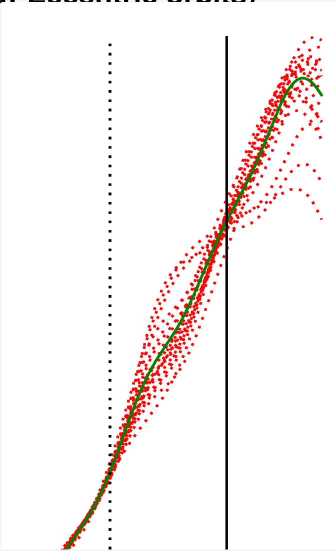

Results (First $185^{\rm y}$-data: Eccentric orbits)

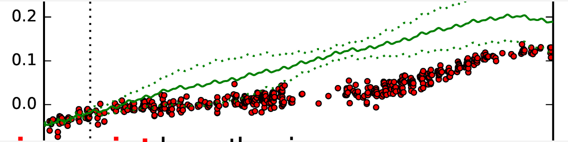

Turning point hypothesis

- O-C data gap close to HJD 2450000 turning point
- Only four values between HJD 2448288 and HJD 2449988 ($\equiv$ 4.6 years)
- No such gaps even during two World Wars

- **Turning point**: **New** data contradicted established long-term $\dot{g}(t) > 0$ and $\ddot{g}(t) < 0$ **old trend**
  $\rightarrow$ Contradicting data was **not published** $\rightarrow$ Gap **began**
- **Five years after turning point**: **New trend** $\dot{g}(t) > 0$ and $\ddot{g}(t) > 0$ securely established
  $\rightarrow$ Supporting data **published** $\rightarrow$ Gap **ended**

Results (Additional experiments)

- **New section** "Additional experiments" (Referee)

  What happens if data divided into two parts?

$\rightarrow$ Both halves ΔT of too short for 219^{y} period detection

  - **Eccentric** orbit $K_2 = 2 \equiv e > 0$ assumption
  - **1st half**: only 137 years signal
  - **2nd half**: 1.86, 30.9, 39.7 and 103.3 years signals
  - **2nd half**: 1.86 year equal to Algol C period
  - What results would have been obtained for **circular** orbit $K_2 = 1 \equiv e = 0$ assumption?

- DCM $K_2 = 1 \equiv e = 0$ **first part** analysis in **ExerciseAlgolOne** **(A2022)**
- DCM $K_2 = 1 \equiv e = 0$ **second part** analysis in **ExerciseAlgolTwo** **(A2022)**

  "Beware of failing models"

Results (Additional experiments)

- **Referee**: **Analysis is based on non-weighted data (i.e. Equal weights $\equiv R$ test statistic). Accuracy of data improves towards modern times. What happens if this improved accuracy is taken into account?**
- **Two alternative experiments** where weights of observations increase linearly towards modern times
- Analysis based on χ^2 test statistic
  1: Weights doubled towards modern times
  2: Weights quadrupled towards modern times
- **Result**: All five signals detected in **weighted data same** as five signals already detected in **non-weighted data**

Results (Signals Identified in All data)

- **New section** "Signals Identified in All data"
- Eccentric orbit analysis: **five signals** in all data
- Correct number **may be six signals**
  - **Periods** $\mathbf{p}_1 < \mathbf{p}_2 < \mathbf{p}_3 < \mathbf{p}_4 < \mathbf{p}_5 < \mathbf{p}_6$
  - **Peak to peak amplitudes** $\mathbf{A}_1$, $\mathbf{A}_2$, $\mathbf{A}_3$, $\mathbf{A}_4$, $\mathbf{A}_5$ and $\mathbf{A}_6$
  - **Tentative names** Algol C, Algol D, Algol E, Algol F, Algol G and Algol H
- Signals identified from comparison of

Table 13: All data	Circular	Eccentric	
Table 14: Eccentric	All data	First 226^y	First 185^y

- **Identification effects**
  - Third-body O-C signal always has only **one minimum** and **one maximum**

  → Other kinds of signals not caused by **one object**

Results (Signals Identified in All data)

- **Additional identification effects**

  "Correct-p": DCM detects the correct period p.
  "Half-p": DCM detects the spurious period $p/2$.
  "Double-p": DCM detects the spurious period $2p$.
  "Interference-p'": DCM detects the spurious period p' caused by p_1 and p_2 interference

- **Fig. A1 extract**: Correct-p and Half-p effects

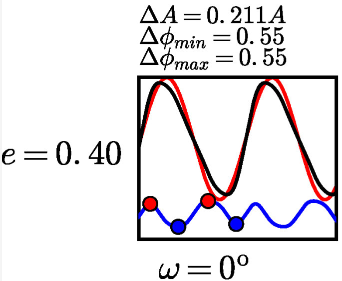

Results (Signal $\mathbf{p}_6 = 219^{\mathrm{y}}.0$)

Here: 28.11.2022

Fig. A8 extract: Signal $\mathbf{p}_6 = 219^{\mathrm{y}}.0$

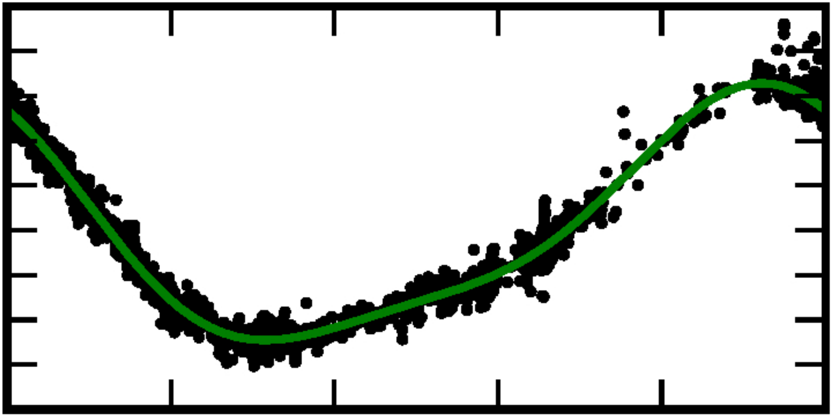

Results (Signal $\mathbf{p}_6 = 219^{\mathrm{y}}.0$)

- **New section** "Signal $\mathbf{p}_6 = 79999^{\mathrm{d}} = 219^{\mathrm{y}}.0$"
  - Signal has only one minimum and one maximum
  - "Correct-*p*" effect: Circular $P_{\mathrm{c},7} = 120740^{\mathrm{d}} \pm 41002^{\mathrm{d}}$ within $\pm 1\sigma$ eccentric $\mathbf{p}_6 = P_{e,5} = 79999^{\mathrm{d}} \pm 1216^{\mathrm{d}}$
  - "Half-*p*" effect: $\mathbf{p}_6$ two times circular $P_{c,6} = 42422^{\mathrm{d}} \pm 640^{\mathrm{d}}$
  - Strongest circular $P_{c,7}$ and $P_{c,6}$ signals "in phase"
  - Signal $\mathbf{p}_6$ detected in all data and First 226^{y}-data, but First 185^{y}-data too short for detection
  - Signal $\mathbf{p}_6$ amplitude $\mathbf{A}_6 = A_{e,5} = 0.^{\mathrm{d}}287 \pm 0.^{\mathrm{d}}005$

Conclusion: DCM confirms that $\mathbf{p}_6 = 79999^{\mathrm{d}} = 219^{\mathrm{y}}.0$ signal is an **eccentric** orbit O-C signal

Results (Signals $\mathbf{p}_5 = 66.^y4$ and $\mathbf{p}_4 = 33.^y7$)

Fig. A8 extract: Signals $\mathbf{p}_5 = 66.^y4$ and $\mathbf{p}_4 = 33.^y7$

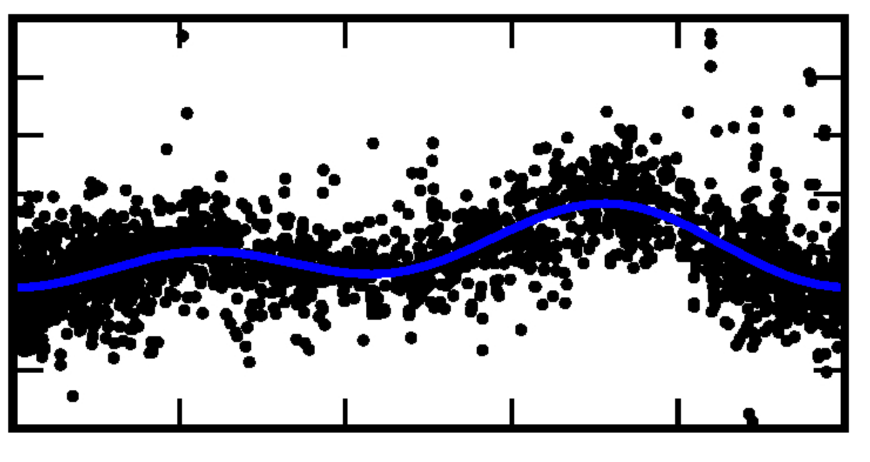

Results (Signals $\mathbf{p}_5 = 66.^{\mathrm{y}}4$ and $\mathbf{p}_4 = 33.^{\mathrm{y}}7$)

- **New section** "Signals $\mathbf{p}_5 = 24247^{\mathrm{d}} = 66.^{\mathrm{y}}4$ and $\mathbf{p}_4 = 12294^{\mathrm{d}} = 33.^{\mathrm{y}}7$"
  - "Correct-p" effect: Connects eccentric $\mathbf{p}_5 = P_{e,4} = 24742^{\mathrm{d}} \pm 141^{\mathrm{d}}$ and circular $P_{c,5} = 24747^{\mathrm{d}} \pm 872^{\mathrm{d}}$
  - "Half-p" effect: Connects eccentric $\mathbf{p}_5$ signal also to circular $P_{c,4} = 12294^{\mathrm{d}} \pm 109^{\mathrm{d}}$
  - **Problem**: $\mathbf{p}_5$ signal has two minima and two maxima
  - **Problem**: Equal circular $P_{\mathrm{c},5}$ and $P_{\mathrm{c},4}$ amplitudes $\mathbf{A}_5 = A_{c,5} = 0.^{\mathrm{d}}018 \pm 0.^{\mathrm{d}}002$ and $\mathbf{A}_4 = A_{c,4} = 0.^{\mathrm{d}}018 \pm 0.^{\mathrm{d}}001$
  - **Solution for both problems**: $\mathbf{p}_5 = 66.^{\mathrm{y}}4$ and $\mathbf{p}_4 = 33.^{\mathrm{y}}7$ independent "off-phase" signals

  $\rightarrow$ "Interference-p'" effect induces two minima /maxima

Conclusion: $\mathbf{p}_5 = 66.^{\mathrm{y}}4$ and $\mathbf{p}_4 = 33.^{\mathrm{y}}7$ probably two independent real signals (Fig. A15: alternative)

Results (Signal $\mathbf{p}_3 = 10144^{\rm d} = 27.^{\rm y}8$)

Fig. A8 extract: Signal $\mathbf{p}_3 = 27.^{\rm y}8$

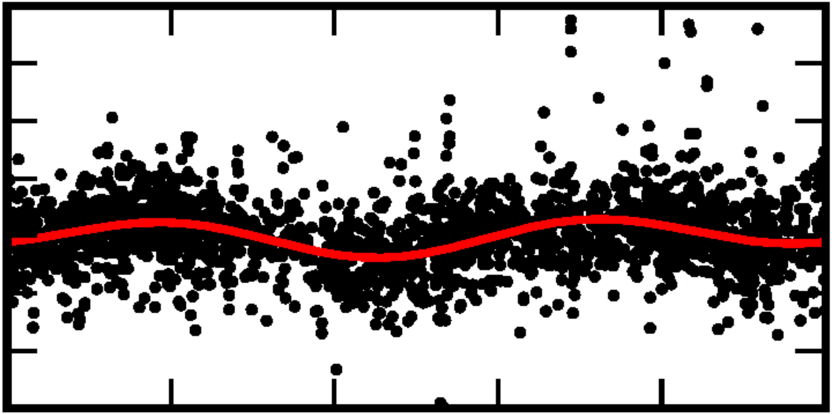

Results (Signal $\mathbf{p}_3 = 10144^{\mathrm{d}} = 27.^{\mathrm{y}}8$)

- **New section** "Signal $\mathbf{p}_3 = 10144^{\mathrm{d}} = 27.^{\mathrm{y}}8$"
  - No eccentric orbit period equal to circular orbit period $\mathbf{p}_3 = P_{c,3} = 10144^{\mathrm{d}} \pm 30^{\mathrm{d}} = 27.^{\mathrm{y}}8 \pm 0.^{\mathrm{y}}1$
  - "Double-p" effect: Connects circular $P_{c,3}$ to eccentric orbit $P_{e,3} = 20358^{\mathrm{d}} \pm 128^{\mathrm{d}}$
  - Symmetric $P_{e,3}$ signal shows two equal maxima and two equal minima = "double-wave" of circular orbit
  - $P_{e,3} = 20358^{\mathrm{d}}$ detected All data, First 226^{y}-data and First 185^{y}-data

  $\rightarrow$ $\mathbf{p}_3 \approx P_{e,3}/2$ also detected in these three samples
  - Signal amplitude $\mathbf{A}_3 = A_{c,3} = 0.^{\mathrm{d}}0097 \pm 0.^{\mathrm{d}}0004$

Conclusion: Eccentric orbit $P_{e,3} = 56.^{\mathrm{y}}0$ signal probably represents "double wave" of circular $\mathbf{p}_3 = 27.^{\mathrm{y}}8$ signal (Fig. A15: alternative)

Results (Signal $\mathbf{p}_2 = 7269^{\mathrm{d}} = 20.^{\mathrm{y}}0$)

Fig. A10 extract: Signal $\mathbf{p}_2 = 20.^{\mathrm{y}}0$"

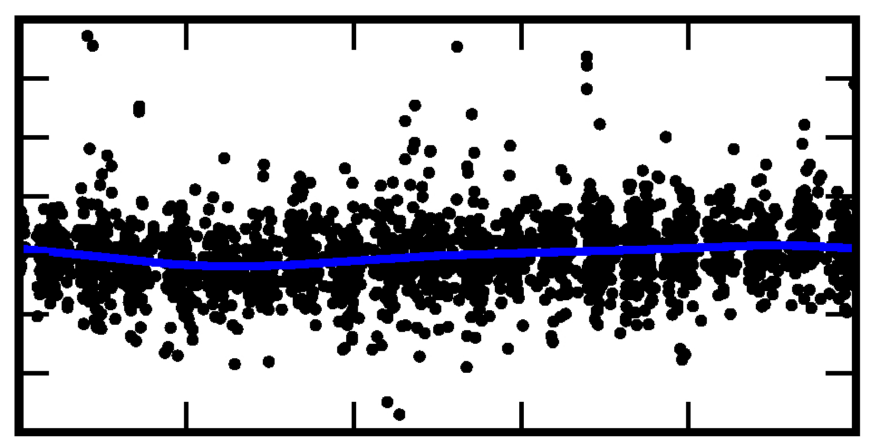

Results (Signal $\mathbf{p}_2 = 7269^{\mathrm{d}} = 20.^{\mathrm{y}}0$)

- **New section** "Signal $\mathbf{p}_2 = 7269^{\mathrm{d}} = 20.^{\mathrm{y}}0$"
  - "Correct-*p*" effect: Eccentric $\mathbf{p}_2 = P_{e,2} = 7269^{\mathrm{d}} \pm 29^{\mathrm{d}}$ connected to circular $P_{c,2} = 7395^{\mathrm{d}} \pm 37^{\mathrm{d}}$
  - Signal shows only one minimum and one maximum
  - Detected directly in All data and First 226^{y}-data
  - "Double-*p*" effect: Signal $\mathbf{p}_2$ detected indirectly in First 185^{y}-data double period $P_3 = 15429^{\mathrm{d}} \pm 222^{\mathrm{d}}$
  - Amplitude $\mathbf{A}_2 = A_{e,2} = 0.^{\mathrm{d}}007 \pm 0.^{\mathrm{d}}001$

Conclusion: Signal $\mathbf{p}_2 = 20.^{\mathrm{y}}0$ is an "ordinary" eccentric orbit O-C signal

Results (Signal $\mathbf{p}_1 = 680.4^{\mathrm{d}} = 1.^{\mathrm{y}}86$)

Fig. A10 extract: Signal $\mathbf{p}_1 = 1.^{\mathrm{y}}86$

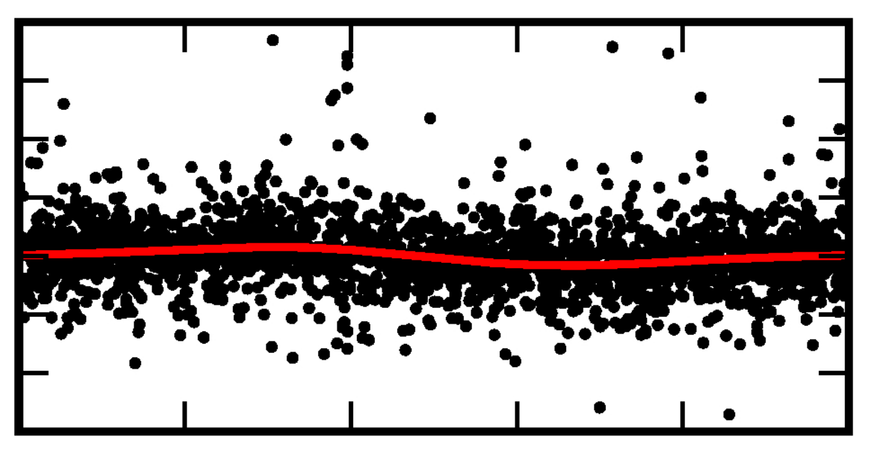

Results (Signal $\mathbf{p}_1 = 680.4^{\mathrm{d}} = 1.^{\mathrm{y}}86$)

- **New section** "Signal $\mathbf{p}_1 = 680.4^{\mathrm{d}} = 1.^{\mathrm{y}}86$"
  - "Correct-p" effect: Eccentric and circular orbits give **same** $\mathbf{p}_1 = 680.^{\mathrm{d}}4 \pm 0.^{\mathrm{d}}4 = 1.^{\mathrm{y}}863 \pm 0.^{\mathrm{y}}001$
  - Signal shows only one minimum and one maximum
  - Detected in All data, First 226^{y}-data and First 185^{y}-data
  - Amplitude $\mathbf{A}_1 = A_{e,1} = 0.^{\mathrm{d}}0064 \pm 0.^{\mathrm{d}}0007$
  - Signal period $\mathbf{p}_1$ equal to Algol C orbital period (discussed later in detail)

Conclusion: Signal $\mathbf{p}_1 = 1.^{\mathrm{y}}86$ is an "ordinary" eccentric orbit O-C signal

- **New section** "Two weakest signals"
  - Weak signals $P_{c,2} = 2986^{\mathrm{d}} \pm 39^{\mathrm{d}} = 8.^{\mathrm{y}}1 \pm 0.^{\mathrm{y}}1$ and $P_2 = 3387^{\mathrm{d}} \pm 17^{\mathrm{d}} = 9.^{\mathrm{y}}27 \pm 0.^{\mathrm{y}}04$ real or spurious

What would it mean?

@depositphotos.com

Table A13

All Data: Comparison of Eccentric and Circular Orbit Results

Col. 1	Col. 2	Col. 3	Col. 4	Col. 5	Col. 6	Col. 7	Col. 8
	Table A7: Eccentric $e > 0 \equiv K_2 = 2$			Table A9: Circular $e = 0 \equiv K_2 = 1$		Connection	Effect
$\mathcal{M} = 3$	$P_{e,5} = 79999 \pm 1216$	$A_{e,5} = 0.287 \pm 0.005$	$\mathcal{M} = 2$	$P_{c,7} = 120740 \pm 41002$ Lp	$A_{c,7} = 0.6 \pm 0.5$ Ad	$P_{e,5} \approx 1 \times P_{c,7}$	Correct-p
			$\mathcal{M} = 2$	$P_{c,6} = 42422 \pm 640$	$A_{c,6} = 0.08 \pm 0.01$	$P_{e,5} \approx 2 \times P_{c,6}$	Half-p
$\mathcal{M} = 3$	$P_{e,4} = 24742 \pm 141$	$A_{e,4} = 0.029 \pm 0.001$	$\mathcal{M} = 2$	$P_{c,5} = 24247 \pm 872$	$A_{c,5} = 0.018 \pm 0.002$	$P_{e,4} \approx 1 \times P_{c,5}$	Correct-p
			$\mathcal{M} = 2$	$P_{c,4} = 12294 \pm 109$	$A_{c,4} = 0.018 \pm 0.001$	$P_{e,4} \approx 2 \times P_{c,4}$	Half-p
$\mathcal{M} = 3$	$P_{e,3} = 20358 \pm 128$	$A_{e,3} = 0.013 \pm 0.001$	$\mathcal{M} = 2$	$P_{c,3} = 10144 \pm 91$	$A_{c,3} = 0.0097 \pm 0.0004$	$P_{e,3} \approx 2 \times P_{c,3}$	Half-p
$\mathcal{M} = 6$	$P_{e,2} = 7269 \pm 29$	$A_{e,2} = 0.007 \pm 0.001$	$\mathcal{M} = 5$	$P_{c,2} = 7395 \pm 37$	$A_{c,2} = 0.0061 \pm 0.0006$	$P_{e,2} \approx 1 \times P_{c,2}$	Correct-p
$\mathcal{M} = 6$	$P_{e,1} = 680.4 \pm 0.4$	$A_{e,1} = 0.0064 \pm 0.0007$	$\mathcal{M} = 5$	$P_{c,1} = 680.7 \pm 0.5$	$A_{c,1} = 0.0057 \pm 0.0009$	$P_{e,1} \approx 1 \times P_{c,1}$	Correct-p

Note. Cols. 1–3: eccentric orbit results (Table A7). Cols. 4–6: circular orbit results (Table A9). Col. 7: connection between eccentric and circular orbit periods. Col. 8: Effects are explained in Section 5.5. Eccentric and circular orbit periods are denoted by subscripts "e" and "c," respectively.

What would it mean, if comparison of circular and eccentric orbit results in Table A13 could not be explained by

- **correct-*p* effect**
- **half-*p* effect**

Discussion

- **New section** “Discussion”
- **What** causes these numerous O-C signals?
  - Applegate (1992)[1] mechanism?
    No: **Magnetic activity** is quasiperiodic, not strictly periodic $\equiv$ Not predictable
  - Apsidal motion?
    No: **Apsidal motion** can cause one period, but not many periods
  - Light Travel Time Effect (LTTE) of “third bodies”
    Yes: **LTTE** could cause strictly periodic signals
- **Tentative** mass and semimajor axis estimates for Algol’s companion candidates (Table 1)
  1. Assumption: circular orbits
  2. Assumption: third body equations valid (interference of other candidates ignored)

Discussion (Hierarchial structure)

- **New section** "Hierarchial structure"
  - Table 1: Case $i = 90^{\mathrm{o}}$
  - Algol A and B = Central Eclipsing binary = cEB
  - Algol C, D, ... = Wide Orbit Companions = WOS
  - We use hierarchial system diagrams introduced by Tokovinin (2021)[37]
- **Configuration 1 (Fig. A15)**
  - Eight members: cEB and six WOSs
  - Algol H: most massive ($m_3 = 2.50 m_{\odot}$) and most distant ($a_3 = 44.7\mathrm{AU}$).
  - Four other low mass WOS ($0.23 m_{\odot} \leq m_3 \leq 0.43 m_{\odot}$)
  - Closest $m_3^{i=90} = 1.16 m_{\odot}$ WOS has period $\mathbf{p}_1 = 680.^{\mathrm{d}}4 \pm 0.^{\mathrm{d}}4$ equal to orbital period $P_{\mathrm{orb}} = 679.^{\mathrm{d}}85 \pm 0.^{\mathrm{d}}04$ of Algol C

Discussion (Hierarchial structure)

- **Fig. A15 extract**
- Eight members: cEB and six WOSs

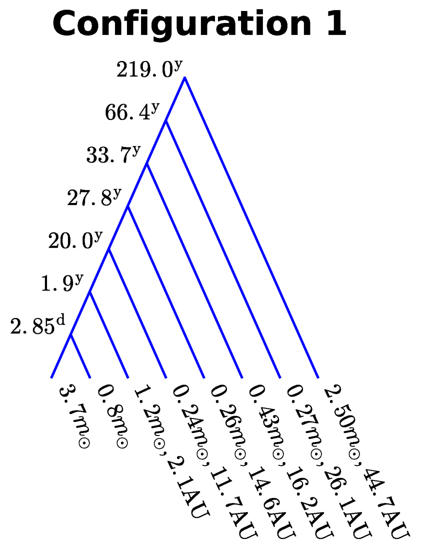

Discussion (Hierarchial structure)

- **Configuration 2 (Fig. A15)**
- Seven members:
  cEB and five WOSs
    - Sum of "off-phase" sinusoidal $\mathbf{p}_5 = 66.^y4$ and $\mathbf{p}_4 \approx \mathbf{p}_5/2 = 33.^y7$ signals causes $\mathbf{p}_5 = 66.^y4$ period double wave
    - $\rightarrow$ Single long-period $\mathbf{p}_5 = 66.^y4$ binary can cause similar curve, if member masses are unequal
    - $\rightarrow$ Unequal two minima and maxima
    - $\rightarrow$ Member masses can not be solved $\equiv$ "?"
    - Configuration 2 diagram: this hypothetical long-period $\mathbf{p}_5 = 66.^y4$ binary has an orbital period $\mathbf{p}_6 = 219.^y0$ around whole system barycentre
    - Three remaining WOS as in Configuration 1

Discussion (Hierarchial structure)

- **Fig. A15 extract**
- Seven members: cEB and five WOSs

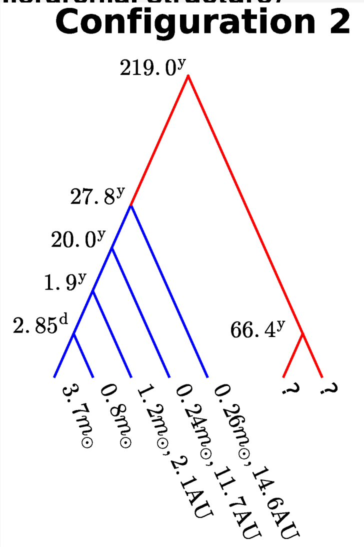

Discussion (Hierarchial structure)

- **Configuration 3 (Fig. A15)**
- Seven members: cEB and five WOSs
- Minor modification of Configuration 2
- Five $\mathcal{M}$=3+6 model periods taken "as such"
  - Signal $66.^{\mathrm{y}}4$ is not separated into two signals, as in Configuration 2
  - Full $P_{e,3} = 55.^{\mathrm{y}}8$ signal period used, not its half period of Configurations 1 and 2
  - $\rightarrow$ Could represent long-period $P_{e,3} = 55.^{\mathrm{y}}8$ binary having equal unknown masses $\equiv$ "?"
  - $\rightarrow$ Symmetric curve with two equal minima and maxima
  - Configuration 3: Long-period $\mathbf{p}_5 = 66.^{\mathrm{y}}4$ and $P_{e,3} = 55.^{\mathrm{y}}8$ binaries orbit each other in $\mathbf{p}_6 = 219.^{\mathrm{y}}0$
  - Two remaining WOS as in Configurations 1 and 2

Discussion (Hierarchial structure)

- **Fig. A15 extract**
- Seven members: cEB and five WOSs

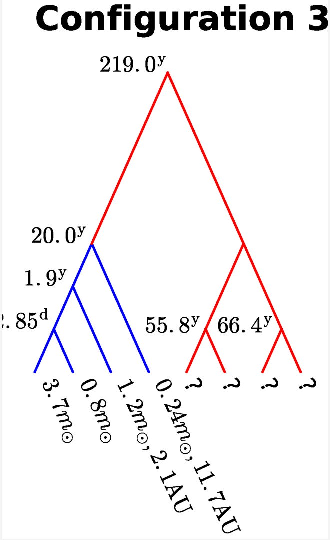

Discussion (Hierarchial structure)

- **Configuration 3**
  - **Inner system**: cEB and two close WOS
  - **Outer system**: Two long-period $55.^{y}8$ and $66.^{y}4$ binaries far away in $219.^{y}0$ orbit
  - → Inner and outer system do not perturb each other
  - → Configuration 3 most stable one of all three alternative configurations
- Algol's O-C data: Many other configurations possible
- **Example of stable hierarchial system of binaries**
  - Sextuple star system **TYC 7037-89-1**
  - Sextuple means six stars
  - Three eclipsing binaries (what are the odds for this!)
  - Spatial diagram on next page
  - → Eclipses of A , B and C systems confirm stability

Discussion (Hierarchial structure)

- Sextuple star system TYC 7037-89-1 with three eclipsing binaries (Powell et al. 2021)[32]

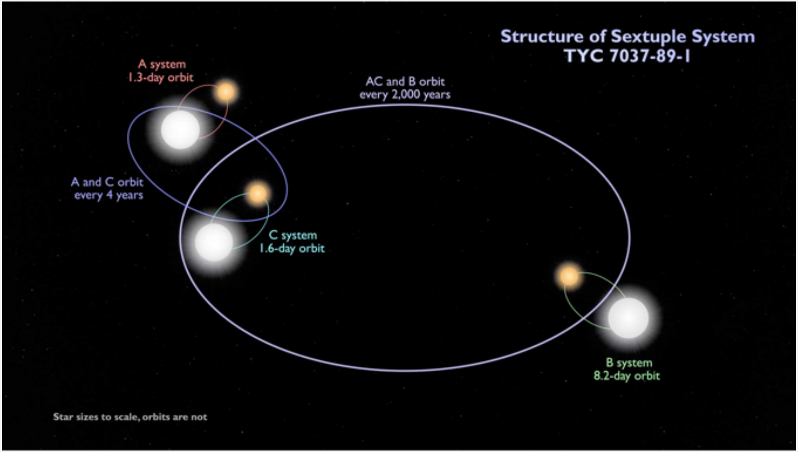

Discussion (Detectability)

- **New section** "Detectability"
- Third body detection data
  - Radial velocity data (e.g. Algol C)
  - O-C data (e.g. This **Paper II**)
  - Astrometric data (e.g. Tokovinin 2021)[37]
- DCM analysis of Algol's O-C data
  - **Can** determine signal periods
  - **Can not** determine exact hierarchial system structure
  - **Can not** determine exact number of stars
- How could Algol's companion candidates be detected?
  - Configuration 1 assumed
  - Circular orbits assumed
  - Orbital plane inclination $i_3 = 90^{\circ}$ assumed

Discussion (Detectability)

- WOSs **maximum and minimum radial velocities**

$$v_{\max} = v_0 + \frac{2\pi a_3}{p_3} \quad (21)$$

$$v_{\min} = v_0 - \frac{2\pi a_3}{p_3}, \quad (22)$$

where $v_0 = 4.0$ km/s Algol's radial velocity

- **Angular distance** between cEB and WOS changes constantly
- **Largest distance changes** occur at O-C curve minima and maxima:

$$\Delta a_{\max}(\Delta t) = 2a_3 \sin\left(\pi \Delta t / p_3\right) \quad (23)$$

during **shorter time intervals** $\Delta t \leq p_3/2$

Discussion (Detectability)

- Largest distance changes for **longer time intervals** $\Delta t > p_3/2$ are

$$\Delta a_{\max} = 2a_3$$

- **Smallest distance changes** coincide with O-C curve mean level
- For **shorter time intervals** $\Delta t \leq p_3$, smallest distance changes are

$$\Delta a_{\min}(\Delta t) = a_3[1 - \cos(\pi \Delta t / p_3)] \tag{24}$$

- **Longer time intervals** $\Delta t > p_3$ have

$$\Delta a_{\min} = 2a_3$$

Discussion (Detectability)

- Proper motion Algol's cEB $\mu_0 = 2.49$ mas/y
- WOS **minimum and maximum proper motion** is

$$\mu_{\min} = \mu_0 - \mu_c \quad (25)$$
$$\mu_{\max} = \mu_0 + \mu_c, \quad (26)$$

where $\mu_c = \Delta a_{\max}(\Delta t = 1^{\mathrm{y}})$ is WOSs maximum proper motion during one year

- All WOS have $\mu_c > \mu_0 \rightarrow \mu_{\min} = 0$
- **Table A15: Estimates** for $v_{\max}$, $v_{\min}$, $\Delta a_{\max}$, $\Delta a_{\min}$, $\mu_{\max}$ and $\mu_{\min}$ computed for observations spanning 5 or 20 years **(Let's have look at Table A15)**
- These can be used to infer, if companion candidates can be observed with different observing techniques

Discussion (Detectability)

Most massive $2.5 m_{\odot}$ candidate Algol H

- Brightest and largest distance from cEB

$\rightarrow$ Easiest to detect

- O-C curve close to mean level

$\rightarrow$ Close to maximum $a_3 = 1569$ mas from cEB

- cEB currently receding from us

$\rightarrow$ Algol H currently approaching us at $v_{\mathrm{min}} = -2$ km/s

- Distance changes between cEB and Algol H only $\Delta a_{\mathrm{min}} = 4$ or 64 mas during next 5 or 20 years

- **Other candidates**
  - Algol C has been detected from radial velocity and interferometry
  - Other remaining candidates much less massive

$\rightarrow$ More difficult to detect

Discussion (Detectability)

2MASS image of Algol: scale 7.58 x 7.58 arc minutes

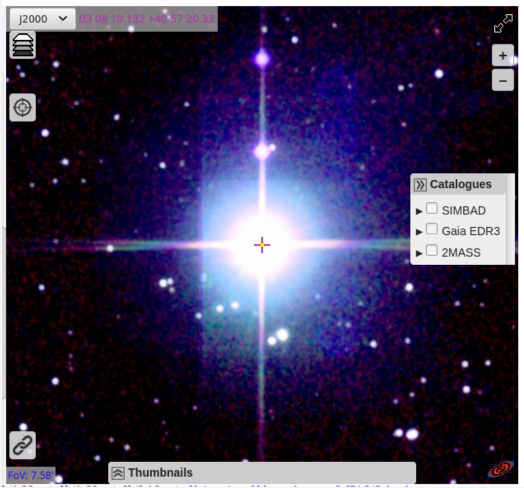

Discussion (Detectability)

Gaia-satellite image centered on Algol: scale 7.58 x 7.58 arc minutes (squares = other detected objects)

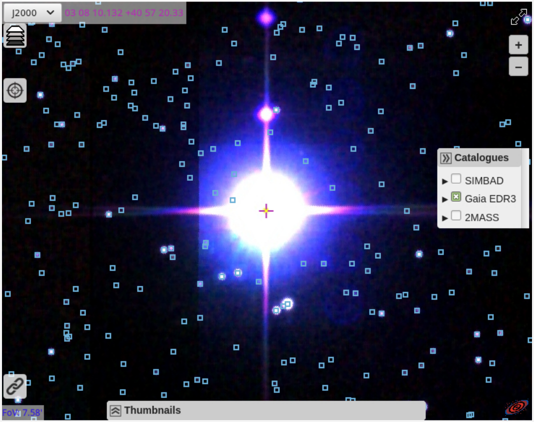

Discussion (Detectability)

Gaia-satellite detection of Algol's new companion candidates?

- Distance between Algol H and cEB is 1569 mas = 1.569" (Table A15: mas = milli arc seconds)
- Other WOS closer to cEB
- GAIA: *"most problems come from the bright sources and the strange image profiles"* (Torra et al. 2020)[38]
- GAIA: Algol "too bright".
- GAIA: Brightness profile constantly changing (movement of Algol A and B, eclipses, movement of companions, like Algol C)

$\rightarrow$ No certain GAIA detections $\pm$4" around Algol

$\rightarrow$ Only one certain $\pm$40" GAIA detection

- **Conclusion**: GAIA-satellite can not detect Algol's new companion candidates

Discussion (Detectability)

Interferometry

- Direct interferometric images of Algol A, Algol B and Algol C: Zavala et al (2010)[39], Baron et al. (2012)[2]

Why did they not detect massive $2.5m_{\odot}$ Algol H?

$\rightarrow$ Algol H **brighter** than **detected** $1.2m_{\odot}$ **Algol C**

1. Imaging area should be 20x20=400 times larger

2a. Algol H may be binary $\rightarrow$ dimmer

2b. Algol H is/has an evolved object $\rightarrow$ dimmer

3. Imaging applied three star model

$\rightarrow$ Algol H flux constant and it did not move during their observations

$\rightarrow$ Algol H contributed constant flux to modelled total flux

- **Conclusion**: Four star model interferometry over a 20x20 larger area may lead to Algol H detection

Discussion (Detectability)

CHARA interferometer image of Algol A, Algol B and Algol C: scale about 10 x 20 mas

Discussion (Detectability)

- **Speckle interferometry detection of Algol's new companion candidates?**
  - Speckle interferometry: many short exposures
  - → Shift-and-add ”image stacking”
  - → Increases ground-based telescope resolution
  - Limited to bright targets
  - → Is Algol ideal target?

Powell et al. (2021)[32]

- Sextuple-eclipsing binary system TIC 168789840 (TYC 7037-89-1 artistic image shown earlier)
- Next page: Speckle interferometry image
- Outer period 2000 years and distance $d \approx 570\mathrm{pc}$
- Algol H period 219 years and 10 times closer
- → Algol H detection might succeed?

Discussion (Hierarchial structure)

Here: 05.12.2022

- Speckle interferometric image of TIC 168789840 (TYC 7037-89-1) by Powell et al. (2021: Fig. 14)[32]

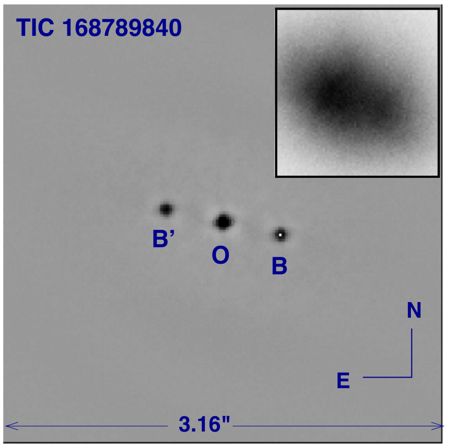

Discussion (Algol C detection)

- **New section** "Algol C detection"
  - Weakest $\mathbf{p}_1 = 680.^{\mathrm{d}}4 \pm 0.^{\mathrm{d}}4$ **signal** detected in all data, First 226^{y}-data and First 185^{y}-data
  - $\mathbf{p}_1$ **signal period** differs 1.4σ from **known** Algol C orbital period $P_{\mathrm{orb}} = 679.^{\mathrm{d}}85 \pm 0.^{\mathrm{d}}04$
  - $\mathbf{p}_6 = 219^{\mathrm{y}}$ signal 44.8 times stronger than $\mathbf{p}_1$ **signal**
  - $\mathbf{p}_1$ **signal "buried under"** five stronger $\mathbf{p}_2$, $\mathbf{p}_3$, $\mathbf{p}_4$ $\mathbf{p}_5$ and $\mathbf{p}_6$ signal interference and linear $p(t)$ trend

  → DCM can not detect Algol C signal full amplitude

  → Our Algol C mass $1.2 m_\odot$ smaller than interferometric mass estimates $1.5 \pm 0.1 m_\odot$ (Zavala et al. 2011)[39] and $1.76 \pm 0.15 m_\odot$ (Baron et al. 2012)[2]
  - Data: 127 Algol C **stable orbit** rounds around cEB
- **All these results indicate** (but do not prove)
  - Other five stronger signals **real periodicities**

What would it mean?

@depositphotos.com

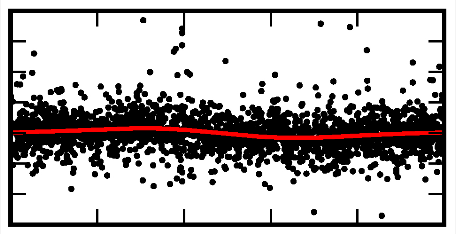

What would it mean, if Algol C signal were not detected with DCM?

Discussion (Stability)

- **New section** "Stability"
- **Is Algol's multiple star systems stable?**
  - **Signals same** in All data and First 226^{y}-data
  - Absence of $\mathbf{p}_2$ and $\mathbf{p}_5$ signals in First 185^{y}-data **can be explained** by "Half-*p*" and "Double-*p*" effects
  - All signals **strictly periodic**
  - Prediction **succeeds** for First 226^{y}-data
  - Trend prediction **fails** for First 185^{y}-data, but turning point prediction **succeeds**
- Strict periodicity does not prove that system is stable
  - Algol AB = cEB orbit **stable**
  - Algol C orbit **stable**
  - Other WOS orbits **stable?**

Discussion (Stability)

- **Angle** Ψ between cEB and WOS orbital planes
- **WOS perturbations** cause periodic cEB **orbital plane changes** (Soderhjelm 1975, Eq. 27)[36]

  $\rightarrow$ cEB eclipses **not always** observed from Earth

  - Orbital plane of cEB **stable** for $\Psi = 0^{\rm o}$ or $90^{\rm o}$
  - Only known WOS Algol C has $\Psi = 90.^{\rm o}20 \pm 0.^{\rm o}32$ (Baron et al. 2012)[2]

  $\rightarrow$ **Modern times**: No changes in Algol's eclipses

  $\rightarrow$ Eclipses observed over three thousand years ago in **ancient Egypt** (Jetsu et a. 2012)[21]

  - If **any WOS** has $\Psi \neq 0^{\rm o}$ or $\Psi \neq 90^{\rm o}$

  $\rightarrow$ System stability reduced

  $\rightarrow$ cEB eclipses **not always** observed on Earth

  - If orbital planes of **all WOS co-planar**

  $\rightarrow$ All WOSs must have $\Psi = 90^{\rm o}$, like Algol C

Discussion (Stability)

- cEB orbital period P_{orb} **should increase** due to **known mass transfer** from the less massive Algol B to the more massive Algol A (Kwee 1958)[23]
  - Mass transfer estimates range from $10^{-13} m_{\odot} \mathrm{yr}^{-1}$ to $10^{-7} m_{\odot} \mathrm{yr}^{-1}$
  - No period increase observed since Goodricke (1783)[9]
- **Other WOS effects** should also perturb cEB
  - **Kozai effect** (Kozai 1962)[22]
  - **Kozai cycle** and **tidal friction** (Fabrysky & Tremaine 2007) [7]
- **Mass transfer**, **Kozai effect**, **Kozai cycle** and **tidal friction** can perturb cEB, and cause cEB period and orbital plane changes

Discussion (Stability)

- Surprisingly, linear $K_3 = 1$ trend for $p(t)$ means that $P_{\rm orb}$ of cEB has been **constant** for past 236 years
- This **constant period** has been

$$P_{\rm orb} = \left(\frac{1}{P_0} - \frac{2M_1}{\Delta T} \right)^{-1} = 2.^{\rm d}86732870, \qquad (27)$$

where $M_1 = 0.1278$ is $p(t)$ coefficient in $\mathcal{M}$= 3 model (Table A7), and $P_0 = 2.^{\rm d}86730431$ (Eq. 1)

$\rightarrow$ **LTTE effects alone** can explain Algol's O-C data

$\equiv$ All members orbit same **stable barycentre**?

$\rightarrow$ **Mass transfer**, **Kozai effect**, **Kozai cycle** and **tidal friction** effects not needed to explain Algol's O-C data

Discussion (Stability)

- **Referee**: **Can stability be confirmed from long-term dynamical orbit integrations?**
  1. Long-term dynamical orbit integrations are not my field of expertise
  2. Number of WOS **unknown**
  3. Hierarchial structure **unknown**
  4. Infinite **unknown number of combinations** for WOS's $p_3, m_3, e_3, a_3, i_3, \omega_3$ and Ψ_3 **initial values** for long-term integrations

  $\rightarrow$ Some combinations may be stable, others may not

$\rightarrow$ **Stability problem**: No unambiguous solution

$\rightarrow$ **Stable** or **unstable**: These p_3 periods observed **now**

Discussion (Predictability)

- **New section** "Predictability"
- Unambiguous **individual signal indentification** from many signal interference not always possible
- **Predictability point of view**:
  - Model $g(t) =$ Sum of **identified signals** is equal to sum of **unidentified signals**
  - $\rightarrow$ **Prediction same** for both alternatives
- **Earlier linear and quadratic EB ephemerides**
  - Future eclipse epoch predictions **fail**
- **Earlier third-dody EB detections**
  - Future eclipse epoch predictions **fail**
- **Our 9.2 years** O-C **prediction for Algol succeeds**
  - Requires **strict periodicities**
  - Requires **corrrect trend**

Discussion (Predictability)

- **Our 50 years** O-C **prediction for Algol fails**
  - **Time span** only $\Delta T = 185$ years
  - $\rightarrow$ **Correct** 219 years period not detected
  - $\rightarrow$ Longest detected 172^{y} period **wrong**
  - $\rightarrow$ Trend **wrong**
  - $\rightarrow$ Prediction **fails**
- **50 years** O-C prediction for HJD 2450000 **turning point epoch succeeds**
- **10 years** prediction **after October 2018**
  - New data will test predictability
  - $\rightarrow$ More accurate peridicities
  - $\rightarrow$ More accurate predictions
  - $\rightarrow$ May, or may not, prove to be strictly periodic **stable orbital periods** (Algol C certainly is!)

Discussion (Predictability)

Fig. 1b: **10 years prediction** after October 2018

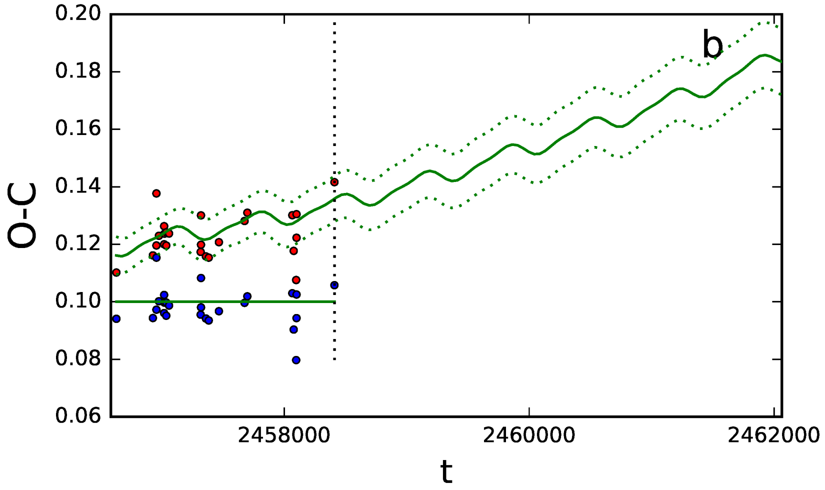

Discussion (Predictability)

- **Origin** of Algol's periodicities **now** uncertain?
- Nothing new in Astronomy
- For example, **one year period** in seasons on Earth easily observed long before **its origin understood**:
  1. Circular shape of Earth
  2. Earth orbits around the Sun
  3. Rotation axis of Earth tilted
- Predictions of seasons or solar motion along ecliptica succeeded, **although origin unknown**
- Algol's periods real, **although origin unknown**
  - $\rightarrow$ For some reason, or another, predictions succeed

Discussion (Look-elsewhere Effect)

- **New section** *"Look-elsewhere Effect"*
- **First**, we test over thirty models having free parameters between $\eta = 6$ and 22
- **Then**, we analyse residuals

$\rightarrow$ Best $\mathcal{M}$=3+6 model for all O-C data has $\eta = 17 + 11 = 28$ free parameters

- Search for correct model over a vast parameter space

$\rightarrow$ Probability for finding **spurious apparently significant** signals **increases**

- This effect called: *"Look-elsewhere Effect"*
  - Some methods can account for *"Look-elsewhere Effect"*, and give **direct** significance estimates *S* for detected periods (e.g. Bayer & Seljak 2020)[3]

$\rightarrow$ Can DCM account for *"Look-elsewhere Effect"*?

Discussion (Look-elsewhere Effect)

Problem: Can DCM account for *"Look-elsewhere Effect"*?

- **Short answer**
  - DCM **can not give direct** S significance estimates
  - DCM **can give indirect** S significance estimates
- **Long answer**: DCM designed for period detection. *"Look-elsewhere Effect"* does not mislead this period detection. Detected periods **not spurious** because
  1. Fisher test approach gives **indirect** S significance estimates, as well as best model. Many **periods detected** at extreme $Q_F < 10^{-16}$ critical levels
  2. Periodograms display no sudden jumps: detected periods do not depend on **number of tested periods**
  3. DCM arrives at **most simple** $K_3 = 1$ trend
  4. $\mathcal{M}$=3+6 model **prediction succeeds**

Discussion (Uncertainties)

- **New section** "Uncertainties"

DCM analysis uncertainties

1. Longest 219 years period **only slightly shorter than** 236 years time span of O-C data. Will new data confirm this periodicity?
2. Except for Algol C, **other WOS not detected directly**. Algol H would be easiest to detect (interferometry, speckle interferometry)
3. **Exact number of WOS** remains uncertain, as well as **hierarchial system structure** and **stability**
4. Short 10 year prediction **succeeds**. Long 50 years prediction **does not succeed**, but turning point epoch prediction **succeeds**

Discussion (Conclusions)

- **New section** “Conclusions”
- O-C ephemerides improved by **removing linear or quadratic trends**
  - $\rightarrow$ Future eclipse epoch **predictions have failed**
- O-C third body LTTE **strictly periodic**
  - $\rightarrow$ Future eclipse epoch **predictions have failed**
- O-C 3rd body detection rate 992/80 000=0.012
- O-C 4th body detection rate 4/80 0000=0.00005
  - Aperiodic trends mislead detection of periodic signals
  - Detections relied on pre-whitening DFT approach
  - $\rightarrow$ Future eclipse epoch **predictions** based on linear or quadratic trends, and LTTE, **have failed**
- **Unprecedented**: DCM detects **five strictly periodic signals** from Algol’s O-C data

Discussion (Conclusions)

All data

- Algol's periods between 1.863 and 219.0 years
- Weakest 680.4 ± 0.4 days signal period differs 1.4σ from **known** 679.85 ± 0.04 days Algol C orbital period
- Exact **number of companions** unknown
- Exact **hierarchial structure** unkown
- System **stability** unkown

Shorter 226.2 years subsample

- **Same five signals** detected
- **Excellent prediction** for last 9.2 years

Shortest 185 years subsample

- Longest 219 years period **not detected**

$\rightarrow$ 50 years **prediction fails**, but **turning point epoch prediction succeeds**

$\rightarrow$ **Turning point** explains odd O-C publication gap!

Discussion (Conclusions)

Linear $K_3 = 1$ trend in Algol's O-C

- $\rightarrow$ **Orbital period constant** since Goodricke (1783)[9]

- **Perpendicular** cEB and Algol C orbital planes
  - $\rightarrow$ Algol's eclipses observed in ancient Egypt
  - $\rightarrow$ If other WOSs **coplanar** with Algol C, then their orbital planes also **perpendicular** to cEB plane
- **General statement**: Predictions for **complex non-linear** models rarely succeed
  - $\rightarrow$ **If** prediction after October 18th, 2018 succeeds, **then** Algol's future O-C data may prove that
  - $\rightarrow$ DCM works for **complex non-linear models**

Paper II completed!

What would it be?

@depositphotos.com

What would be the next logical step with DCM?

References I

[1] J. H. Applegate.
A mechanism for orbital period modulation in close binaries.
ApJ, 385:621–629, Feb. 1992.

[2] F. Baron, J. D. Monnier, E. Pedretti, M. Zhao, G. Schaefer, R. Parks, X. Che, N. Thureau, T. A. ten Brummelaar, H. A. McAlister, S. T. Ridgway, C. Farrington, J. Sturmann, L. Sturmann, and N. Turner.
Imaging the Algol Triple System in the H Band with the CHARA Interferometer.
ApJ, 752(1):20, June 2012.

[3] A. E. Bayer and U. Seljak.
The look-elsewhere effect from a unified Bayesian and frequentist perspective.
JCAP, 2020(10):009, Oct. 2020.

[4] T. Borkovits, E. Forgács-Dajka, and Z. Regály.
The combined effect of the perturbations of a third star and the tidally forced apsidal motion on the O–C curve of eccentric binaries.
Astronomical Society of the Pacific Conference Series, 333:128, 2005.

References II

[5] R. H. Curtiss.
on the Orbital Elements of Algol.
ApJ, 28:150, Sept. 1908.

[6] X.-W. Duan, X. Chen, W. Sun, L. Deng, H. Zhang, F. Yang, and C. Liu.
Blueshifted hydrogen emission and shock wave of RR Lyrae variables in SDSS and LAMOST.
ApJ, 918(3):arXiv:2107.13573, Sept. 2021.

[7] D. Fabrycky and S. Tremaine.
Shrinking Binary and Planetary Orbits by Kozai Cycles with Tidal Friction.
ApJ, 669(2):1298–1315, Nov. 2007.

[8] H. Frieboes-Conde, T. Herczeg, and E. Høg.
The multiple system of Algol.
A&A, 4:78, Feb. 1970.

References III

[9] J. Goodricke.
A Series of Observations on, and a Discovery of, the Period of the Variation of the Light of the Bright Star in the Head of Medusa, Called Algol. In a Letter from John Goodricke, Esq. to the Rev. Anthony Shepherd, D. D. F. R. S. and Plumian Professor at Cambridge.
Philosophical Transactions of the Royal Society of London Series I, 73:474–482, Jan. 1783.

[10] T. Hajdu, T. Borkovits, E. Forgács-Dajka, J. Sztakovics, G. Marschalkó, and G. Kutrovátz.
Eclipse timing variation analysis of OGLE-IV eclipsing binaries towards the Galactic Bulge - I. Hierarchical triple system candidates.
MNRAS, 485(2):2562–2572, May 2019.

[11] D. I. Hoffman, T. E. Harrison, B. J. McNamara, W. T. Vestrand, J. A. Holtzman, and T. Barker.
The Case for Third Bodies as the Cause of Period Changes in Selected Algol Systems.
AJ, 132(6):2260–2267, Dec. 2006.

References IV

[12] J. B. Irwin.
The Determination of a Light-Time Orbit.
ApJ, 116:211, July 1952.

[13] L. Jetsu.
Real light curves of FK Comae Berenices: Farewell flip-flop.
arXiv e-prints, page arXiv:1808.02221, Aug. 2019.

[14] L. Jetsu.
About ten stars orbit eclipsing binary XZ Andromedae (**Paper III**).
JAAVSO (submitted), 2020.

[15] L. Jetsu.
Discrete Chi-square Method for Detecting Many Signals (**Paper I**).
The Open Journal of Astrophysics, 3(1):4, Apr. 2020.

[16] L. Jetsu.
Say Hello to Algol's New Companion Candidates (**Paper II**).
ApJ, 920(2):137, Oct. 2021.

References V

[17] L. Jetsu, J. Huovelin, I. Tuominen, O. Vilhu, B. . W. Bopp, and V. Piirola.
Rotational and long-term variations of HD 199 178 - A double period activity cycle.
A&A, 236:423–439, Sept. 1990.

[18] L. Jetsu and J. Pelt.
Three stage period analysis and complementary methods.
A&AS, 139:629–643, Nov. 1999.

[19] L. Jetsu, J. Pelt, and I. Tuominen.
Time series analysis of V 1794 Cygni long-term photometry.
A&A, 351:212–224, Nov. 1999.

[20] L. Jetsu and S. Porceddu.
Shifting Milestones of Natural Sciences: The Ancient Egyptian Discovery of Algol's Period Confirmed.
PLoS ONE, 10(12):e0144140, Dec. 2015.

References VI

[21] L. Jetsu, S. Porceddu, J. Lyytinen, P. Kajatkari, J. Lehtinen, T. Markkanen, and J. Toivari-Viitala.
Did the Ancient Egyptians Record the Period of the Eclipsing Binary Algol - The Raging One?
ApJ, 773:1, Aug. 2013.

[22] Y. Kozai.
Secular perturbations of asteroids with high inclination and eccentricity.
AJ, 67:591–598, Nov. 1962.

[23] K. K. Kwee.
Investigation of variations in the period of sixteen bright short-period eclipsing binary stars.
BAN, 14:131, Apr. 1958.

[24] J. Lehtinen, L. Jetsu, T. Hackman, P. Kajatkari, and G. W. Henry.
The continuous period search method and its application to the young solar analogue HD 116956.
A&A, 527:A136, Mar. 2011.

References VII

[25] J. Lehtinen, L. Jetsu, T. Hackman, P. Kajatkari, and G. W. Henry.
Activity trends in young solar-type stars.
A&A, 588:A38, Apr. 2016.

[26] M. C. A. Li, N. J. Rattenbury, I. A. Bond, T. Sumi, D. P. Bennett, N. Koshimoto, F. Abe, Y. Asakura, R. Barry, A. Bhattacharya, M. Donachie, P. Evans, A. Fukui, Y. Hirao, Y. Itow, K. Masuda, Y. Matsubara, Y. Muraki, M. Nagakane, K. Ohnishi, T. Saito, A. Sharan, D. J. Sullivan, D. Suzuki, P. J. Tristram, and A. Yonehara.
A study of the light travel time effect in short-period MOA eclipsing binaries via eclipse timing.
MNRAS, 480(4):4557–4577, Nov. 2018.

[27] G. L. Loumos and T. J. Deeming.
Spurious results from Fourier analysis of data with closely spaced frequencies.
Ap&SS, 56:285–291, July 1978.

[28] R. Miller.
Simultaneous Statistical Inference.
Springer New York, 1981.

References VIII

[29] P. Moskalik and Z. Kołaczkowski.
Frequency analysis of Cepheids in the Large Magellanic Cloud: new types of classical Cepheid pulsators.
MNRAS, 394(3):1649–1666, Apr. 2009.

[30] S. Porceddu, L. Jetsu, T. Markkanen, J. Lyytinen, P. Kajatkari, J. Lehtinen, and J. Toivari-Viitala.
Algol as horus in the cairo calendar: The means and the motives of the observations.
Open Astronomy, 27:232–263, sep 2018.

[31] S. Porceddu, L. Jetsu, T. Markkanen, and J. Toivari-Viitala.
Evidence of periodicity in ancient egyptian calendars of lucky and unlucky days.
Cambridge Archaeological Journal, 18(03):327, oct 2008.

[32] Powell et al.
TIC 168789840: A Sextuply Eclipsing Sextuple Star System.
AJ, 161(4):162, Apr. 2021.

References IX

[33] M. J. Sarna.
The evolutionary status of beta Per.
MNRAS, 262:534–542, May 1993.

[34] J. D. Scargle.
Studies in astronomical time series analysis. II - Statistical aspects of spectral analysis of unevenly spaced data.
ApJ, 263:835–853, Dec. 1982.

[35] T. Shibayama, H. Maehara, S. Notsu, Y. Notsu, T. Nagao, S. Honda, T. T. Ishii, D. Nogami, and K. Shibata.
Superflares on Solar-type Stars Observed with Kepler. I. Statistical Properties of Superflares.
ApJS, 209(1):5, Nov. 2013.

[36] S. Soderhjelm.
The three-body problem and eclipsing binaries. Application to Algol and lambda Tauri.
A&A, 42:229–236, Aug. 1975.

References X

[37] A. Tokovinin.
Inner and Outer Orbits in 13 Resolved Hierarchical Stellar Systems.
AJ, 161(3):144, Mar. 2021.

[38] Torra et al.
Gaia Early Data Release 3. Building the Gaia DR3 source list – Cross-match of Gaia observations.
arXiv e-prints, page arXiv:2012.06420, Dec. 2020.

[39] R. T. Zavala, C. A. Hummel, D. A. Boboltz, R. Ojha, D. B. Shaffer, C. Tycner, M. T. Richards, and D. J. Hutter.
The Algol Triple System Spatially Resolved at Optical Wavelengths.
ApJL, 715(1):L44–L48, May 2010.